



Structure determination of
genomes and genomic
domains by satisfaction of
spatial restraints

Marc A. Marti-Renom

CNAG-CRG · ICREA

<http://marciuslab.org>
<http://3DGenomes.org>
<http://cnag.crg.eu>

Photo by David Oliete - www.davidoliete.com

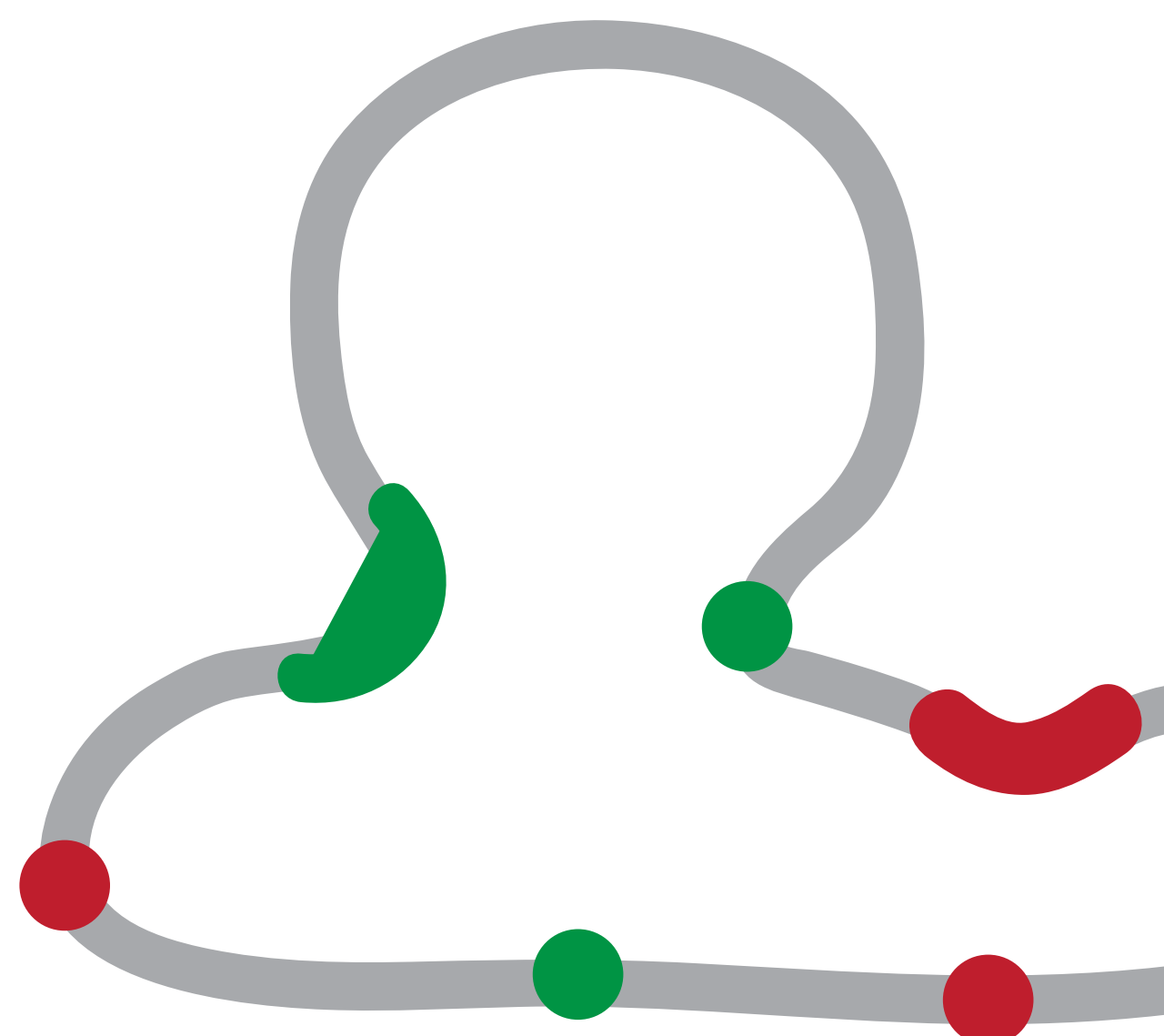
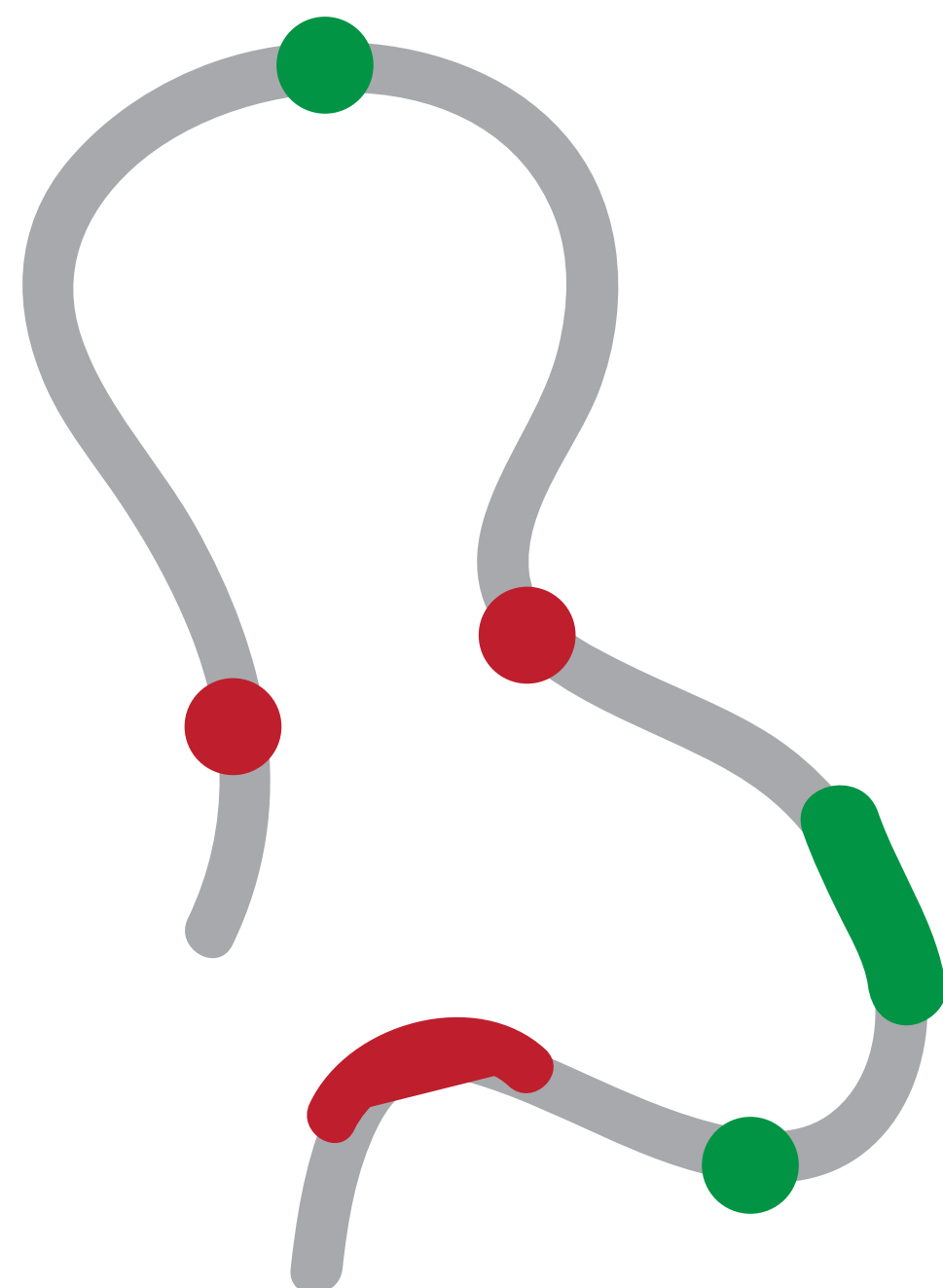
cnag CRG[®] ICREA

All you will see in the screen will be stored here:

<http://sgt.cnag.eu/www/presentations/>

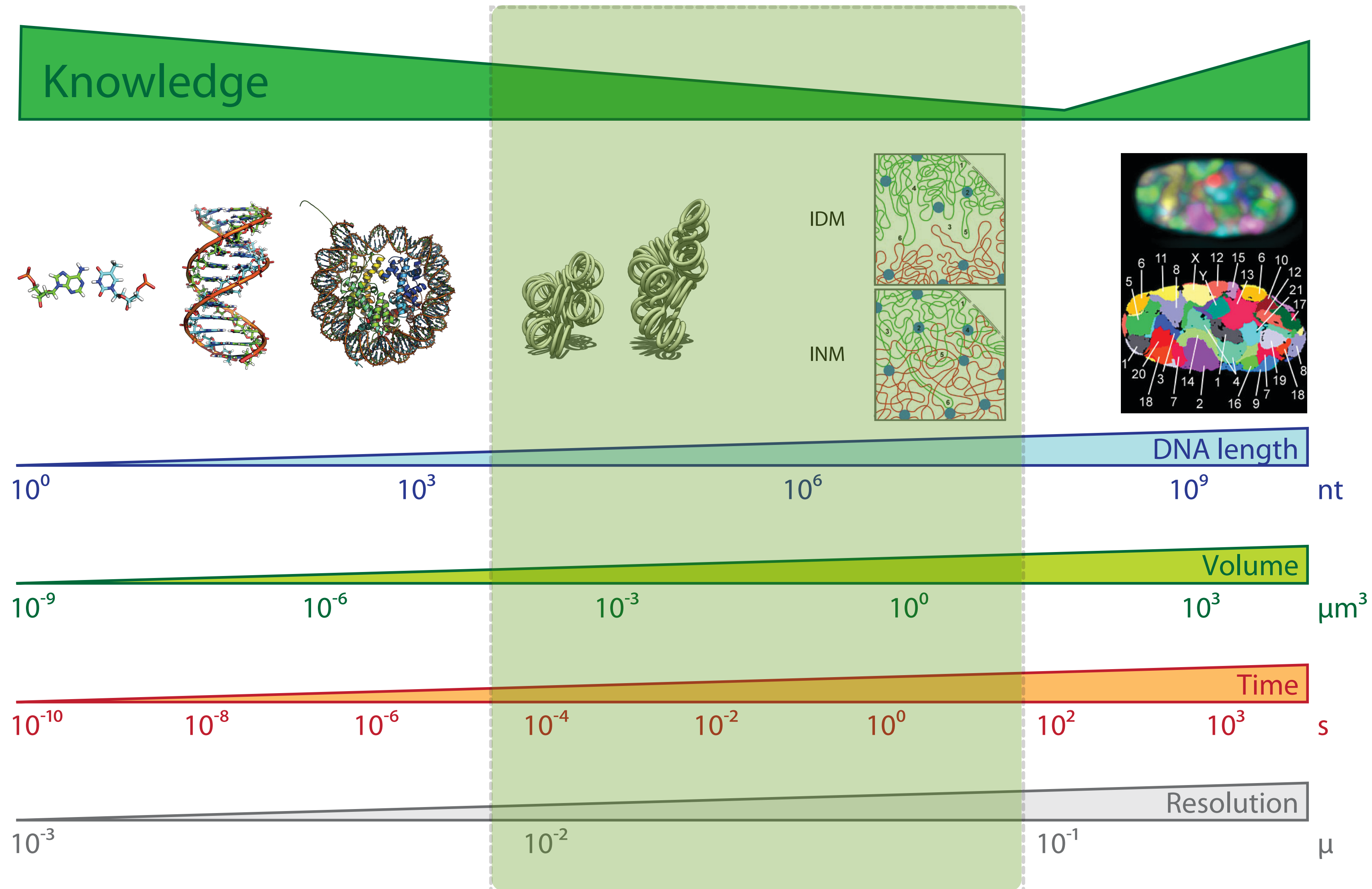
I encourage you to:

You can ask for question any time



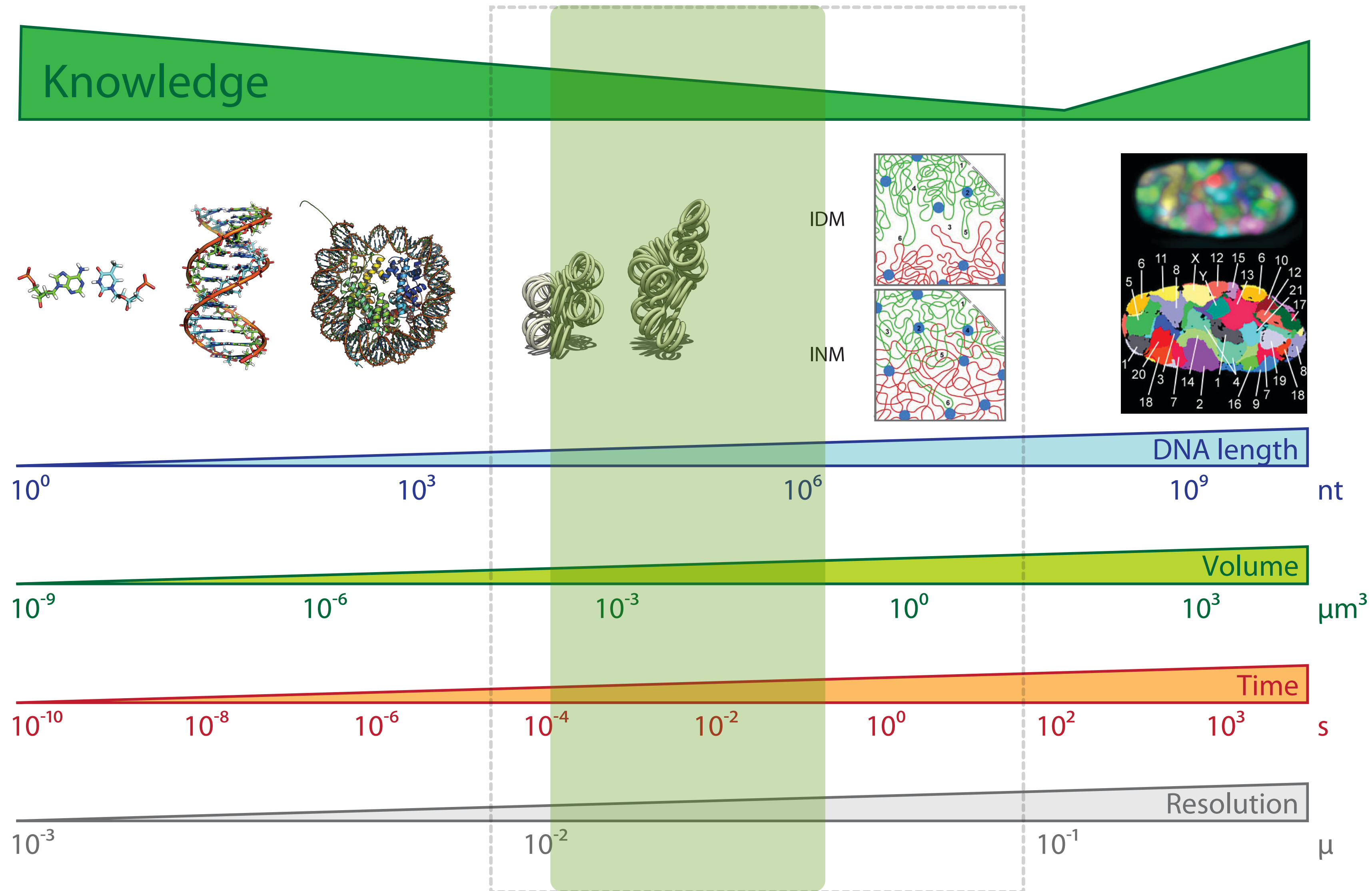
Resolution Gap

Marti-Renom, M. A. & Mirny, L. A. PLoS Comput Biol 7, e1002125 (2011)



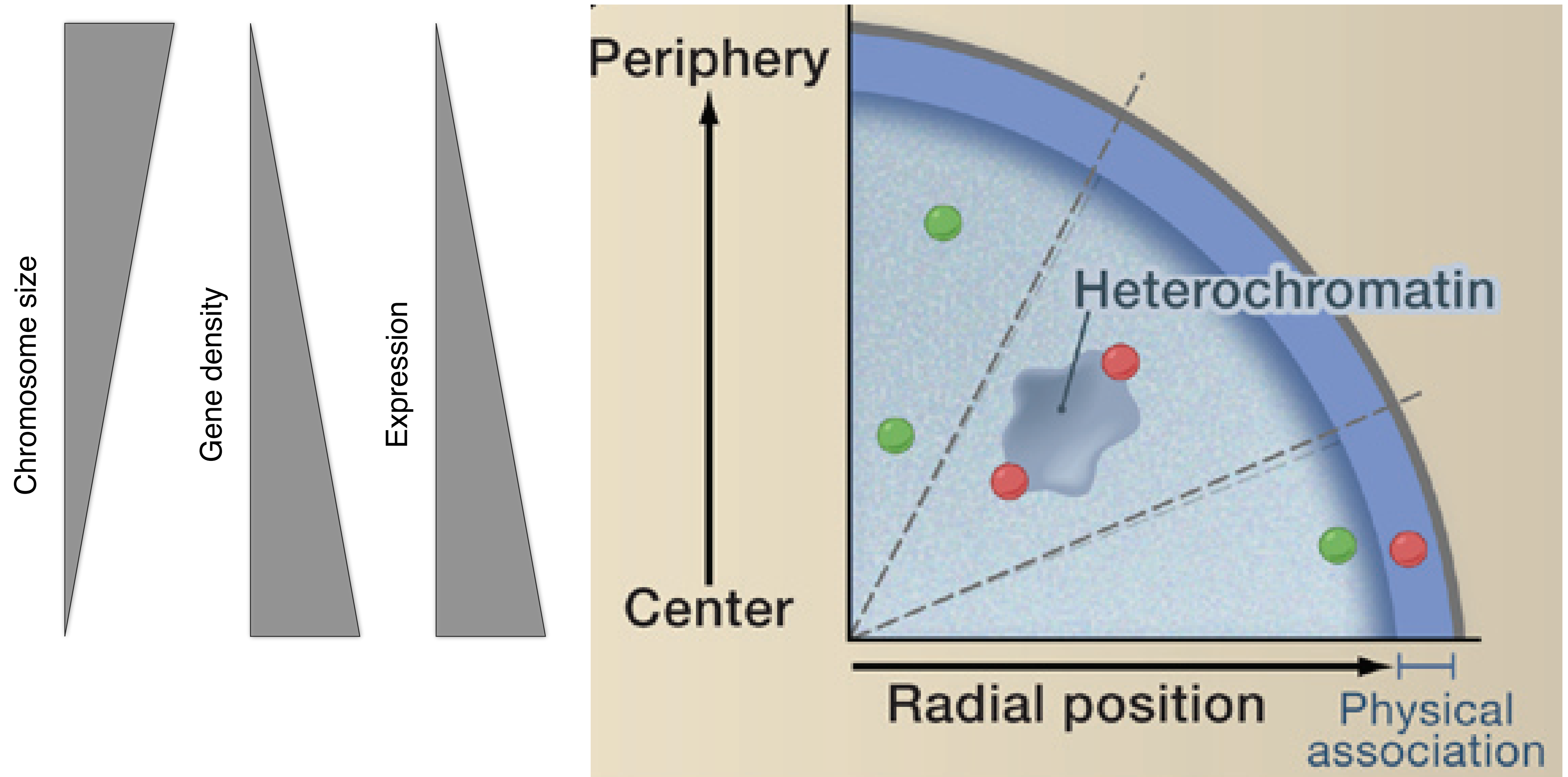
Resolution Gap

Marti-Renom, M. A. & Mirny, L. A. PLoS Comput Biol 7, e1002125 (2011)



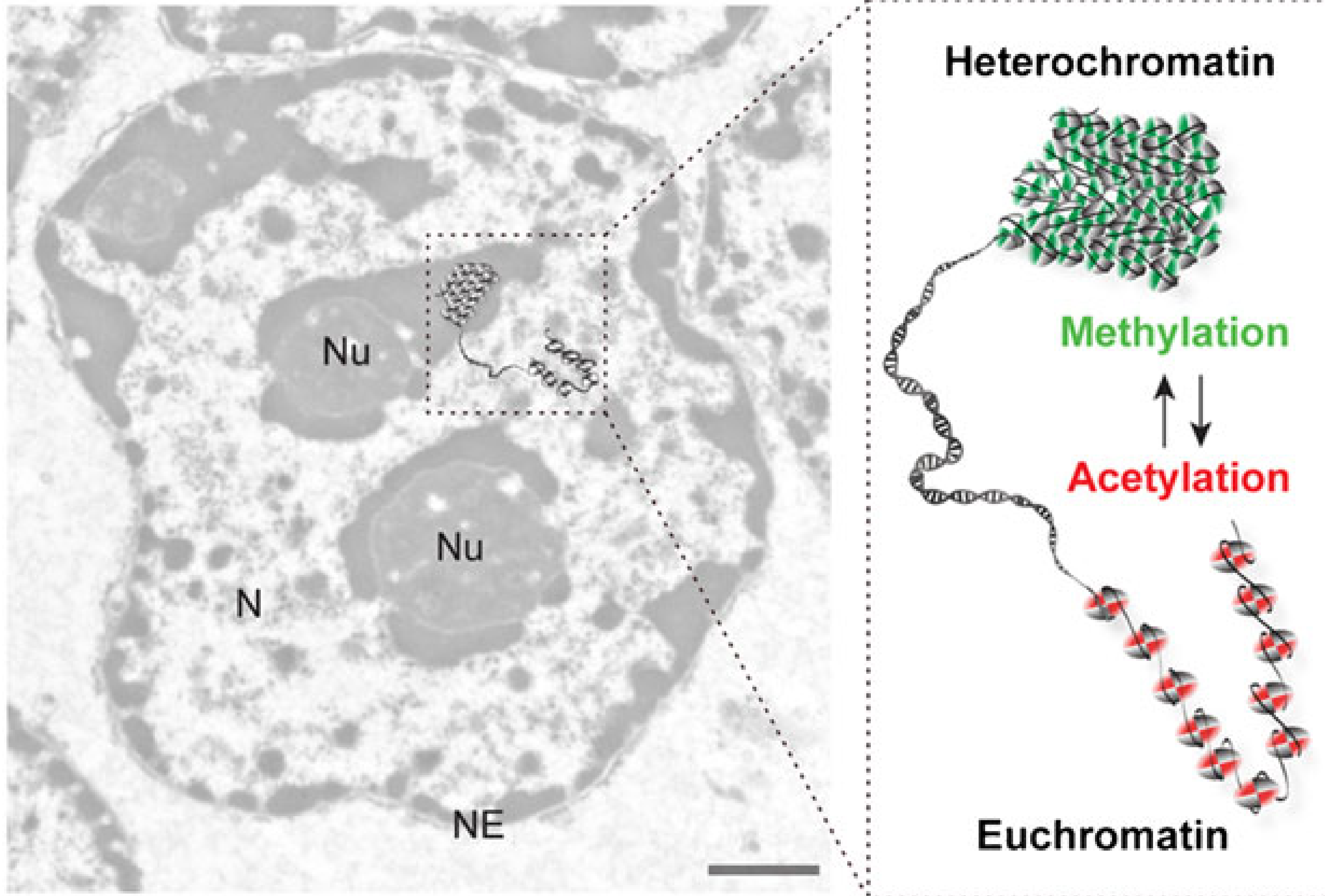
Level I: Radial genome organization

Takizawa, T., Meaburn, K. J. & Misteli, T. The meaning of gene positioning. Cell 135, 9–13 (2008).

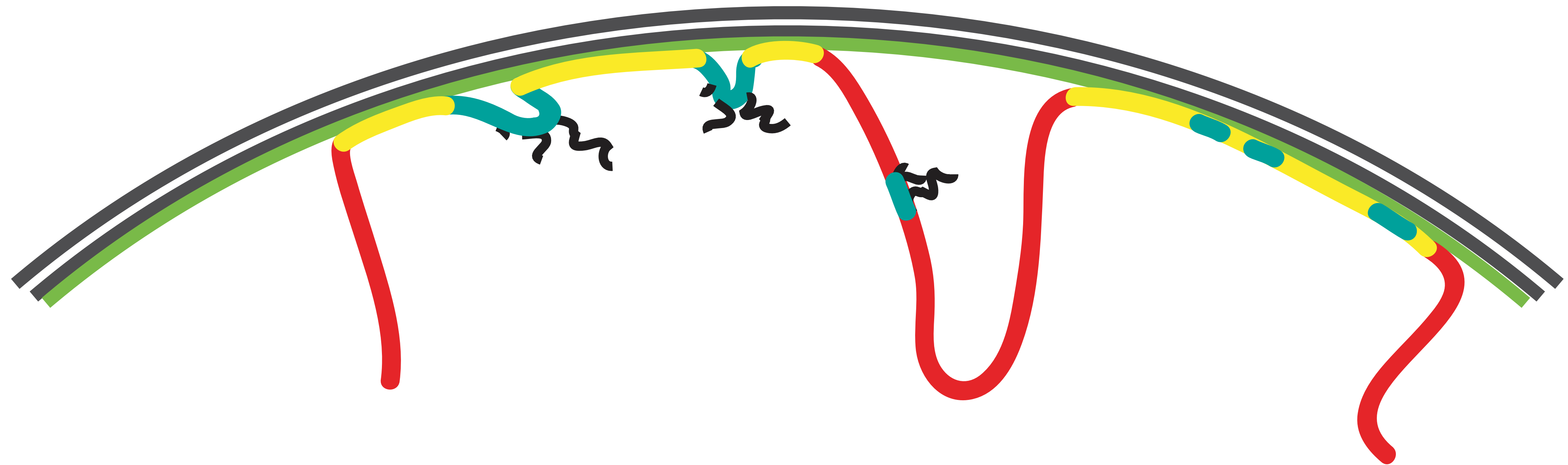


Level II: Euchromatin vs heterochromatin

Electron microscopy



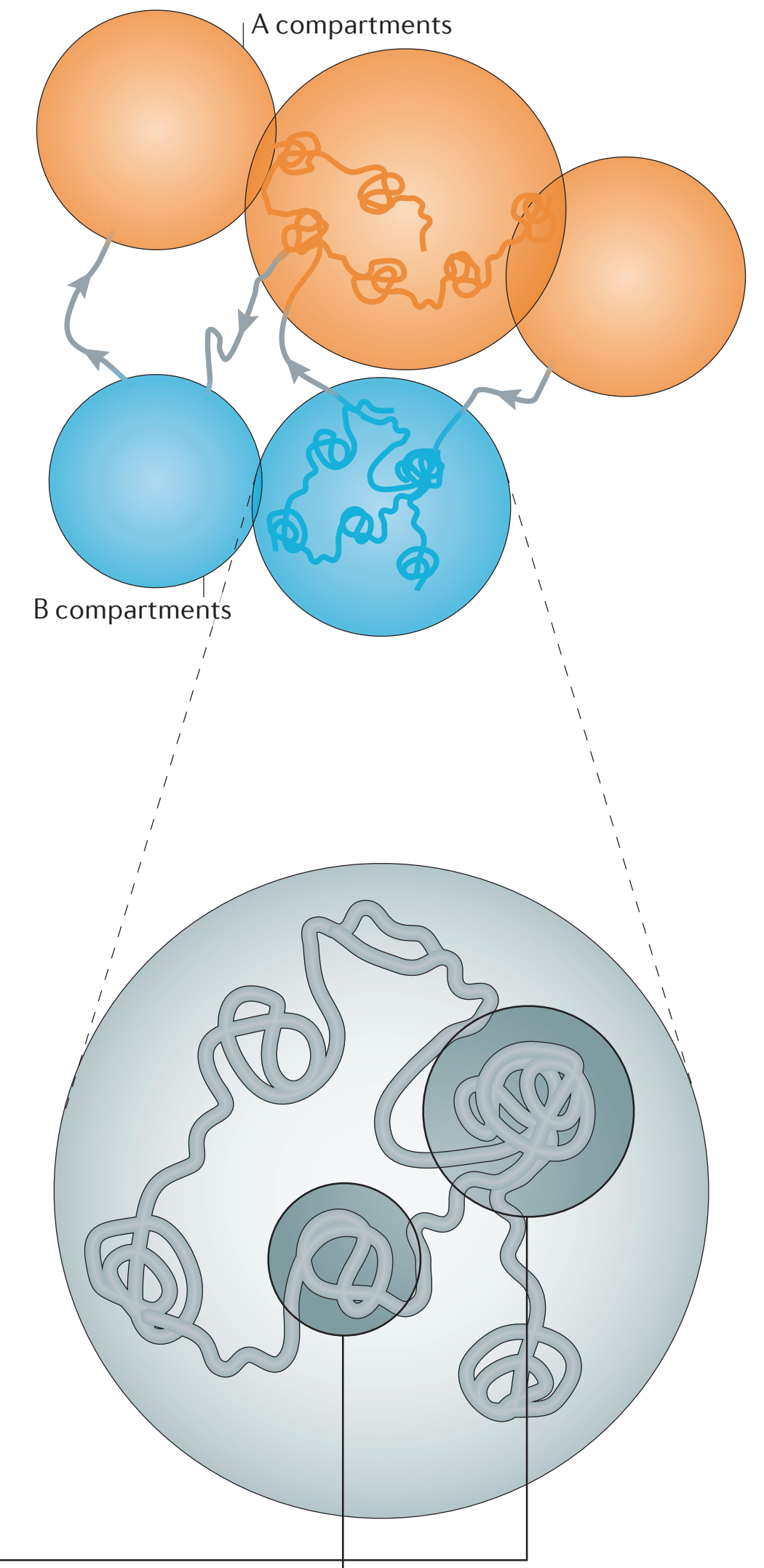
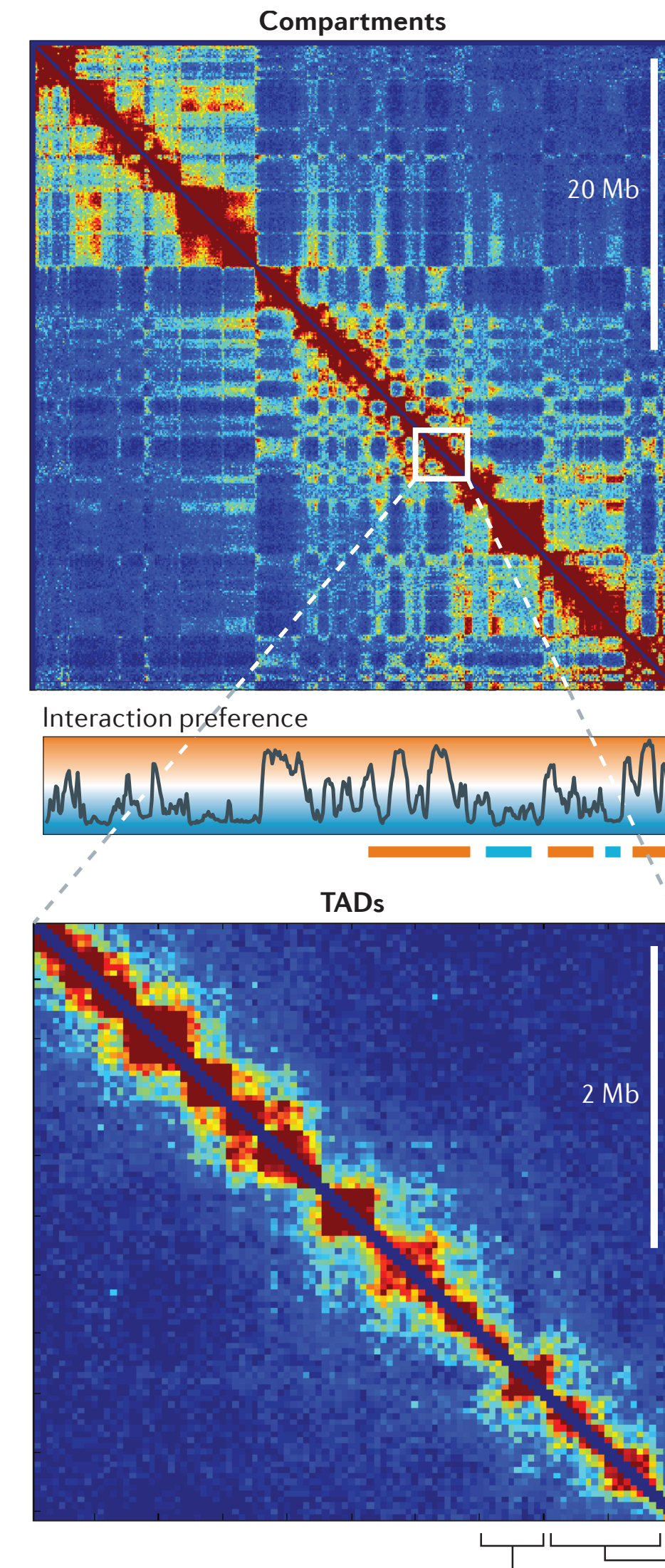
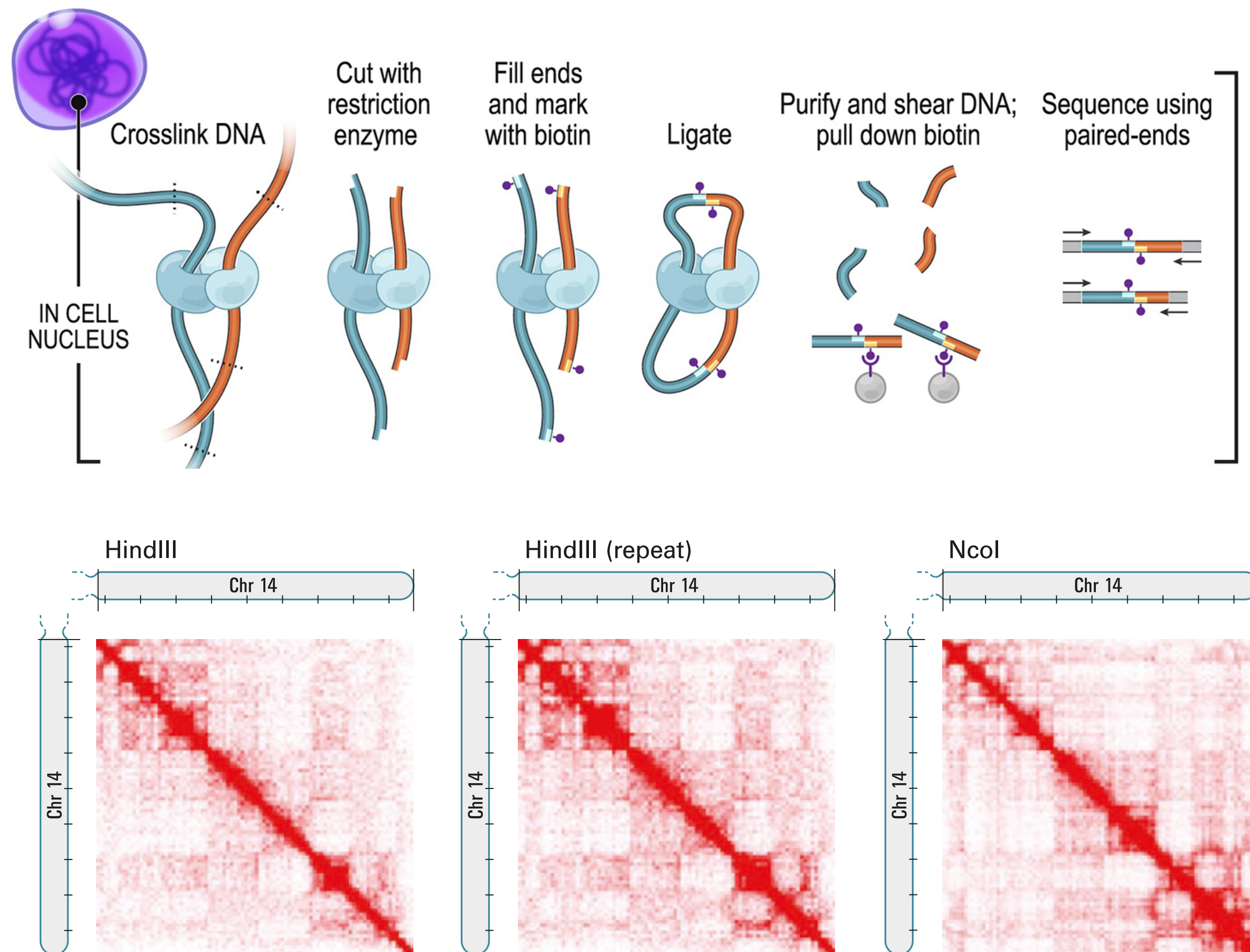
Level III: Lamina-genome interactions



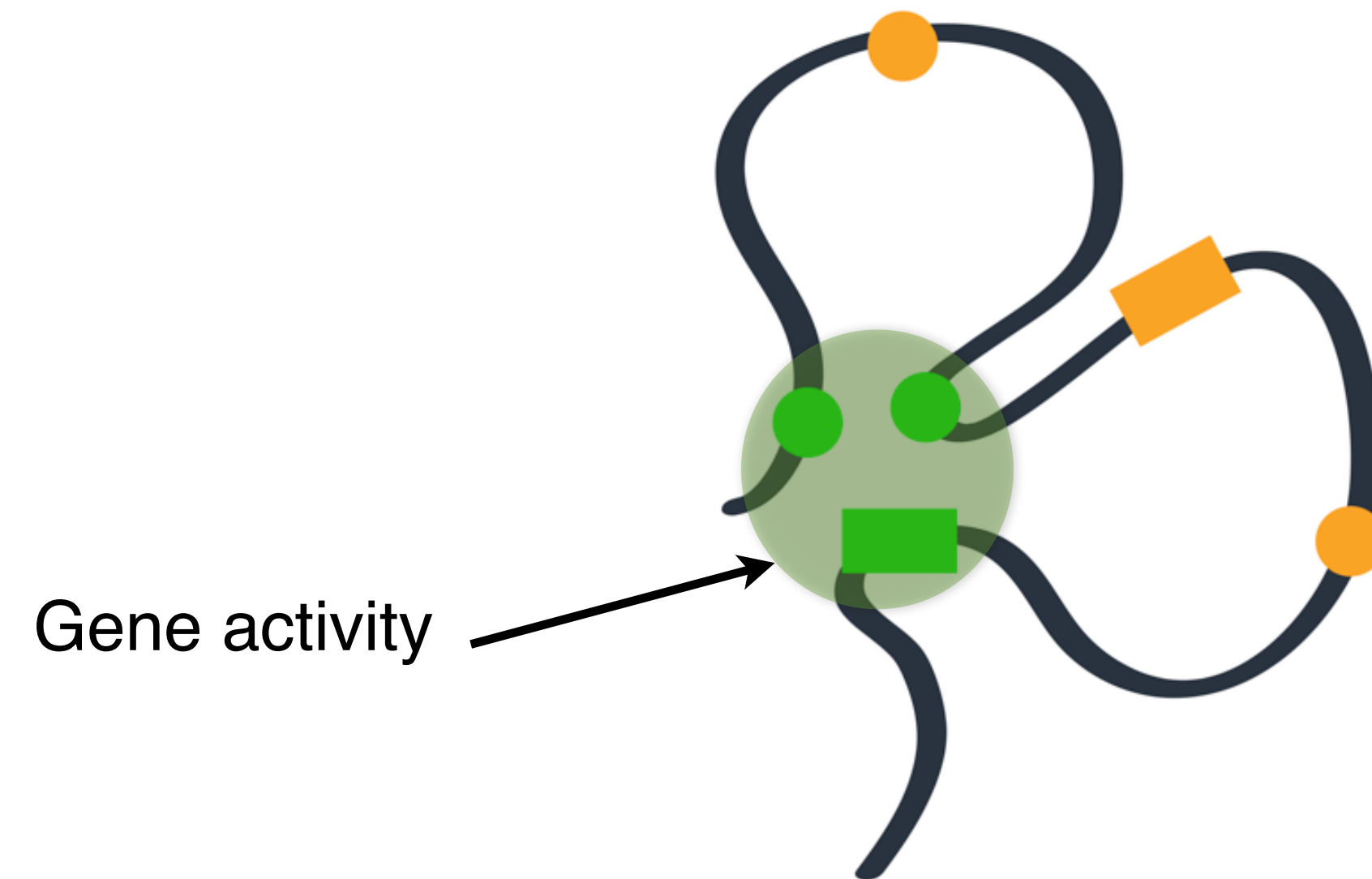
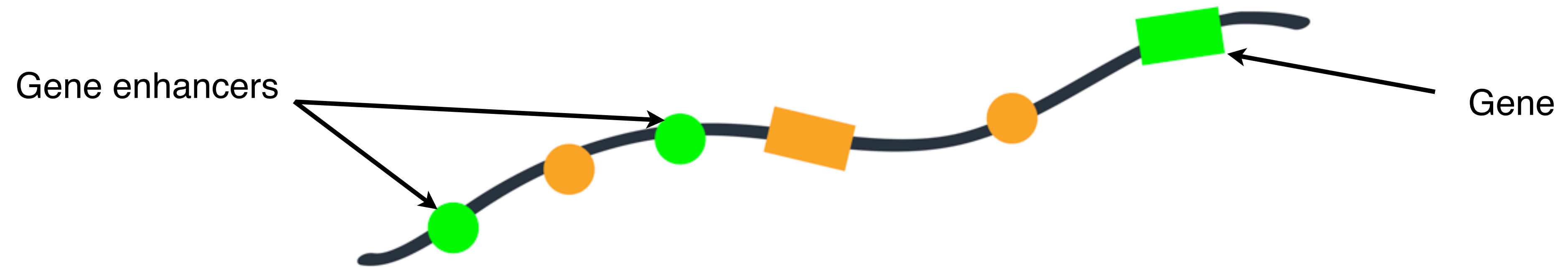
- nuclear membrane
- nuclear lamina
- internal chromatin (mostly active)
- lamina-associated domains (repressed)
- Genes
- mRNA

Level IV: Higher-order organization

Dekker, J., Marti-Renom, M. A. & Mirny, L. A. Nat Rev Genet 14, 390–403 (2013).



Level V: Chromatin loops

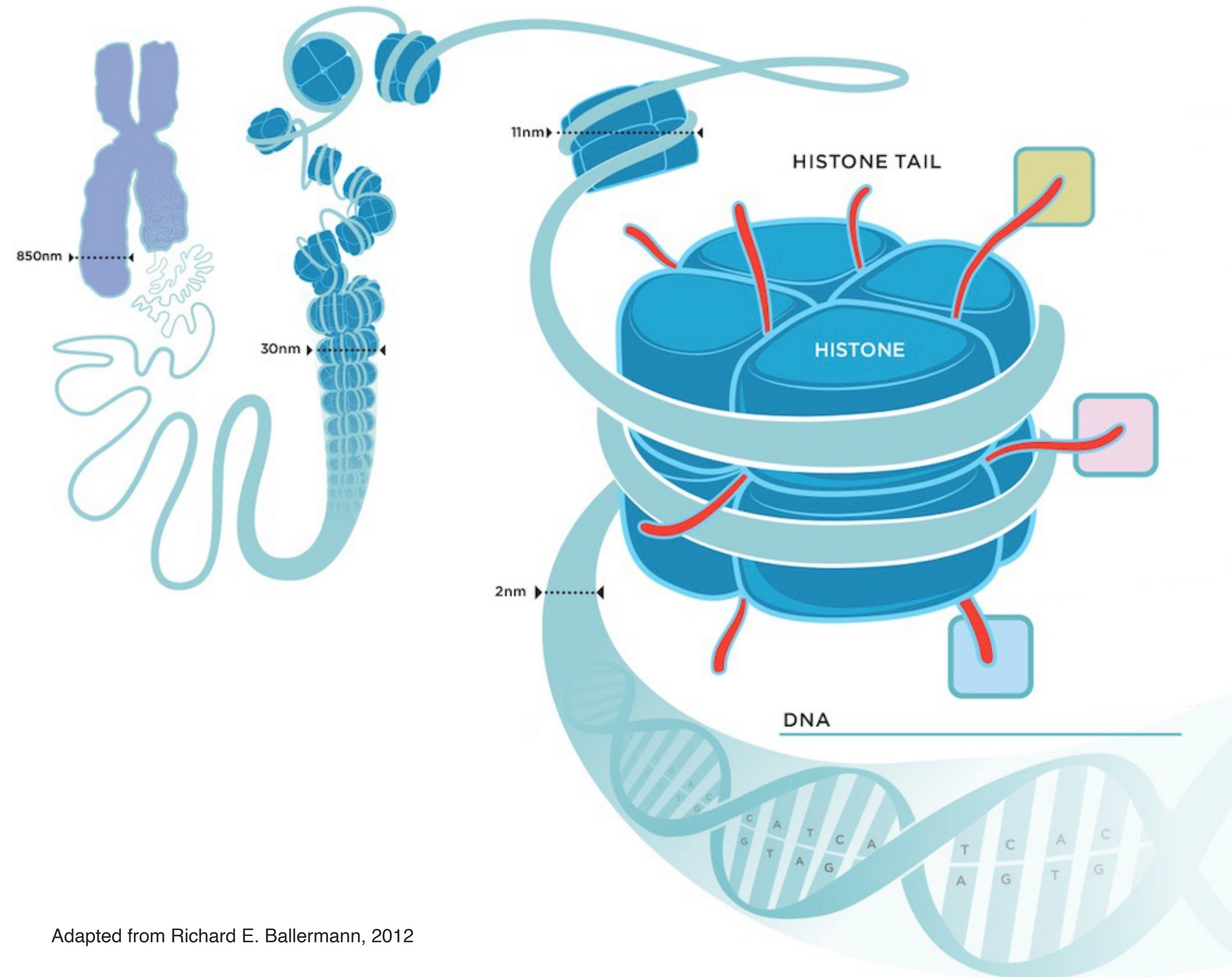


Level VI: Nucleosome

Chromosome

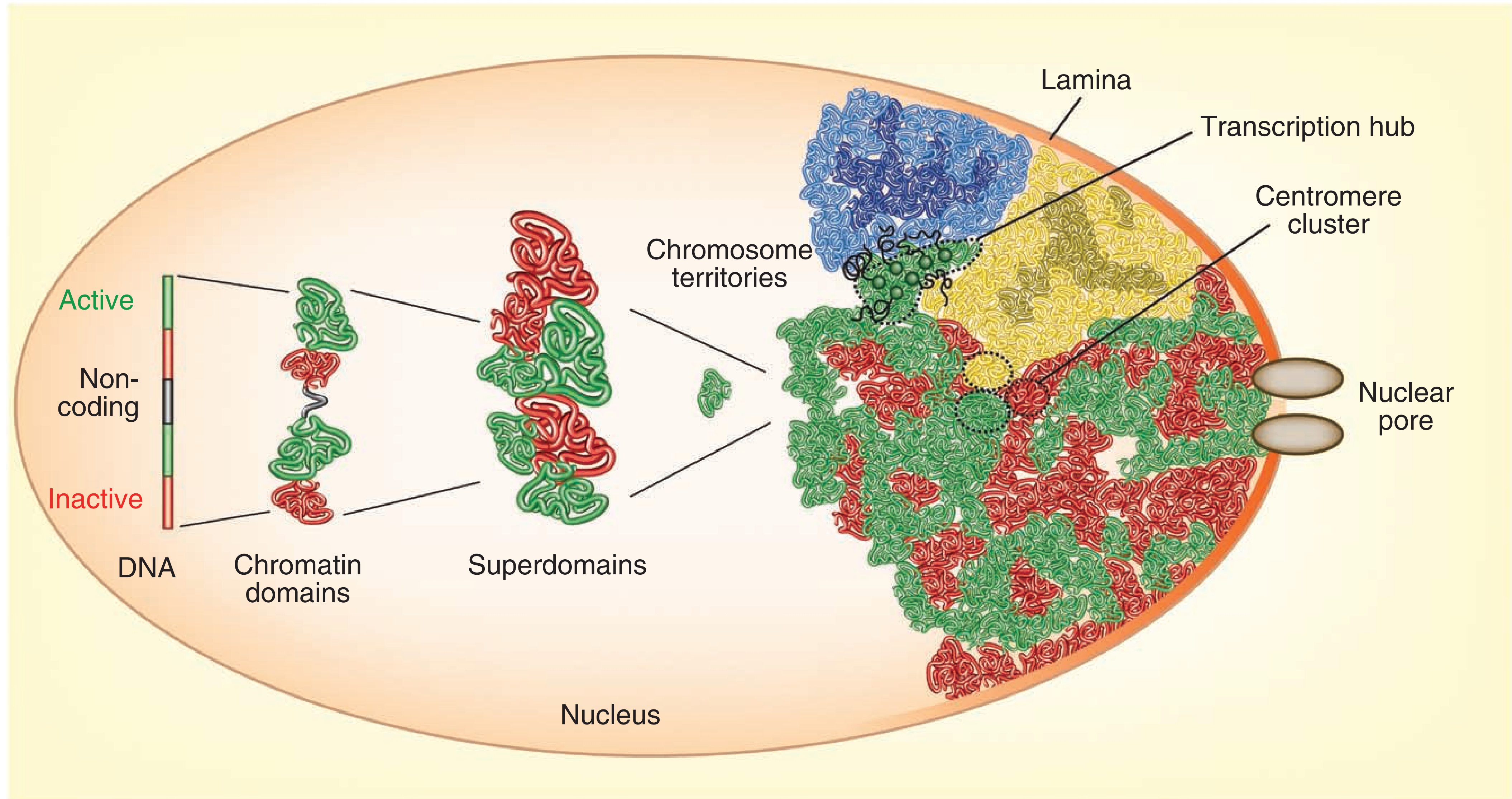
Chromatin fibre

Nucleosome

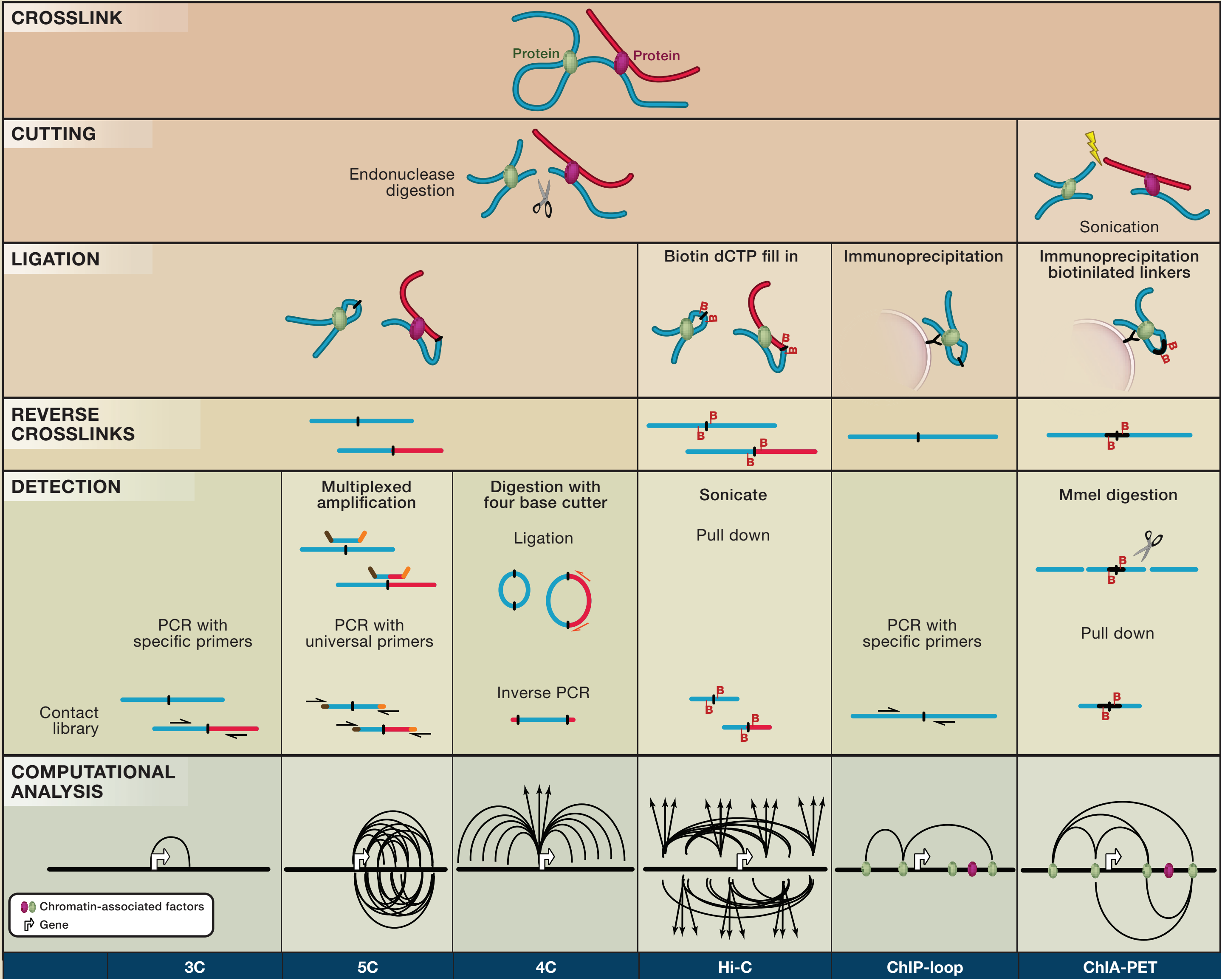


Complex genome organization

Cavalli, G. & Misteli, T. Functional implications of genome topology. Nat Struct Mol Biol 20, 290–299 (2013).



Chromosome Conformation Capture



ARTICLE

doi:10.1038/nature12593

Single-cell Hi-C reveals cell-to-cell variability in chromosome structure

Takashi Nagano^{1*}, Yaniv Lubling^{2*}, Tim J. Stevens^{3*}, Stefan Schoenfelder¹, Eitan Yaffe², Wendy Dean⁴, Ernest D. Laue³, Amos Tanay² & Peter Fraser²

LETTER

doi:10.1038/nature20158

Capturing pairwise and multi-way chromosomal conformations using chromosomal walks

Pedro Olivares-Chauvet¹, Zohar Mukamel¹, Aviezer Lifshitz¹, Omer Schwartzman¹, Noa Oded Elkayam¹, Yaniv Lubling¹, Gintaras Deikus², Robert P. Sebra² & Amos Tanay¹

ARTICLES

https://doi.org/10.1038/s41588-018-0161-5

Enhancer hubs and loop collisions identified from single-allele topologies

Amin Allahyar^{1,2,7}, Carlo Vermeulen^{3,7}, Britta A. M. Bouwman³, Peter H. L. Krijger³, Marjon J. A. M. Versteegen³, Geert Geeven³, Melissa van Kranenburg³, Mark Pieterse³, Roy Straver³, Judith H. I. Haarhuis⁴, Kees Jalink⁵, Hans Teunissen⁶, Ivo J. Renkens¹, Wigard P. Kloosterman¹, Benjamin D. Rowland⁴, Elzo de Wit⁴, Jeroen de Ridder^{3*} and Wouter de Laat^{3*}

Cell

Higher-Order Inter-chromosomal Hubs Shape 3D Genome Organization in the Nucleus

Graphical Abstract

Authors: Sofia A. Quinodoz, Noah Ollikainen, Barbara Tabak, ..., Patrick McDonel, Manuel Garber, Mitchell Guttman

Correspondence: mguttman@caltech.edu



ARTICLE

DOI: 10.1038/s41467-018-06961-0 OPEN

Chromatin conformation analysis of primary patient tissue using a low input Hi-C method

Noelia Díaz¹, Kai Kruse¹, Tabea Erdmann², Annette M. Staiger^{3,4,5}, German Ott³, Georg Lenz² & Juan M. Vaquerizas¹

Liquid chromatin Hi-C characterizes compartment-dependent chromatin interaction dynamics

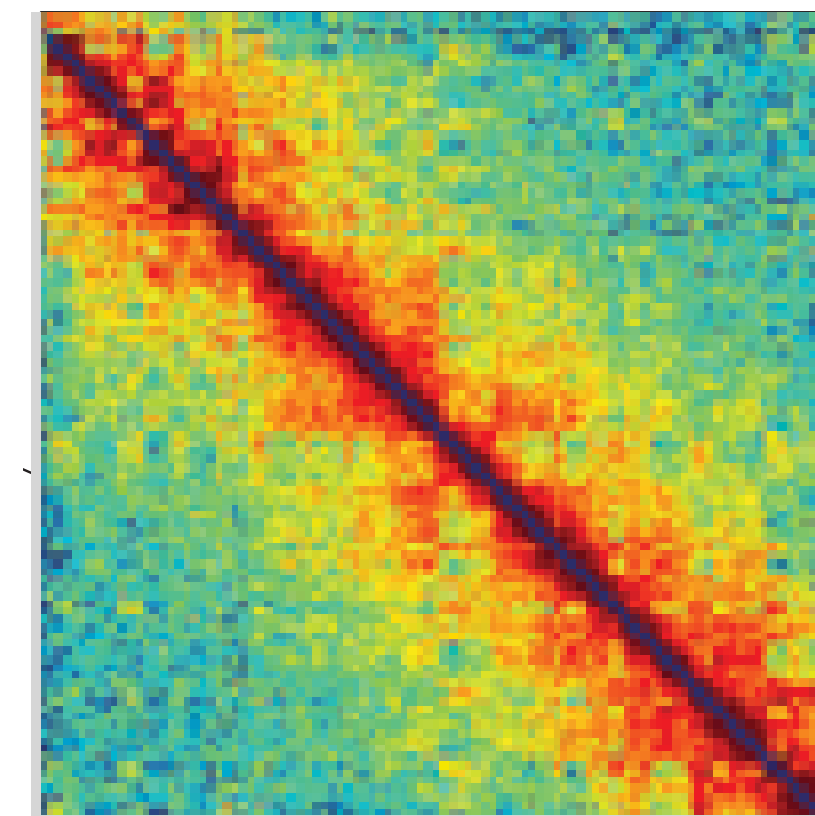
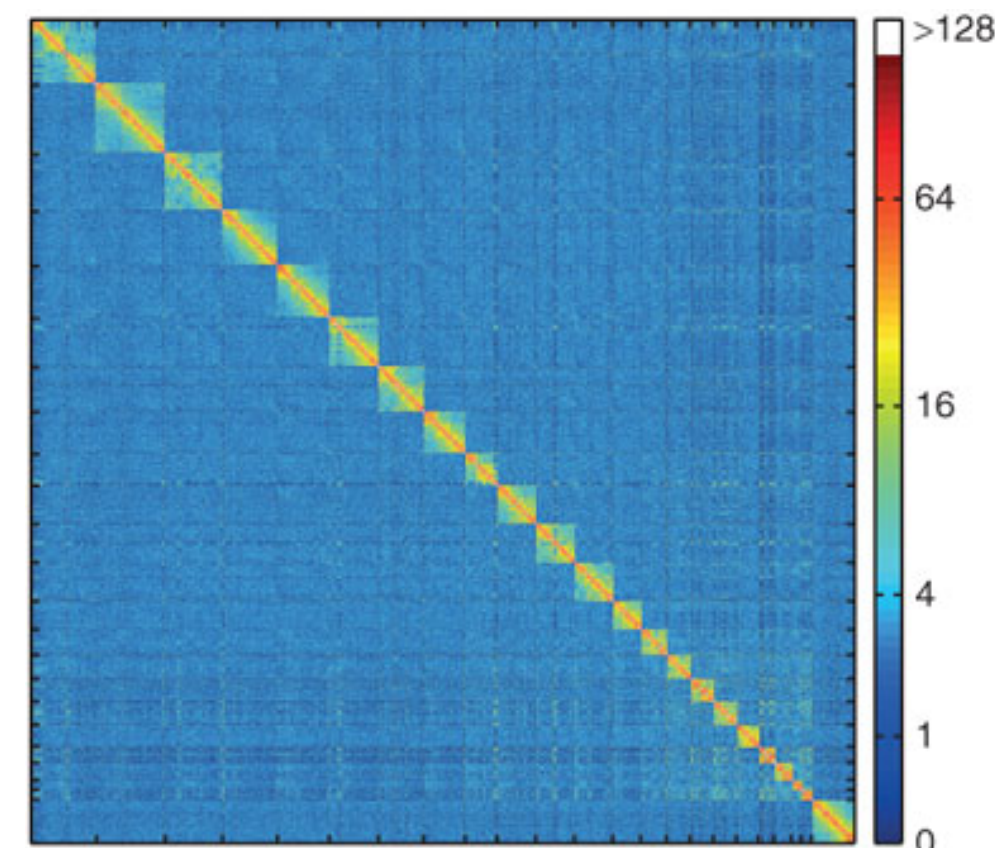
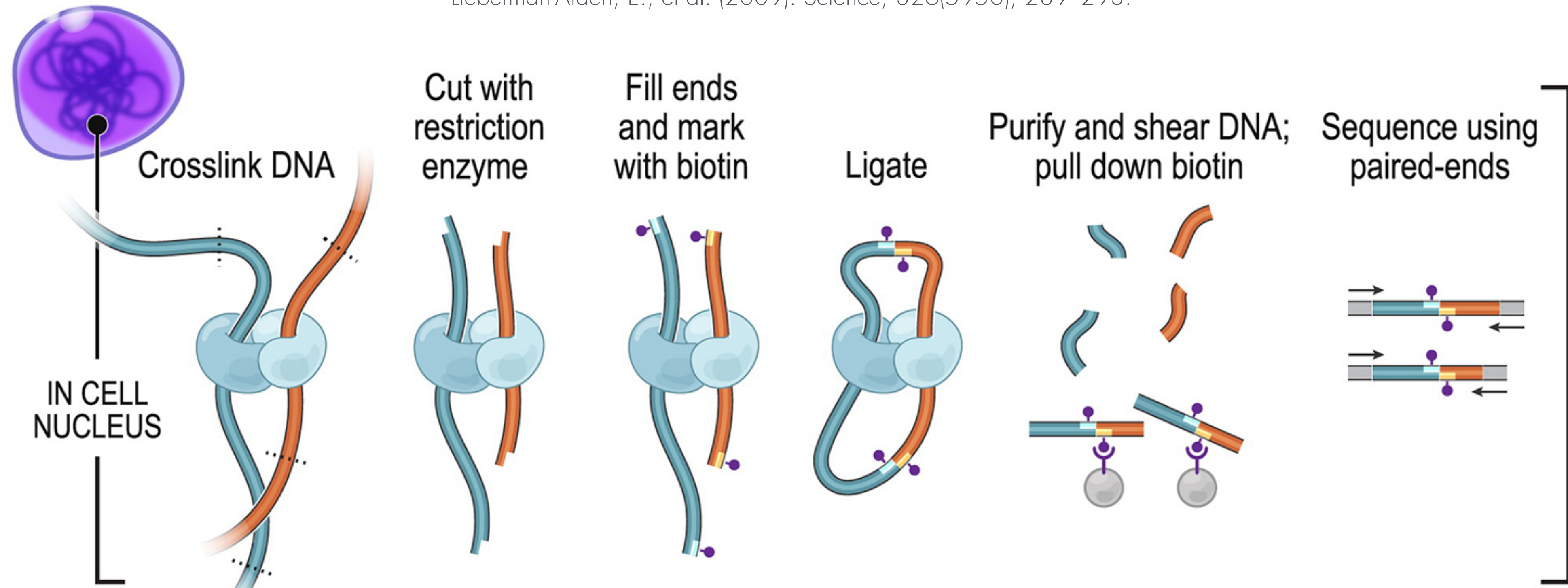
Houda Belaghzal, Tyler Borrmann, Andrew D. Stephens, Denis L. Lafontaine, Sergey V. Venev, Zhiping Weng, John F. Marko & Job Dekker

Nature Genetics 53, 367–378 (2021) | Cite this article
7436 Accesses | 8 Citations | 20 Altmetric | Metrics

Chromosome Conformation Capture

Dekker, J., Rippe, K., Dekker, M., & Kleckner, N. (2002). *Science*, 295(5558), 1306–1311.

Lieberman-Aiden, E., et al. (2009). *Science*, 326(5950), 289–293.



Hi-C 3.0

Akgol Oksuz, et al. Nature Methods 2021

ANALYSIS

<https://doi.org/10.1038/s41592-021-01248-7>

nature **methods**



OPEN

Systematic evaluation of chromosome conformation capture assays

Betul Akgol Oksuz^{1,10}, Liyan Yang^{1,10}, Sameer Abraham², Sergey V. Venev¹, Nils Krietenstein³, Krishna Mohan Parsi^{4,5}, Hakan Ozadam^{1,6}, Marlies E. Oomen², Ankita Nand², Hui Mao^{4,5}, Ryan M. J. Genga^{4,5}, Rene Maehr^{4,5}, Oliver J. Rando², Leonid A. Mirny^{2,7,8}, Johan H. Gibcus²✉ and Job Dekker²✉✉

Chromosome conformation capture (3C) assays are used to map chromatin interactions genome-wide. Chromatin interaction maps provide insights into the spatial organization of chromosomes and the mechanisms by which they fold. Hi-C and Micro-C are widely used 3C protocols that differ in key experimental parameters including cross-linking chemistry and chromatin fragmentation strategy. To understand how the choice of experimental protocol determines the ability to detect and quantify aspects of chromosome folding we have performed a systematic evaluation of 3C experimental parameters. We identified optimal protocol variants for either loop or compartment detection, optimizing fragment size and cross-linking chemistry. We used this knowledge to develop a greatly improved Hi-C protocol (Hi-C 3.0) that can detect both loops and compartments relatively effectively. In addition to providing benchmarked protocols, this work produced ultra-deep chromatin interaction maps using Micro-C, conventional Hi-C and Hi-C 3.0 for key cell lines used by the 4D Nucleome project.

Chromosome conformation capture (3C)-based assays¹ have become widely used to generate genome-wide chromatin interaction maps². Analysis of chromatin interaction maps has led to detection of several features of the folded genome. Such features include precise looping interactions (at the 0.1–1 Mb scale) between pairs of specific sites that appear as local dots in interaction maps. Many of such dots represent loops formed by cohesin-mediated loop extrusion that is stalled at convergent CCCTC-binding factor (CTCF) sites^{3–5}. Loop extrusion also produces other features in interaction maps such as stripe-like patterns anchored at specific sites that block loop extrusion. The effective depletion of interactions across such blocking sites leads to domain boundaries (insulation). At the megabase scale, interaction maps of many organisms including mammals display checkerboard patterns that represent the spatial compartmentalization of two main types of chromatin: active and open A-type chromatin domains, and inactive and more closed B-type chromatin domains⁶.

The Hi-C protocol has evolved over the years. While initial protocols used restriction enzymes such as HindIII that produces relatively large fragments of several kilobases⁶, over the last 5 years Hi-C using DpnII or MboI digestion has become the protocol of choice for mapping chromatin interactions at kilobase resolution⁷. More recently, Micro-C, which uses MNase instead of restriction enzymes as well as a different cross-linking protocol, was shown to allow generation of nucleosome-level interaction maps^{7–9}. It is critical to ascertain how key parameters of these 3C-based methods, including cross-linking and chromatin fragmentation, quantitatively

influence the detection of chromatin interaction frequencies and the detection of different chromosome folding features that range from local looping between small intra-chromosomal (cis) elements to global compartmentalization of megabase-sized domains. Here, we systematically assessed how different cross-linking and fragmentation methods yield quantitatively different chromatin interaction maps.

Results

We explored how two key parameters of 3C-based protocols, cross-linking and chromatin fragmentation, determine the ability to quantitatively detect chromatin compartment domains and loops. We selected three cross-linkers widely used for chromatin: 1% formaldehyde (FA), conventional for most 3C-based protocols; 1% FA followed by incubation with 3 mM disuccinimidyl glutarate (the FA + DSG protocol); and 1% FA followed by incubation with 3 mM ethylene glycol bis(succinimidylsuccinate) (the FA + EGS protocol) (Fig. 1a). We selected four different nucleases for chromatin fragmentation: MNase, DdeI, DpnII and HindIII, which fragment chromatin in sizes ranging from single nucleosomes to multiple kilobases. Combined, the three cross-linking and four fragmentation strategies yield a matrix of 12 distinct protocols (Fig. 1b). To determine how performance of these protocols varies for different states of chromatin we applied this matrix of protocols to multiple cell types and cell cycle stages. We analyzed four different cell types: pluripotent H1 human embryonic stem cells (H1-hESCs), differentiated endoderm (DE) cells derived from H1-hESCs, fully

¹Program in Systems Biology, Department of Biochemistry and Molecular Pharmacology, University of Massachusetts Medical School, Worcester, MA, USA. ²Department of Physics, Massachusetts Institute of Technology, Cambridge, MA, USA. ³Department of Biochemistry and Molecular Pharmacology, University of Massachusetts Medical School, Worcester, MA, USA. ⁴Program in Molecular Medicine, University of Massachusetts Medical School, Worcester, MA, USA. ⁵Program in Molecular Medicine, Diabetes Center of Excellence, University of Massachusetts Medical School, Worcester, MA, USA. ⁶Department of Molecular Biosciences, University of Texas at Austin, Austin, TX, USA. ⁷Institute for Medical Engineering and Science, Massachusetts Institute of Technology, Cambridge, MA, USA. ⁸Graduate Program in Biophysics, Harvard University, Cambridge, MA, USA. ⁹Howard Hughes Medical Institute, Chevy Chase, MD, USA. ¹⁰These authors contributed equally: Betul Akgol Oksuz, Liyan Yang. ✉e-mail: Johan.Gibcus@umassmed.edu; Job.Dekker@umassmed.edu

NATURE METHODS

ANALYSIS

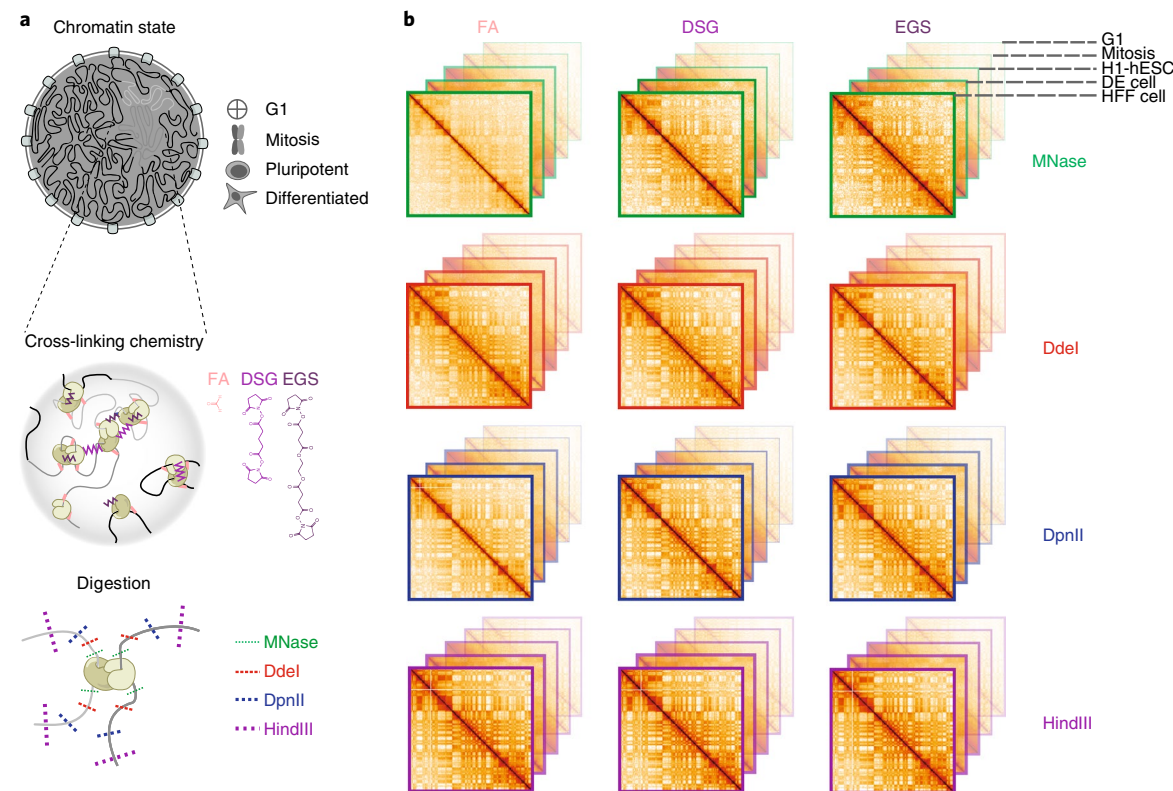


Fig. 1 | Outline of the experimental design. a, Experimental design for conformation capture for various cells, cross-linkers and enzymes. **b**, Representation of interaction maps from experiments in **a**.

differentiated human foreskin fibroblast (HFF) cells (12 protocols for each), and HeLa-S3 cells (9 protocols). We analyzed two cell cycle stages: G1 and mitosis, in HeLa-S3 cells (9 protocols for each; Fig. 1). Each interaction library was then sequenced on a single lane of a HiSeq4000 instrument, producing ~150–200 million uniquely mapping read pairs (Supplementary Table 1). We used the Distiller pipeline to align the sequencing reads, and pairtools and cooler¹⁰ packages to process mapped reads and create multi-resolution contact maps (Methods). Given that the density of restriction sites for DdeI, DpnII and HindIII fluctuates along chromosomes, we observed different read coverages in raw interaction maps obtained from datasets using these enzymes (Extended Data Fig. 1h). These differences were removed after matrix balancing¹¹.

We first assessed the size range of the chromatin fragments produced after digestion by the 12 protocols for HFF cells (Methods). Digestion with HindIII resulted in 5–20-kb DNA fragments; DpnII and DdeI produced fragments of 0.5–5 kb; and MNase protocols included a size selection step to ensure that the ligation product involved two mononucleosome-sized fragments (~150 bp) (Extended Data Fig. 1). Different cross-linkers did not affect the size ranges produced by the different nucleases, although DSG cross-linking lowered digestion efficiency slightly (Extended Data Fig. 1b).

All 3C-based protocols can differentiate between cell states. We first assessed the similarity between the 63 datasets by global and pairwise correlations using HiCRep and hierarchical clustering (Extended Data Fig. 1c)^{12,13}. We found that the datasets are highly correlated and cluster primarily by cell type and state and then by cell type similarity, for example H1-hESCs and H1-hESC-derived DE cells cluster together; and the most distinct cluster is formed by mitotic HeLa cells. MNase protocols show slightly lower correlations with Hi-C experiments.

Extra cross-linking yields more intra-chromosomal contacts.

Given that chromosomes occupy individual territories, intra-chromosomal (cis) interactions are more frequent than inter-chromosomal (trans) interactions¹⁴. The cis:trans ratio is commonly used as an indicator of Hi-C library quality given that inter-chromosomal interactions are a mixture of true chromatin interactions and interactions that are the result of random ligations^{14,15}. For all enzymes and cell types, we found that the addition of DSG or EGS to FA cross-linking decreased the percentage of trans interactions (Fig. 2a for HFF and Extended Data Fig. 2a for H1-hESC, DE, HeLa-S3).

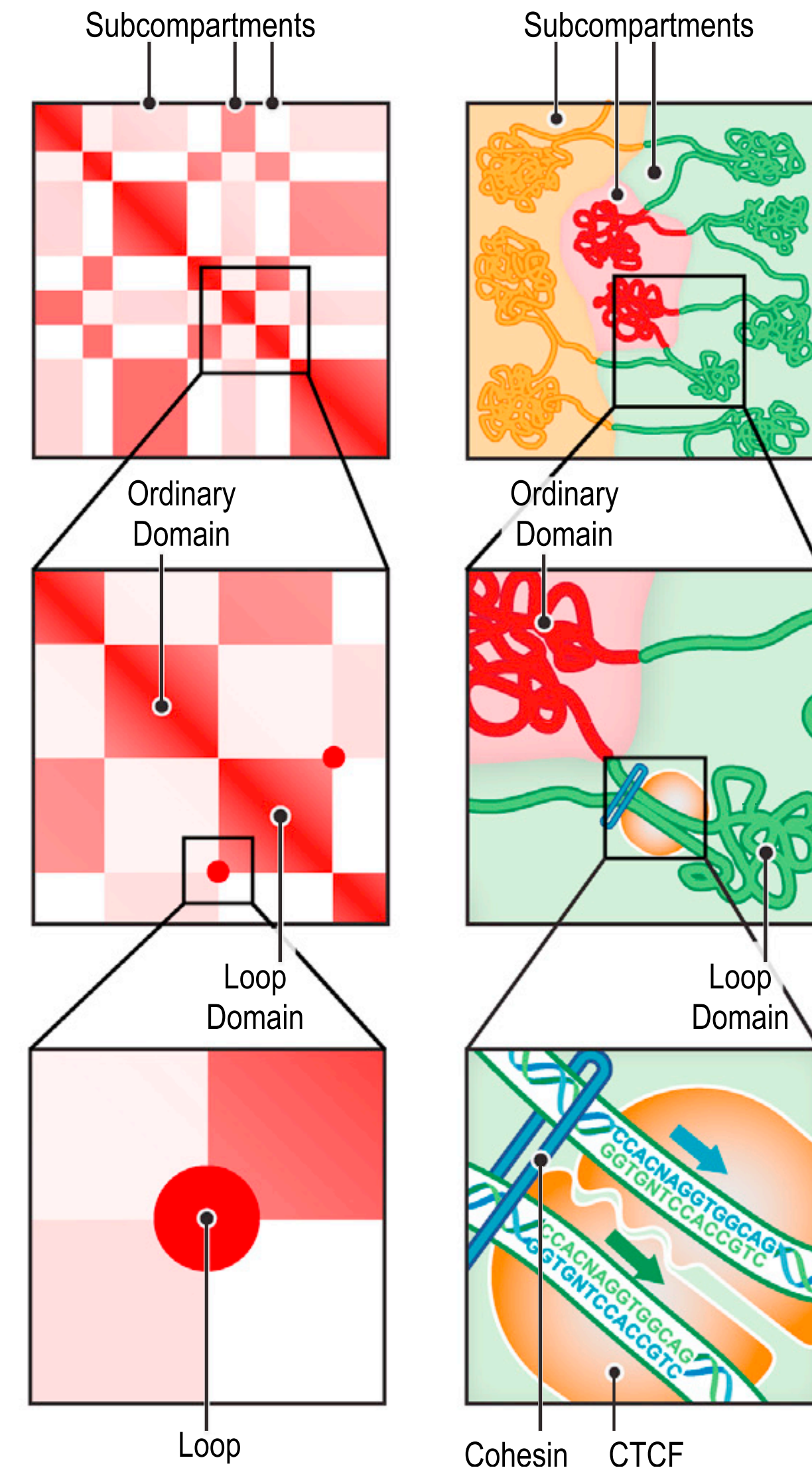
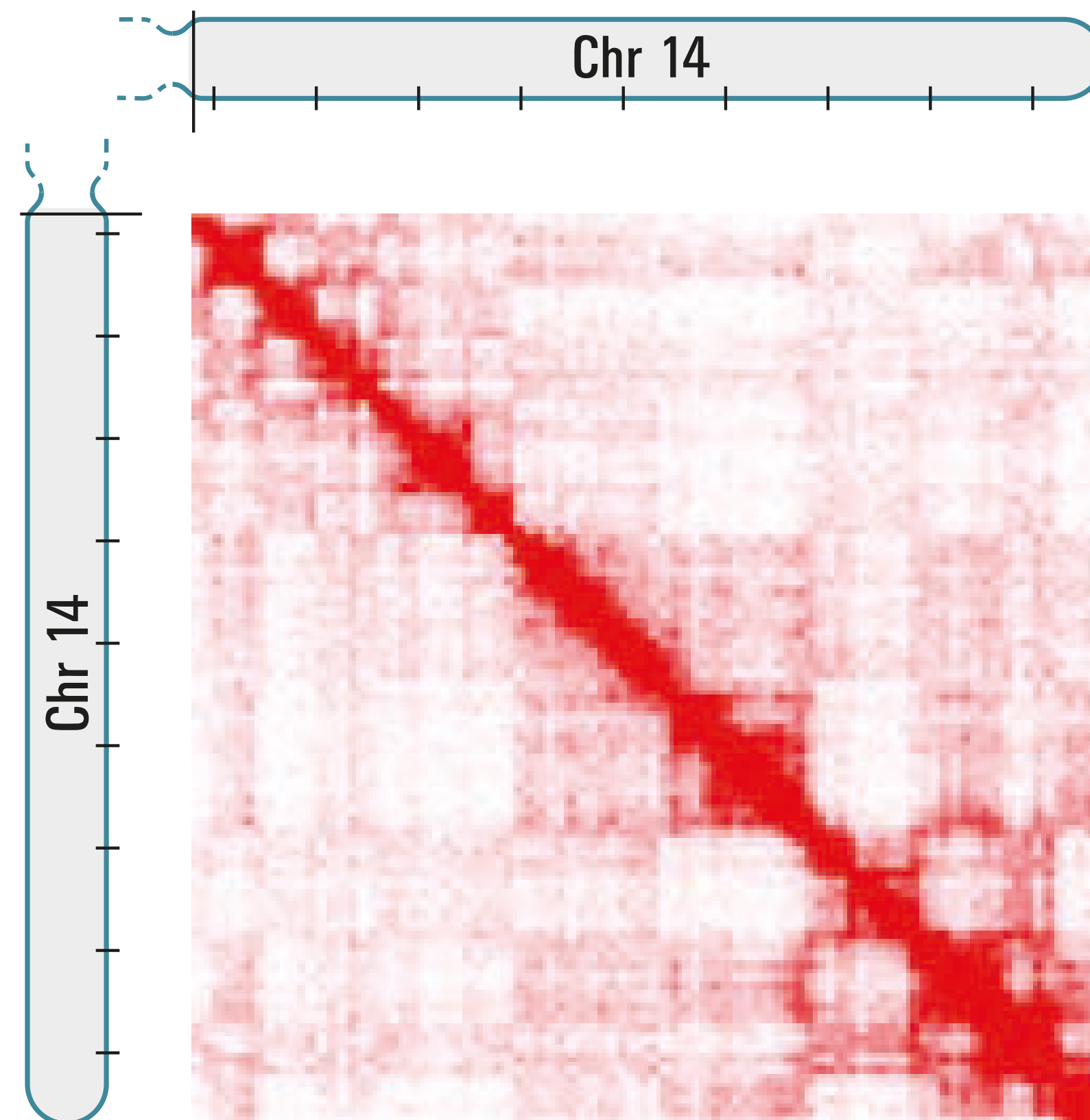
Regarding intra-chromosomal interactions, we noticed two distinct patterns. First, digestion into smaller fragments increased short-range interactions. MNase digestion generated more interactions between loci separated by less than 10 kb, whereas digestion with either DdeI, DpnII or HindIII resulted in a relatively larger number of interactions between loci separated by more than 10 kb (Fig. 2a,b for HFF and Extended Data Fig. 2a,b for DE, H1-hESC, HeLa-S3). Second, *P(s)* plots showed that the addition of either DSG or EGS resulted in a steeper decay in interaction frequency as a function of genomic distance for all fragmentation protocols. Moreover, for a given chromatin fragmentation level, additional cross-linking with DSG or EGS reduced trans interactions, as shown for HFF cells and all other cell types and cell stages studied (Fig. 2c,d and Extended Data Fig. 2c). The addition of DSG or EGS could have reduced fragment mobility and the formation of spurious ligations, resulting in a steeper slope of the *P(s)*. We note a difference in slopes for data obtained with different cell types and cell cycle stages, which could reflect state-dependent differences in chromatin compaction.

Random ligation events between un-cross-linked, freely diffusing fragments lead to noise that is mostly seen in trans and long-range cis interactions. Experiments that use DpnII and

Hierarchical genome organisation

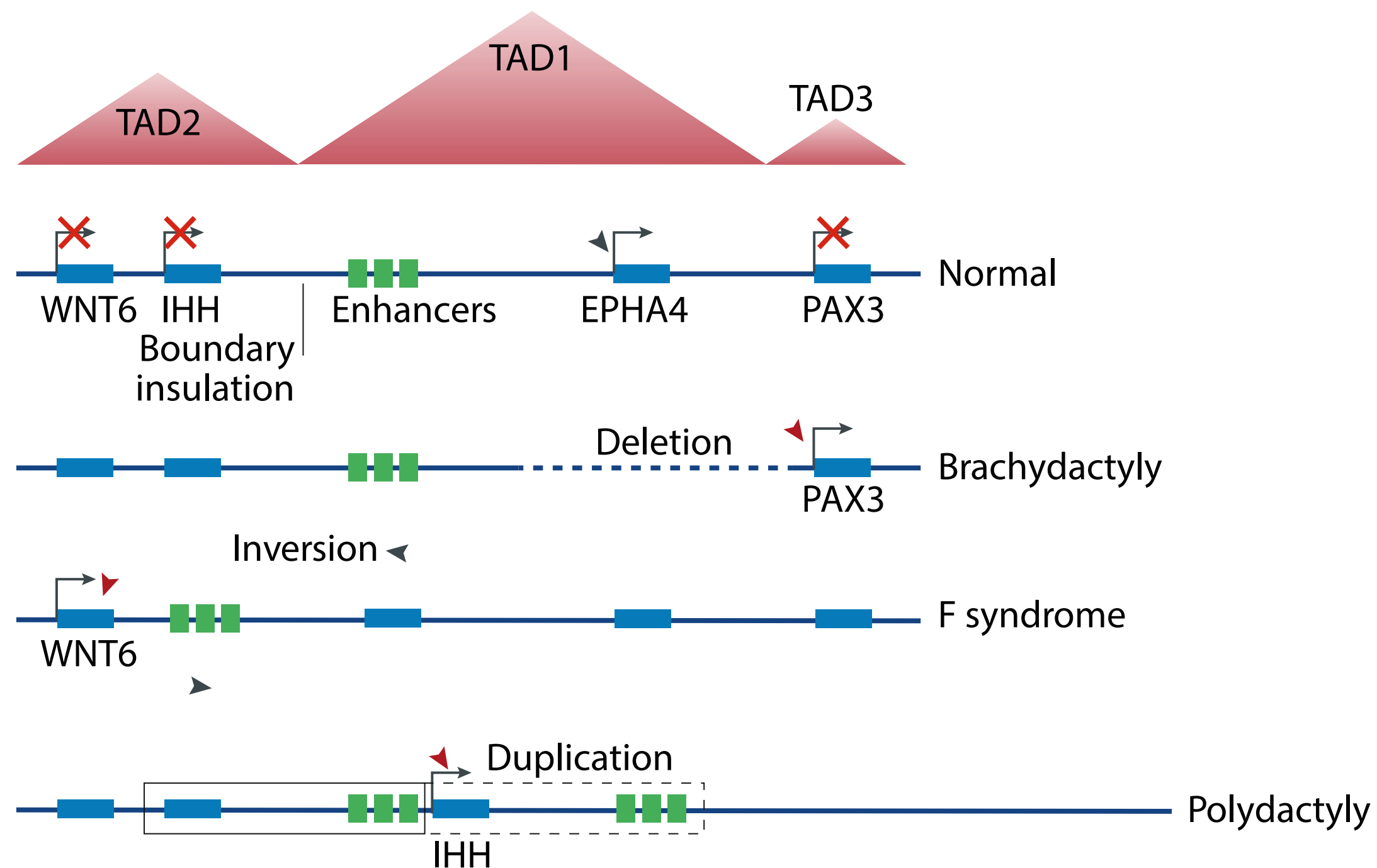
Lieberman-Aiden, E., et al. (2009). *Science*, 326(5950), 289–293.

Rao, S. S. P., et al. (2014). *Cell*, 1–29.

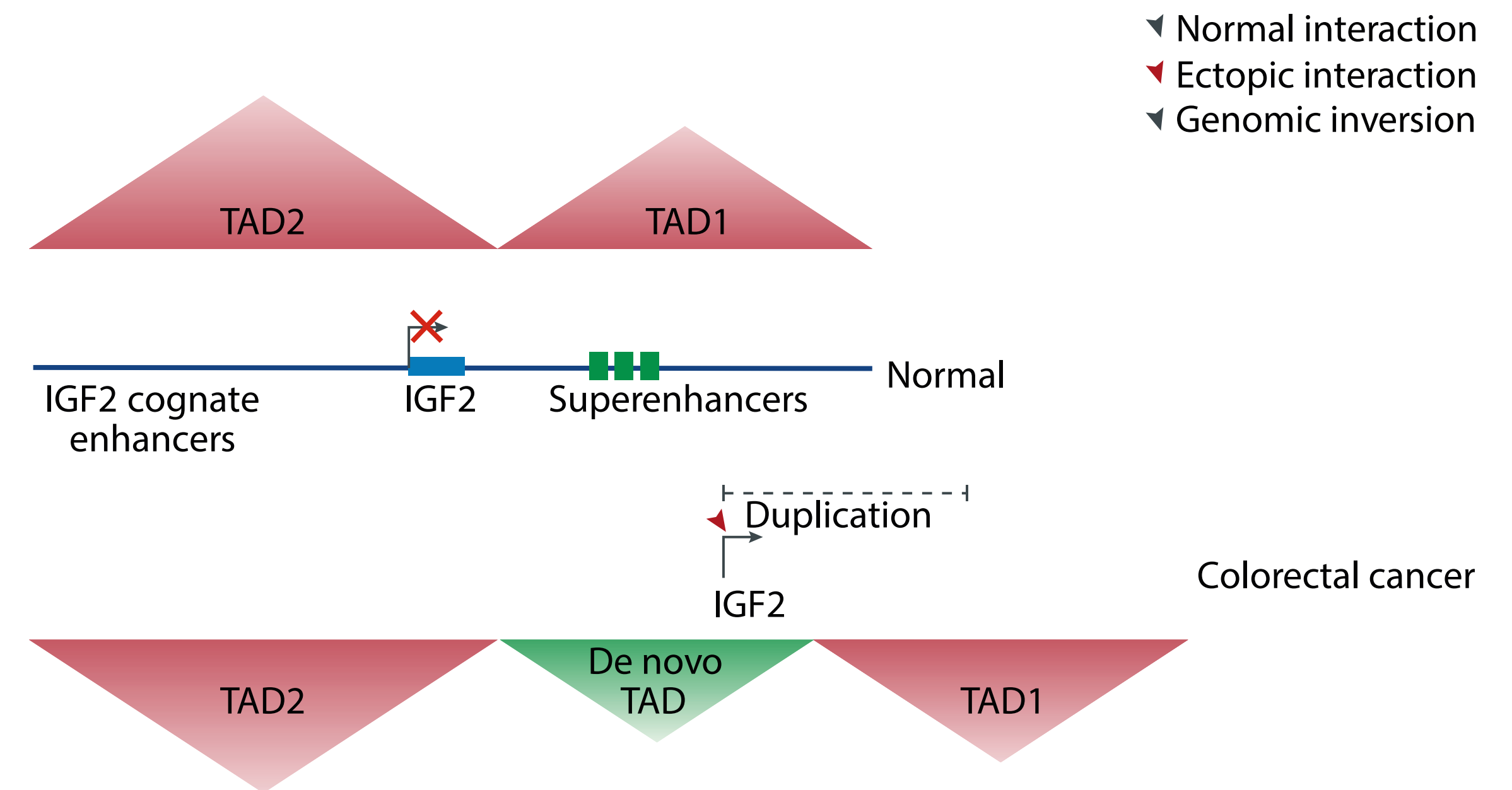


TADs are functional units

Figure adapted from Hui Zheng and Wei Xie. Nature Reviews Molecular Cell Biology (2019)



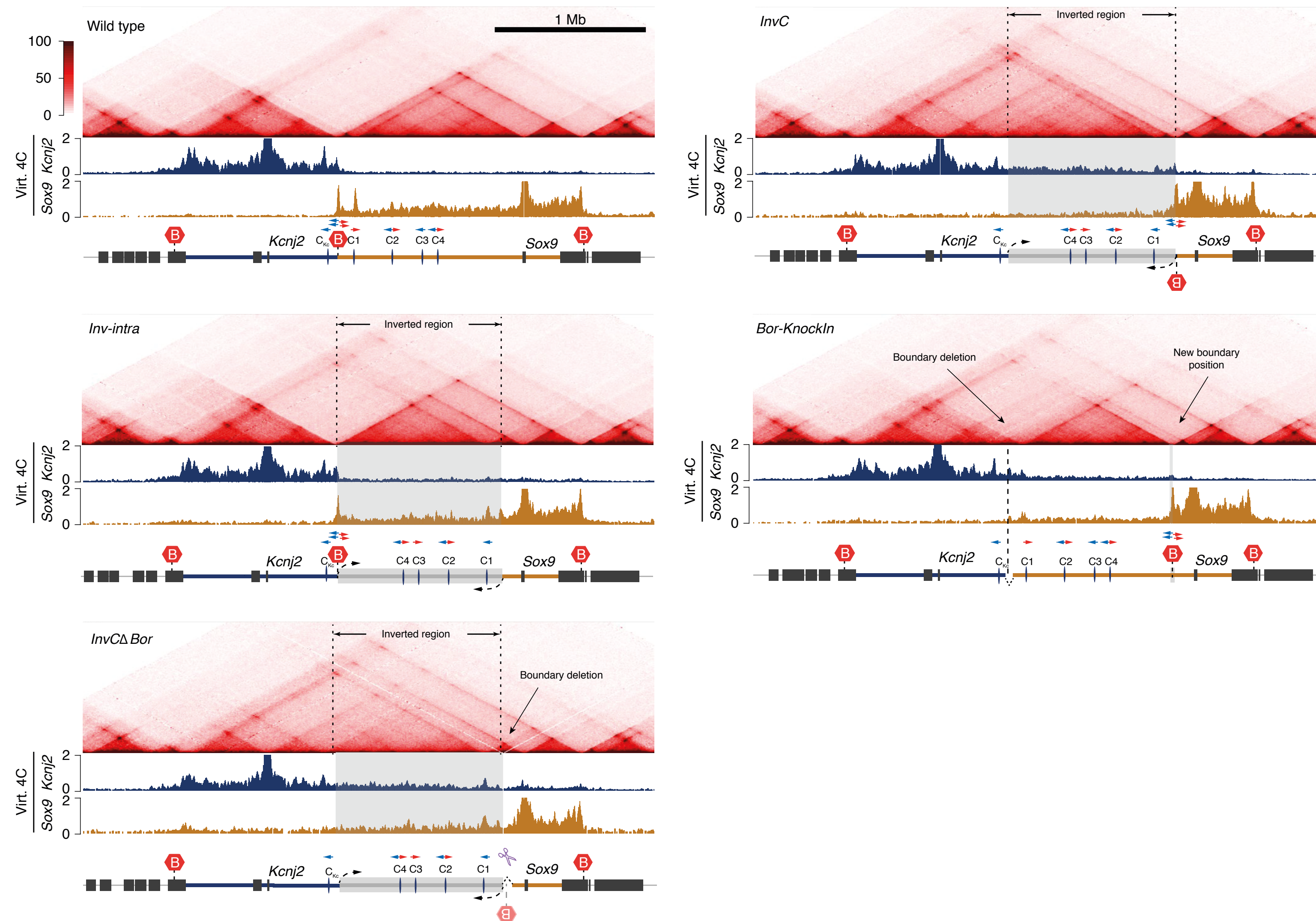
Lupianez, D. G. et al. Cell 161, 1012–1025 (2015)



Flavahan, W. A. et al. Nature 529, 110–114 (2016).

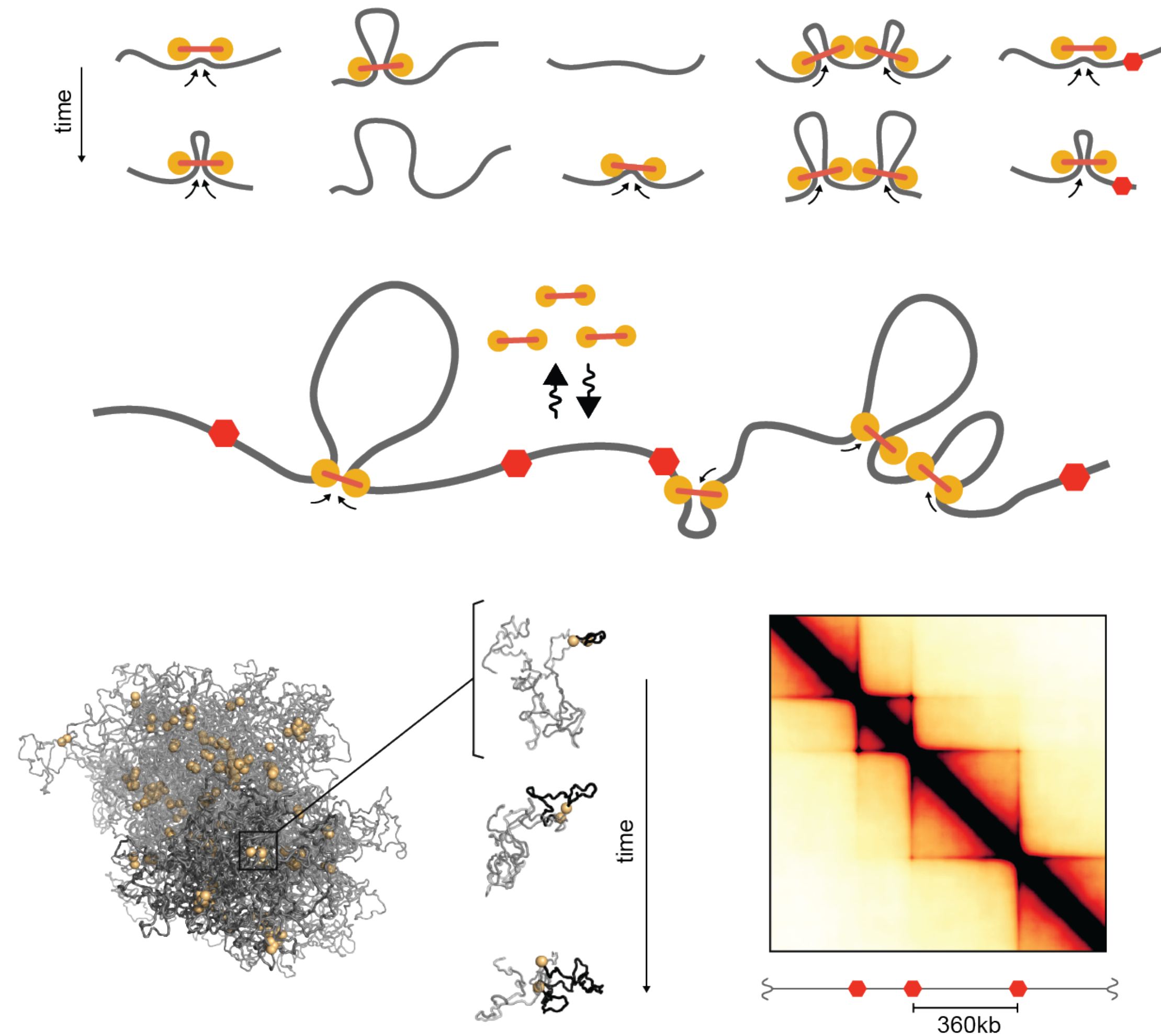
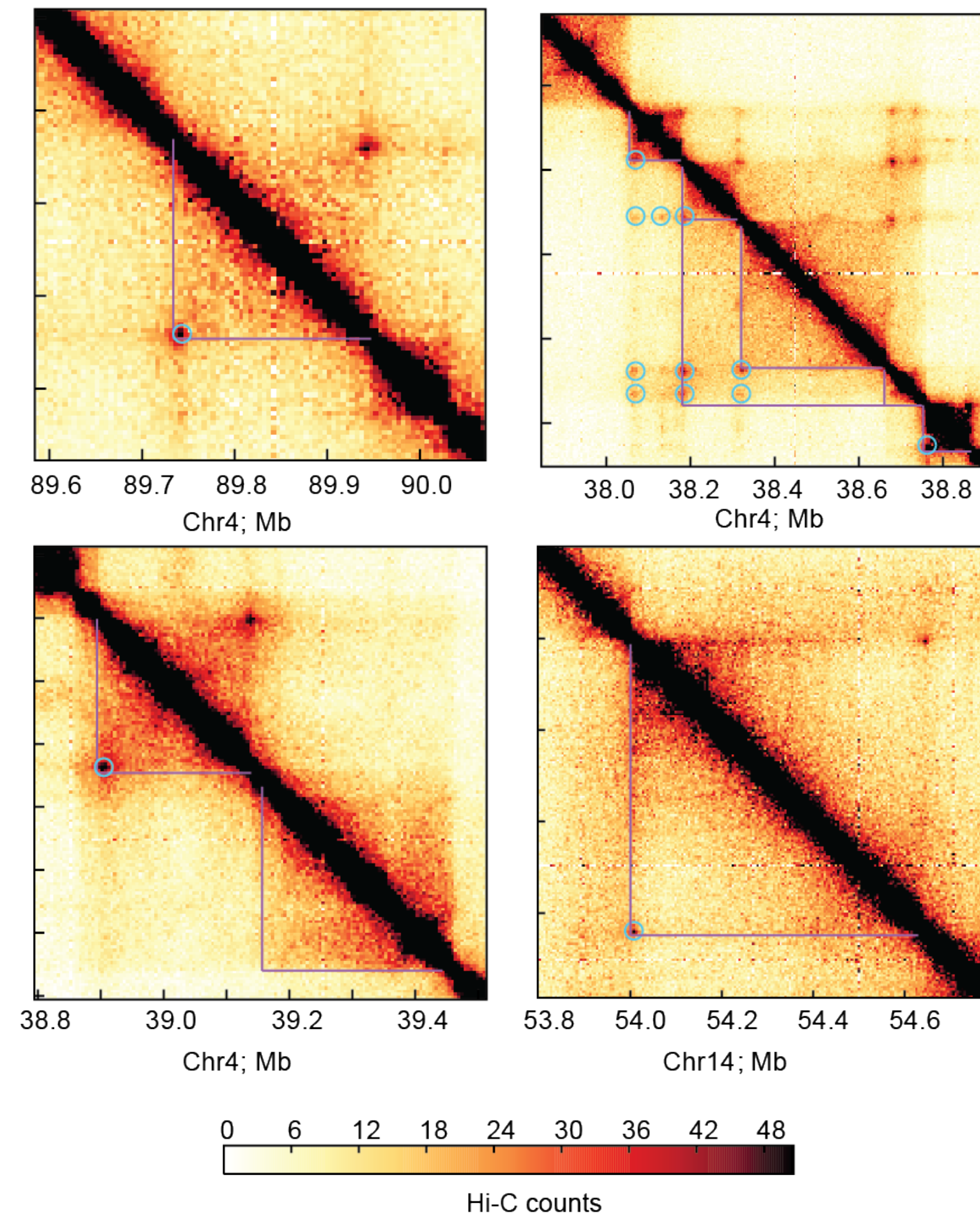
TADs are functional units

Despang, et al. (2019). Nature Genetics 51,1263–1271 (2019)



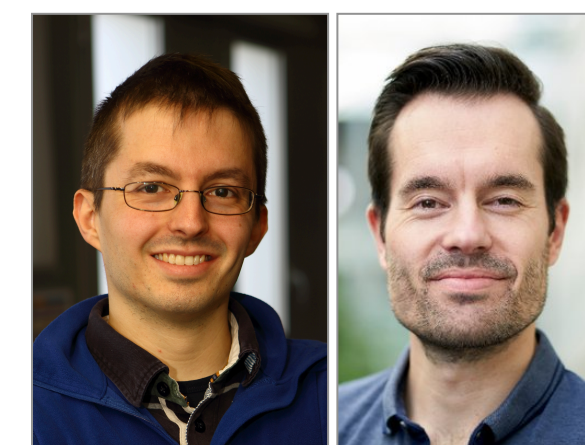
Loop-extrusion as a TAD forming mechanism

Fudenberg, G., Imakaev, M., Lu, C., Goloborodko, A., Abdennur, N., & Mirny, L. A. (2018).
Cold Spring Harb Symp Quant Biol 2017. 82: 45-55





Dynamics of gene activation

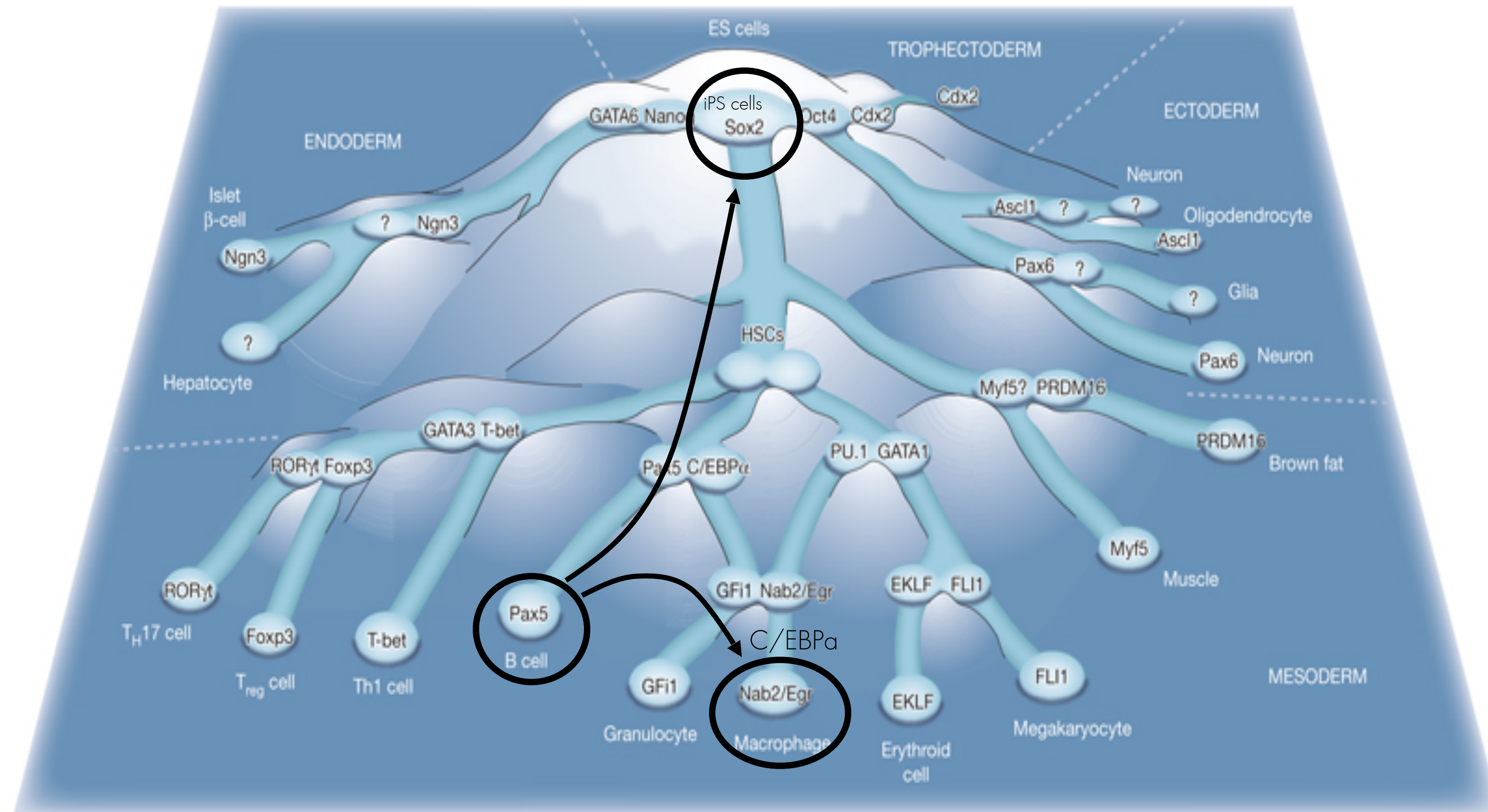


Marco di Stefano
Ralph Stadhouders
with Graf Lab (CRG, Barcelona)

Nature Genetics (2018) 50 p238
Nature Communications (2020) 11 p2564

Transcription factors dictate cell fate

Graf & Enver (2009) Nature



Transcription factors (TFs) determine cell identity through gene regulation

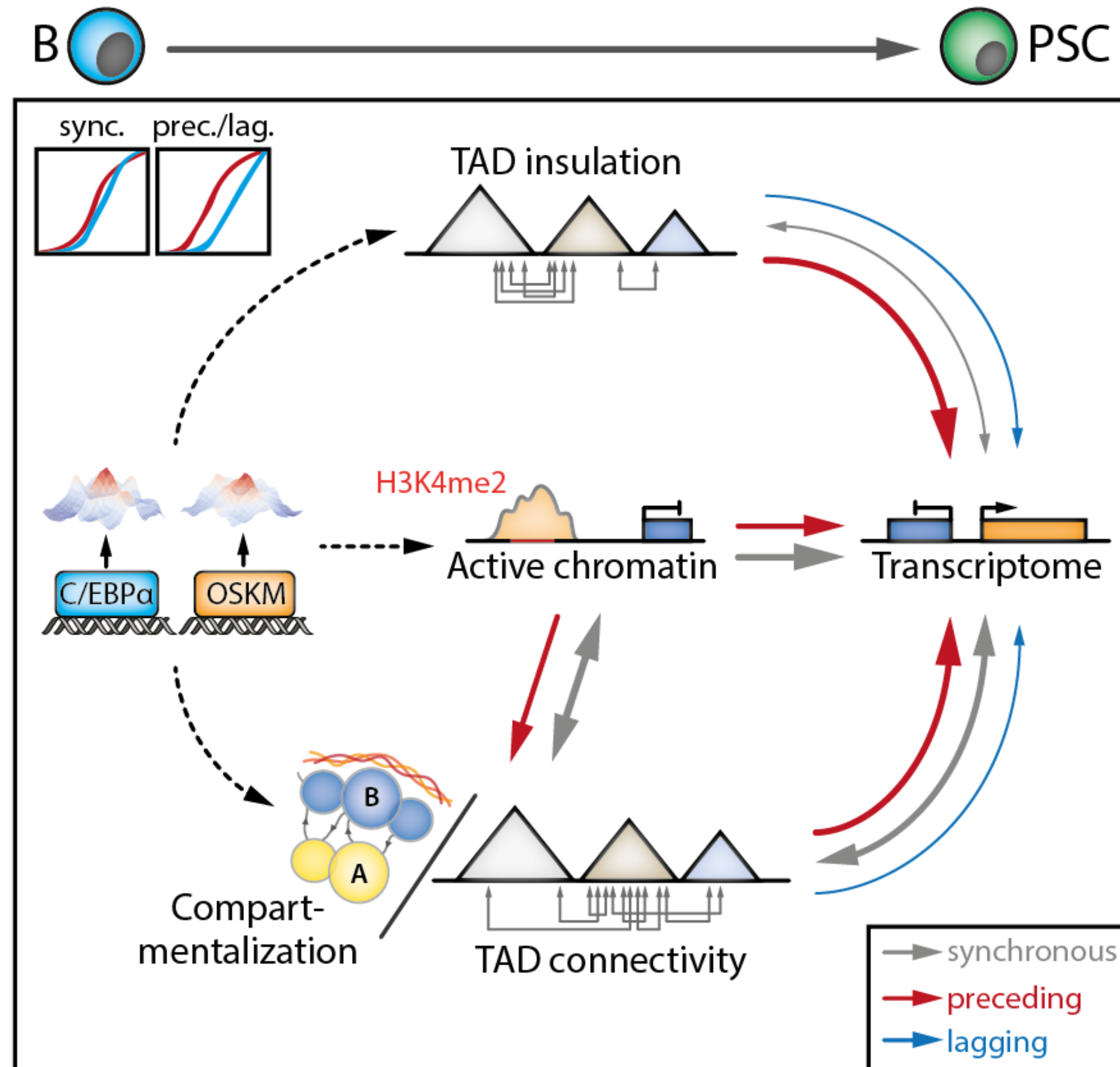
Normal 'forward' differentiation

Cell fates can be converted by enforced TF expression

Transdifferentiation or reprogramming

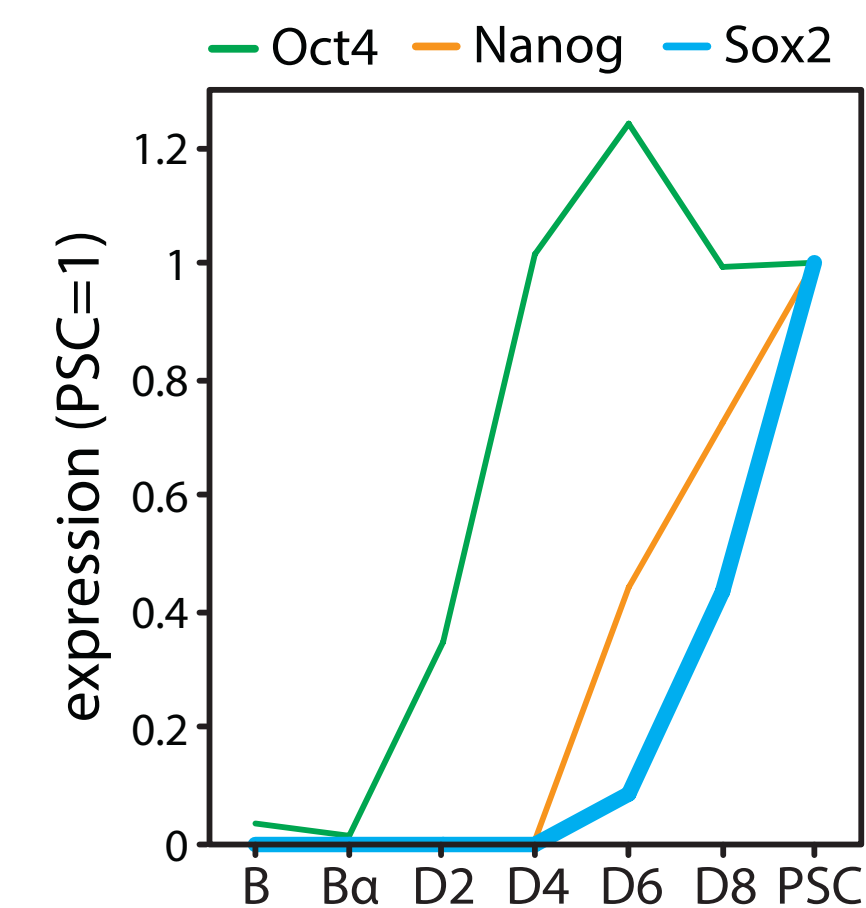
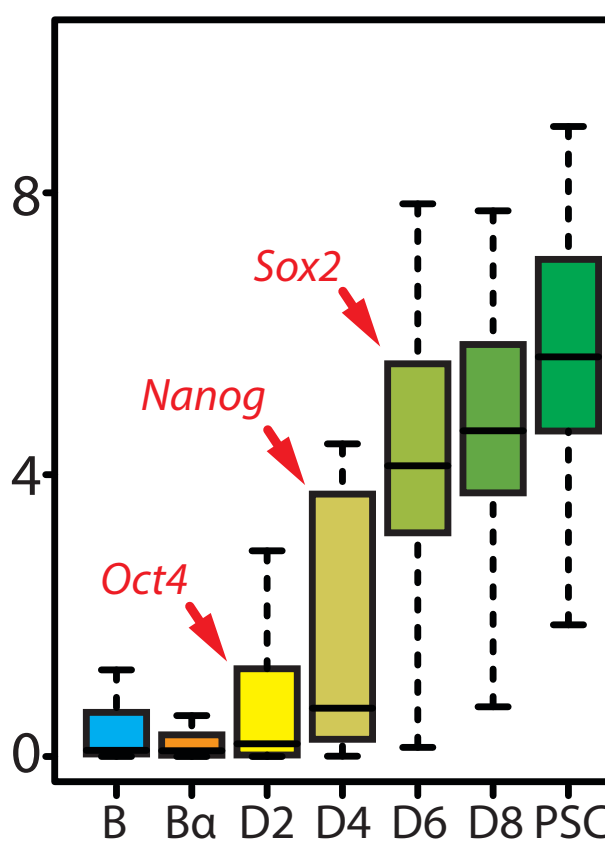
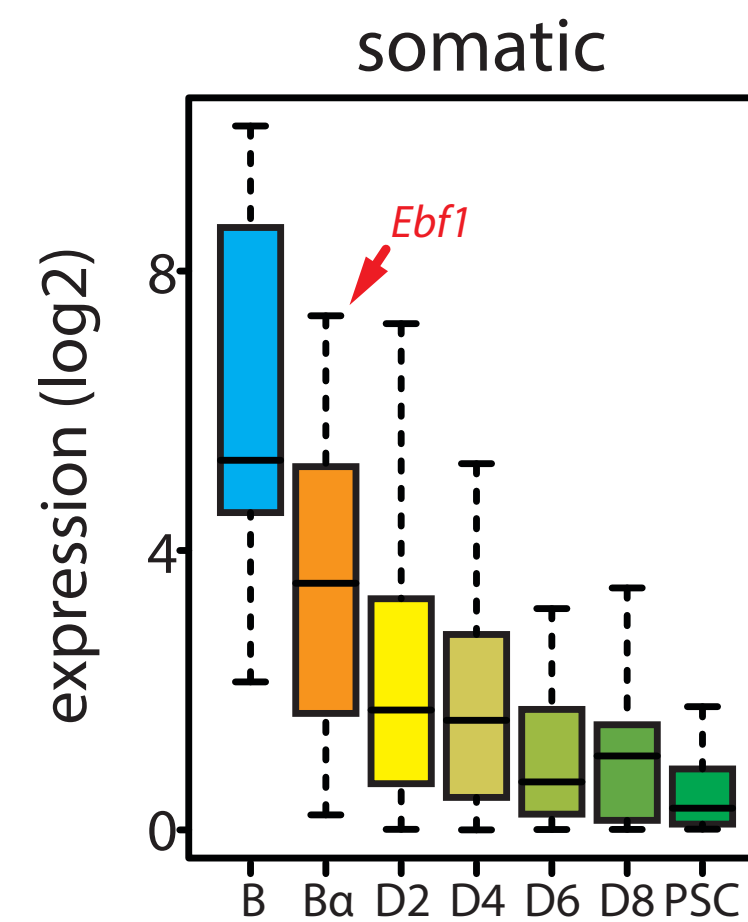
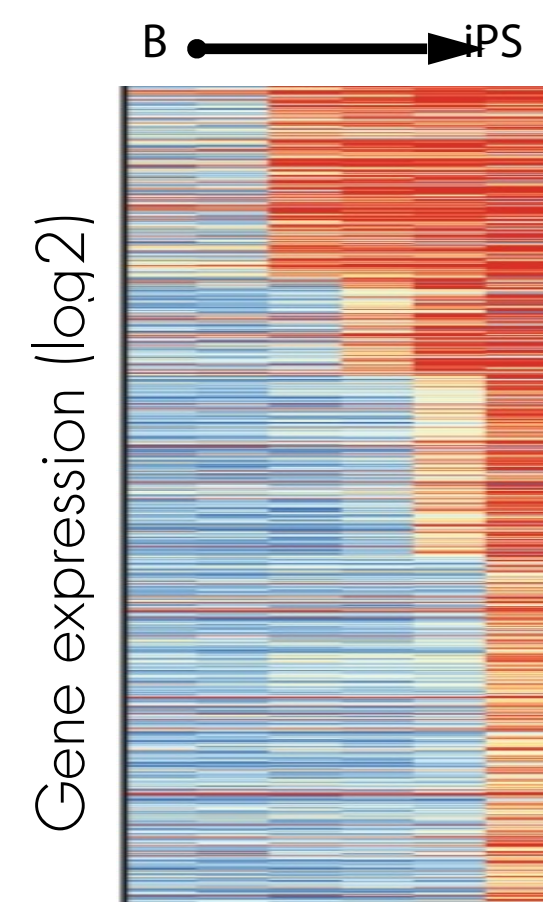
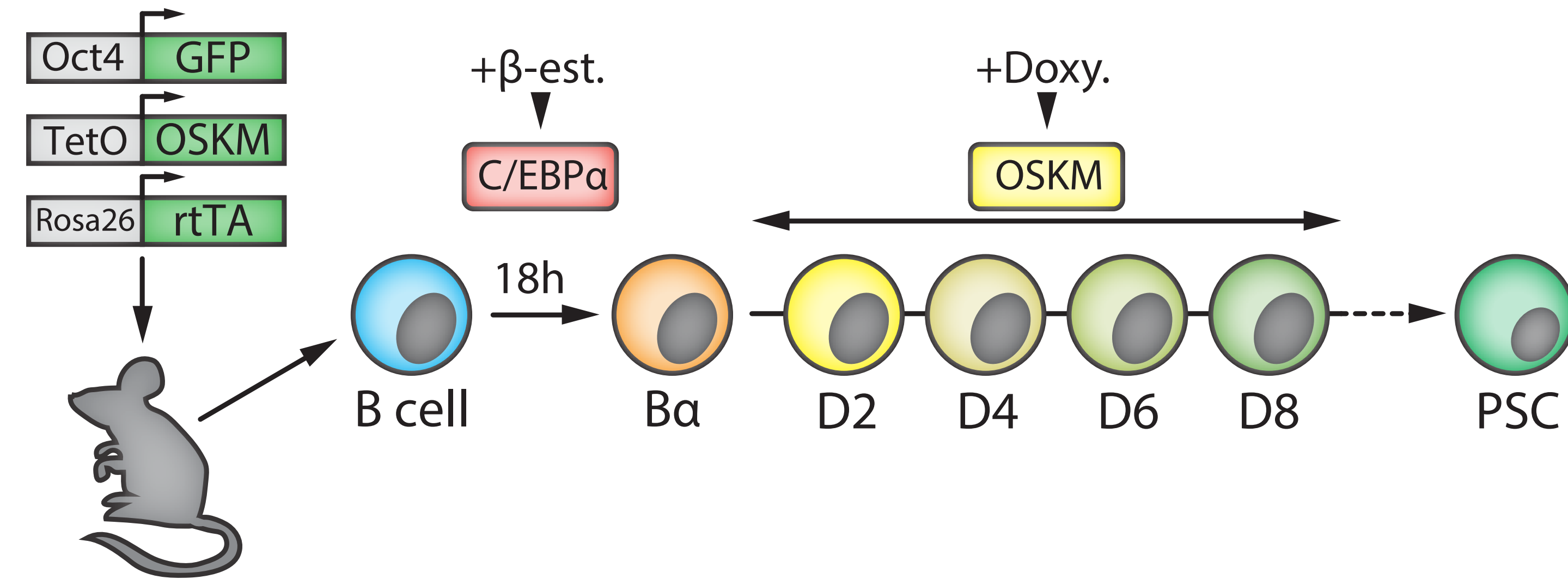
Interplay: topology, gene expression & chromatin

Stadhouders, R., Vidal, E. et al. (2018) Nature Genetics



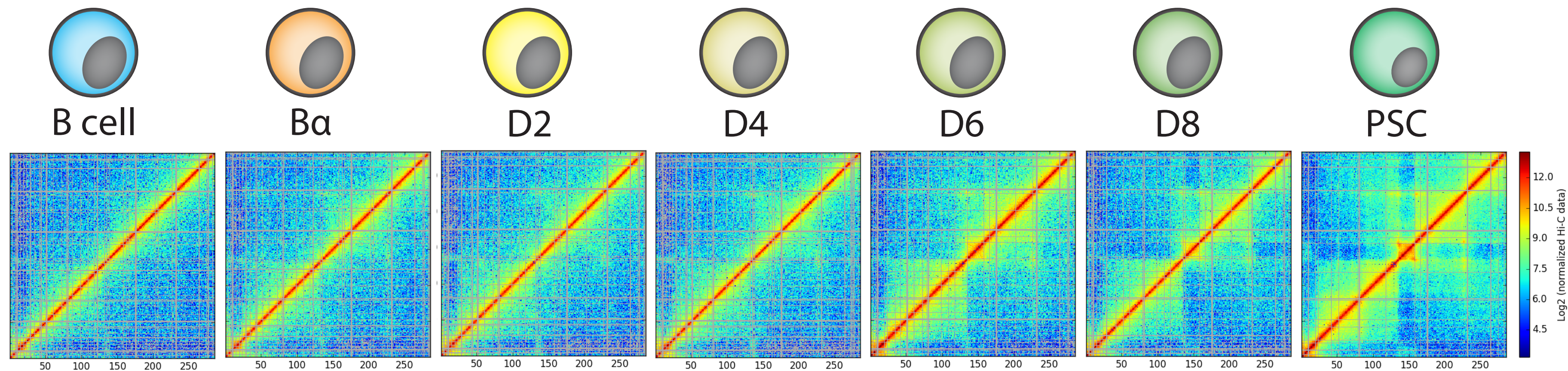
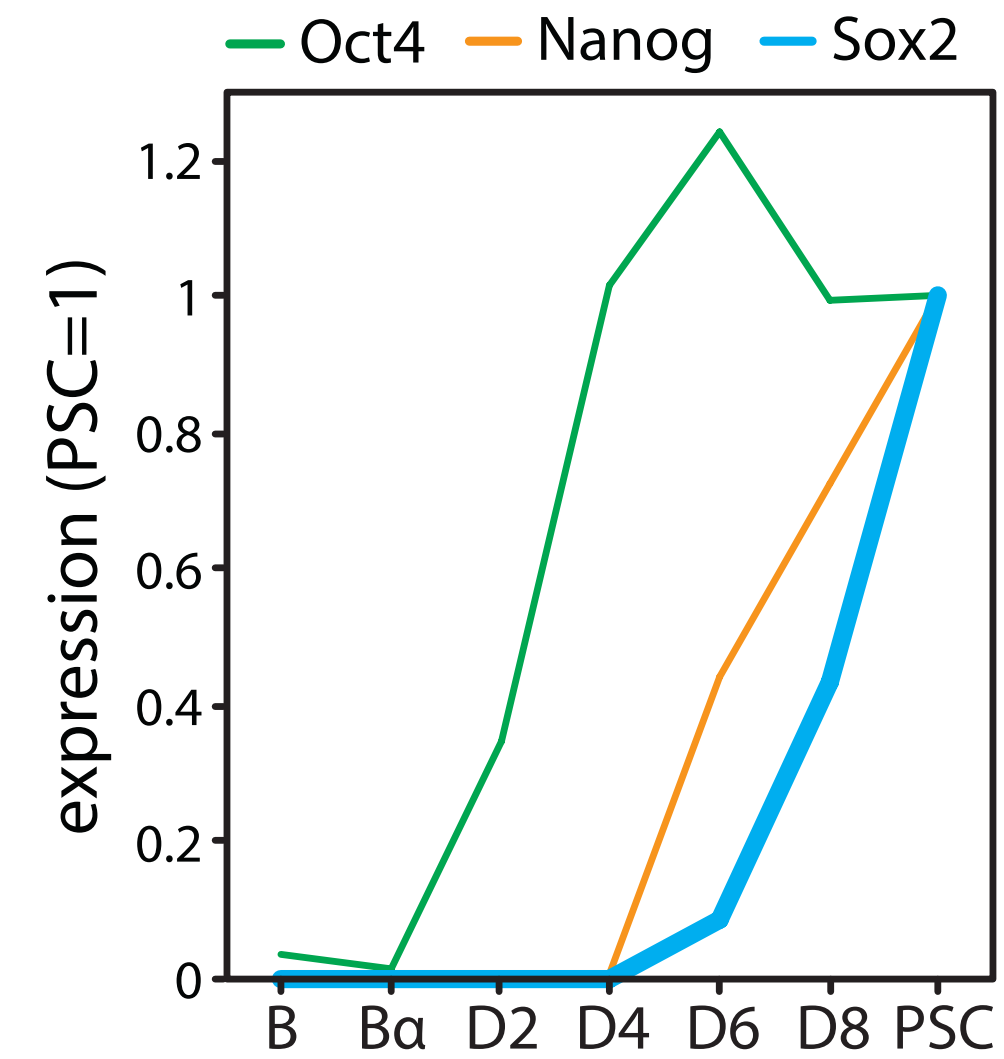
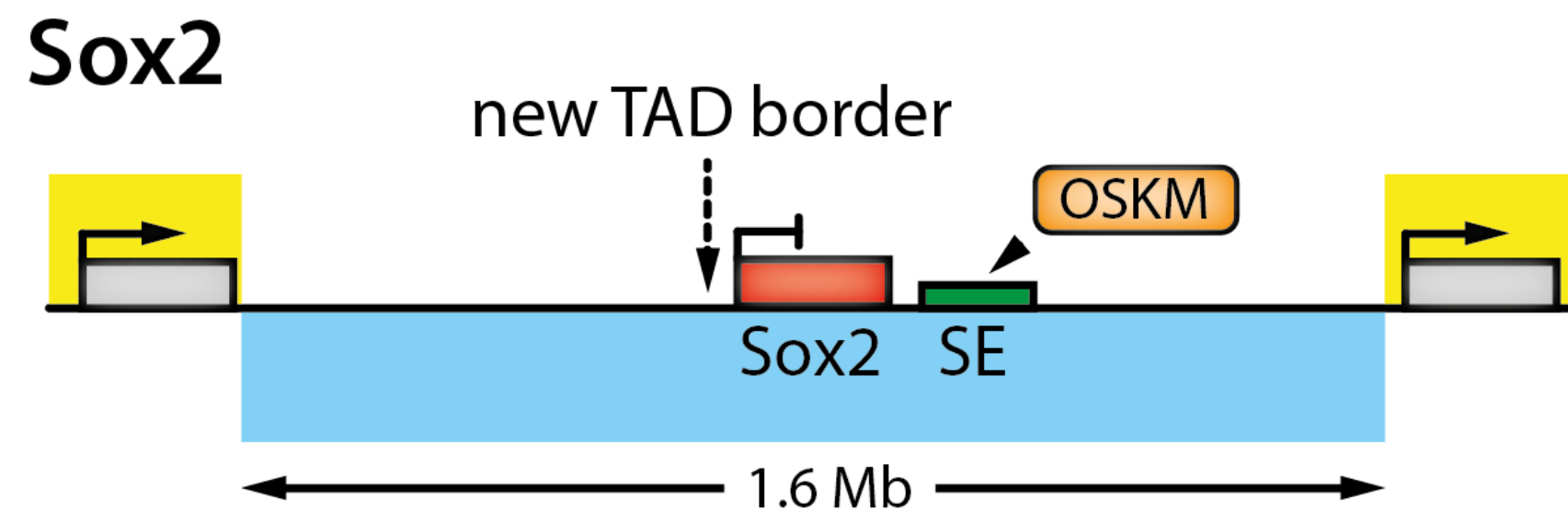
Reprogramming from B to PSC

Stadhouders, R., Vidal, E. et al. (2018) Nature Genetics



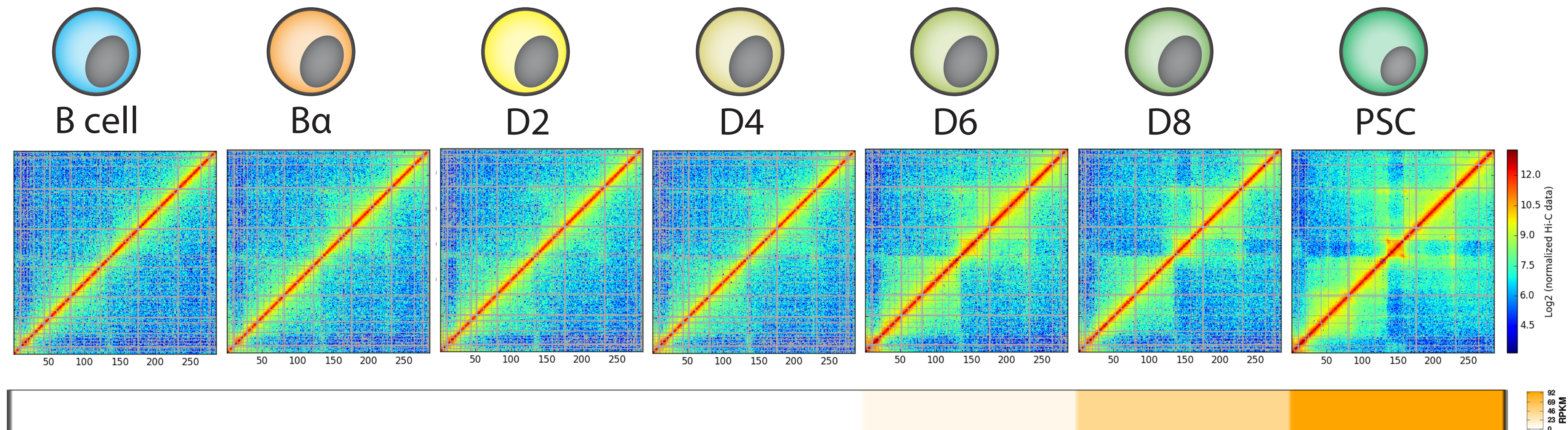
Hi-C maps of reprogramming from B to PSC

The SOX2 locus



Hi-C maps of reprogramming from B to PSC

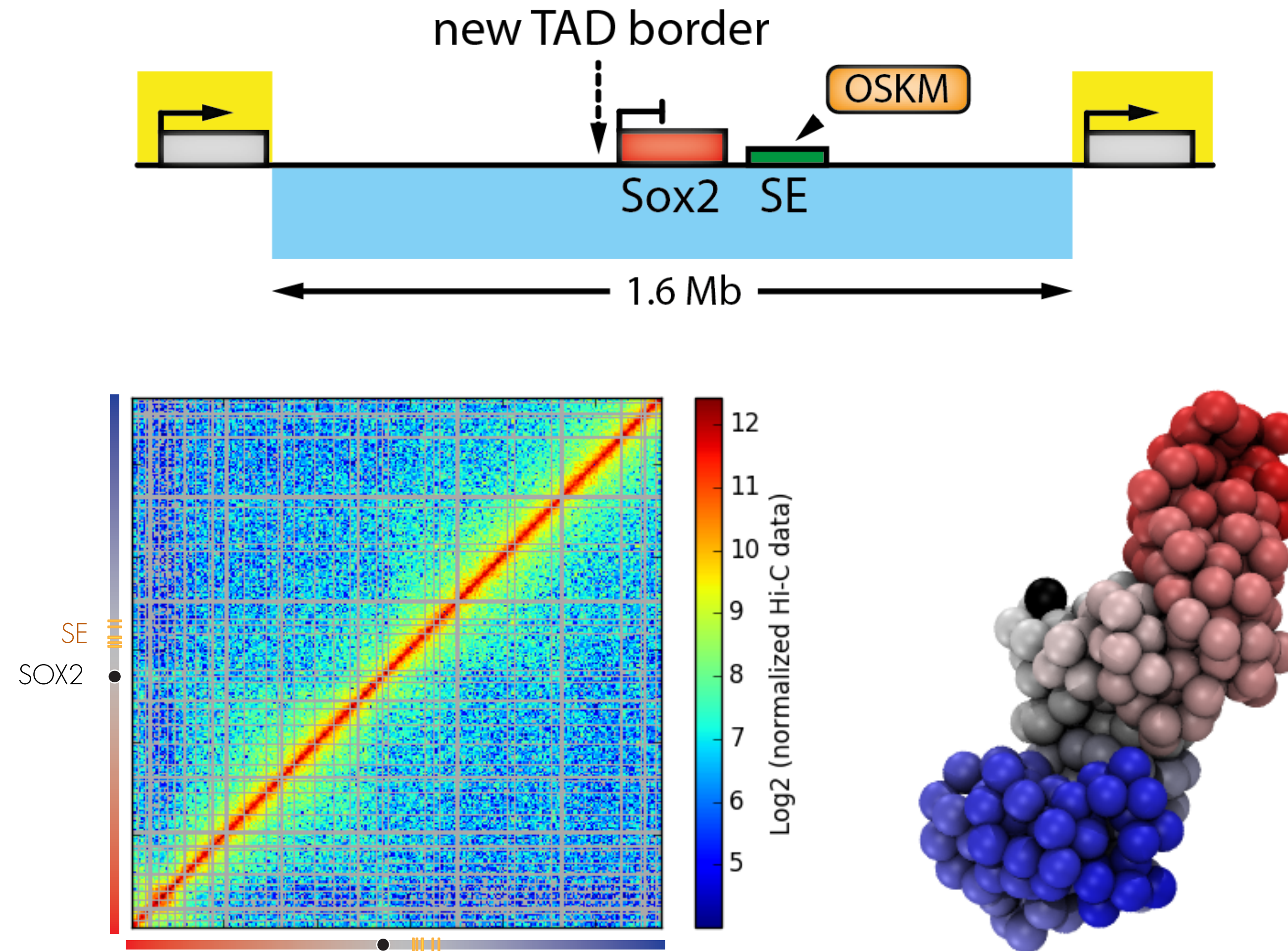
The SOX2 locus



How do these structural rearrangements interplay with the transcription activity?

What are the main drivers of structural transitions?

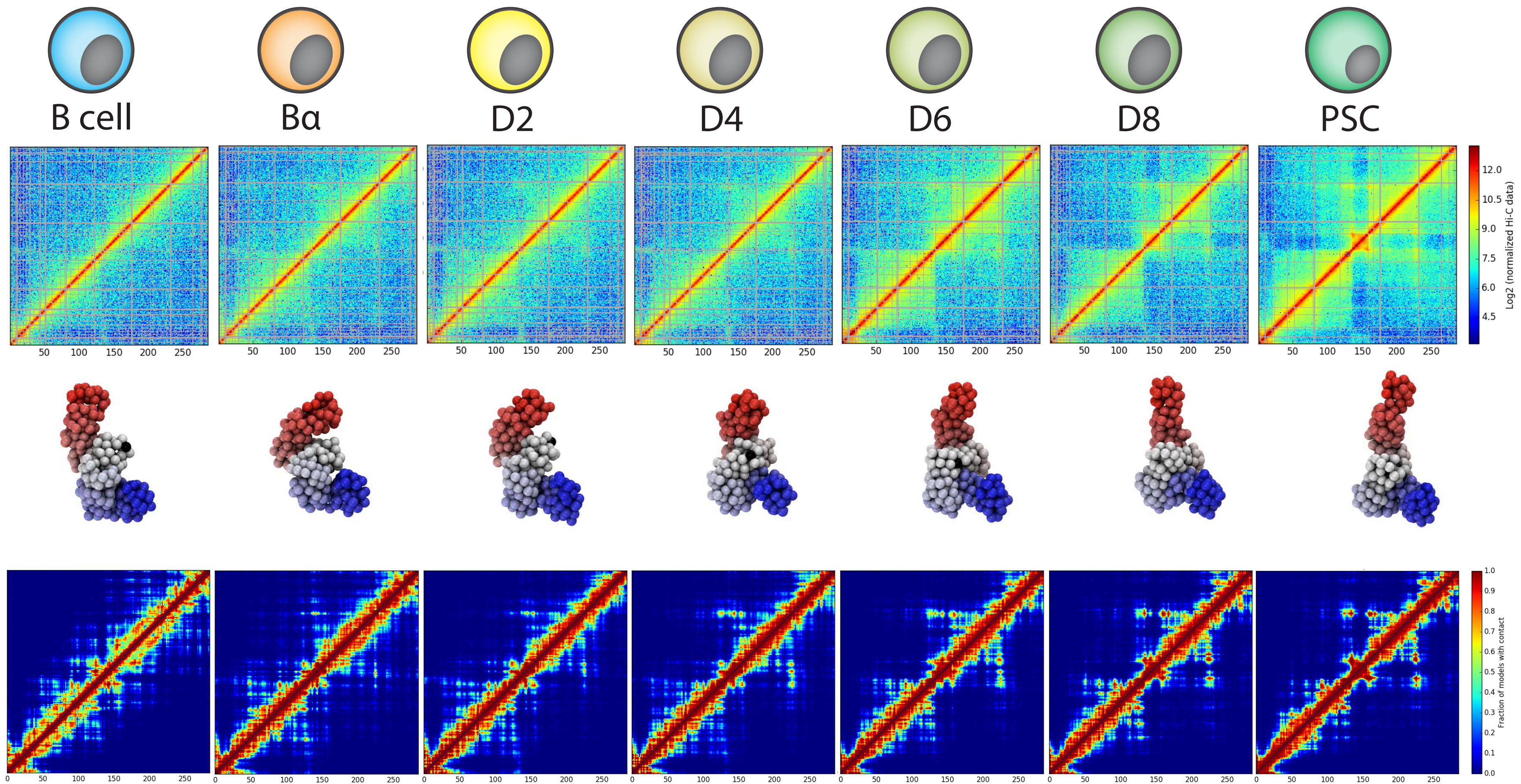
TADbit modeling of SOX2 from B cells Hi-C



Optimal IMP parameters
lowfreq=0 , upfreq=1 , maxdist=200nm, dcutoff=125nm, particle size=50nm (5kb)

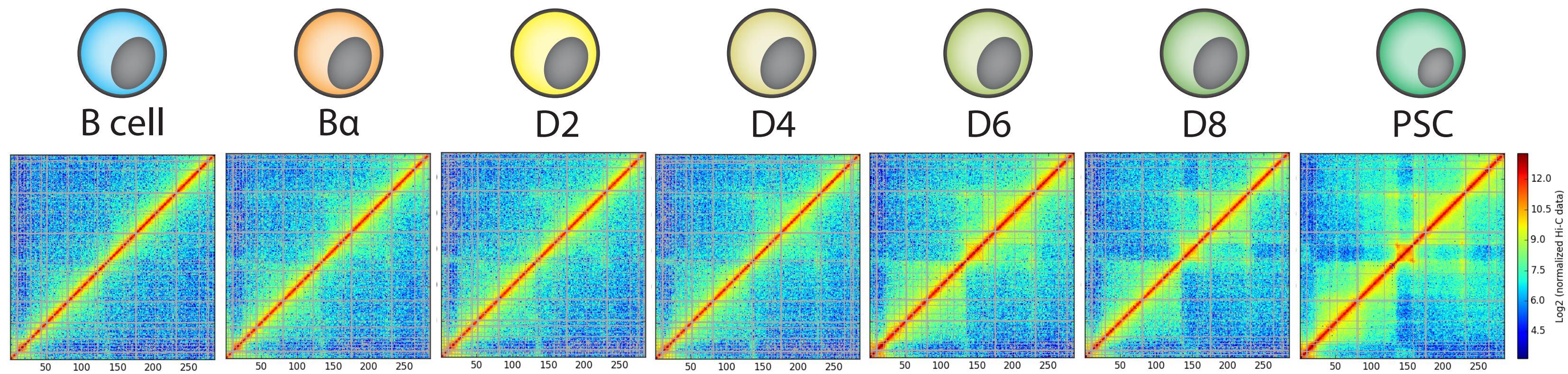
Models of reprogramming from B to PSC

The SOX2 locus



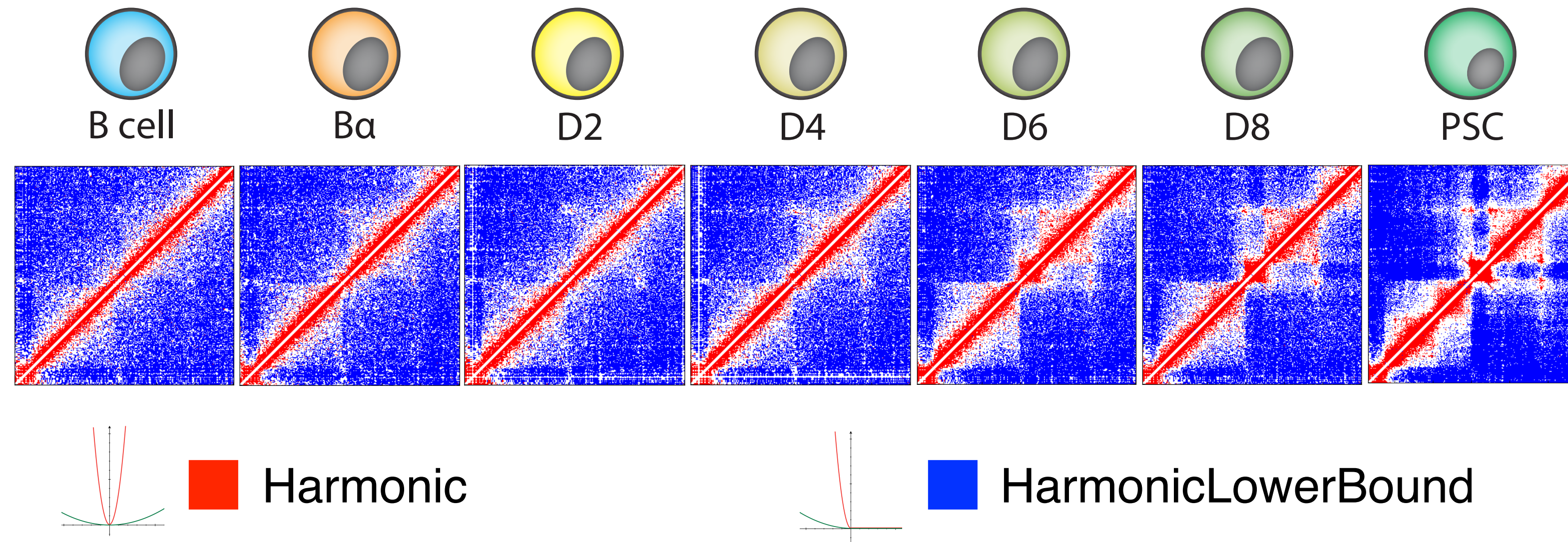
TADdyn: from time-series Hi-C maps to dynamic restraints

The SOX2 locus



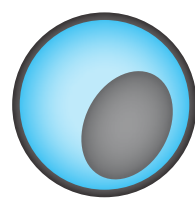
TADdyn: from time-series Hi-C maps to dynamic restraints

The SOX2 locus

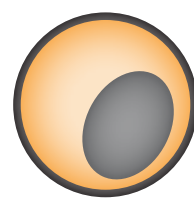


TADdyn: from time-series Hi-C maps to dynamic restraints

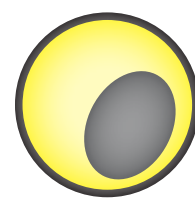
The SOX2 locus



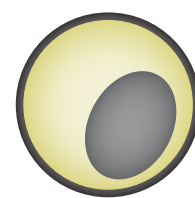
B cell



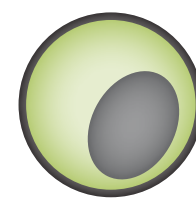
B α



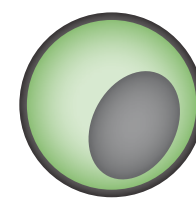
D2



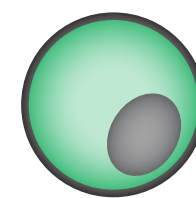
D4



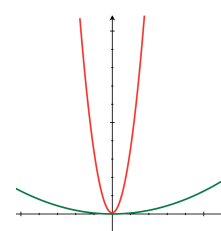
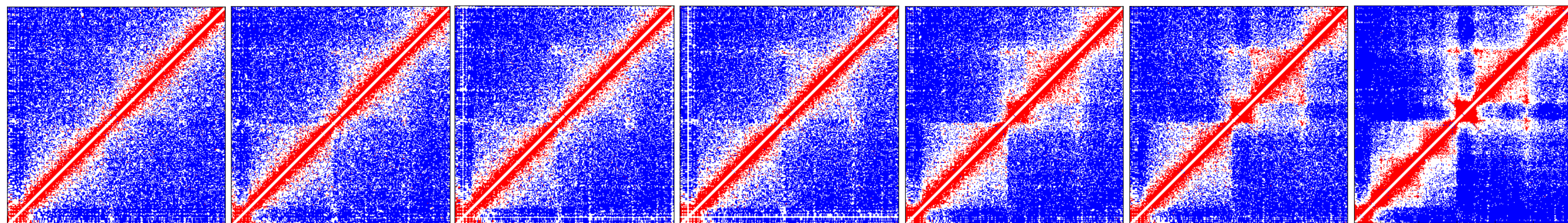
D6



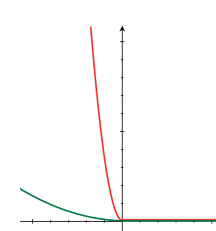
D8



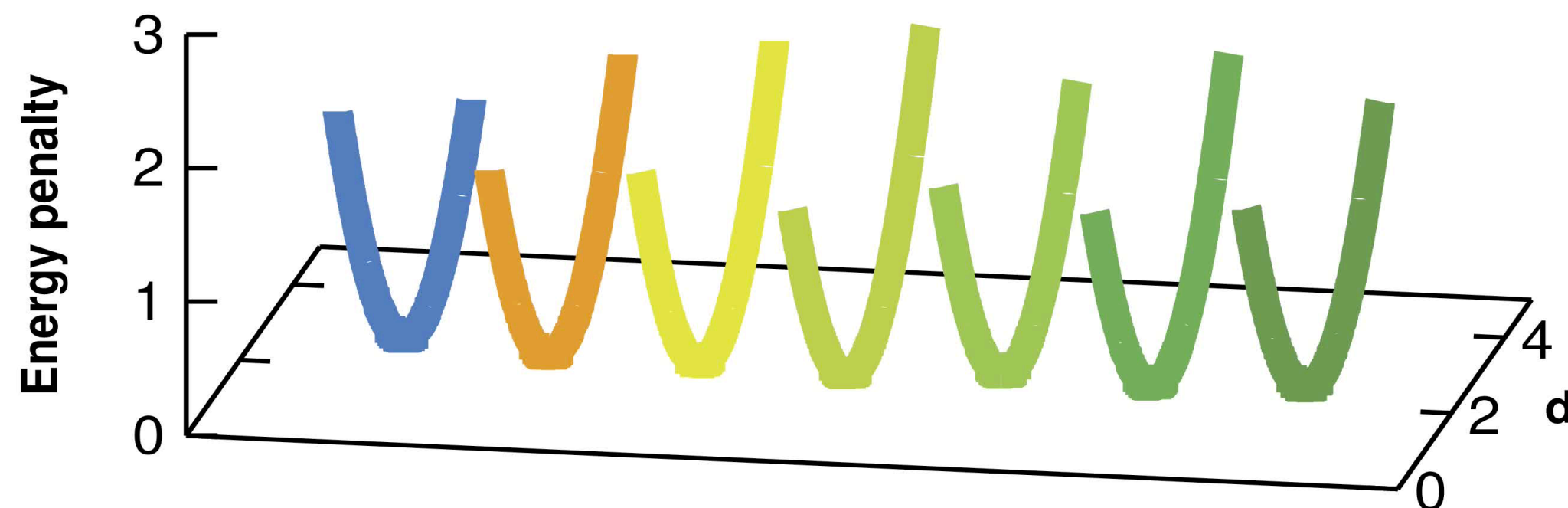
PSC



Harmonic



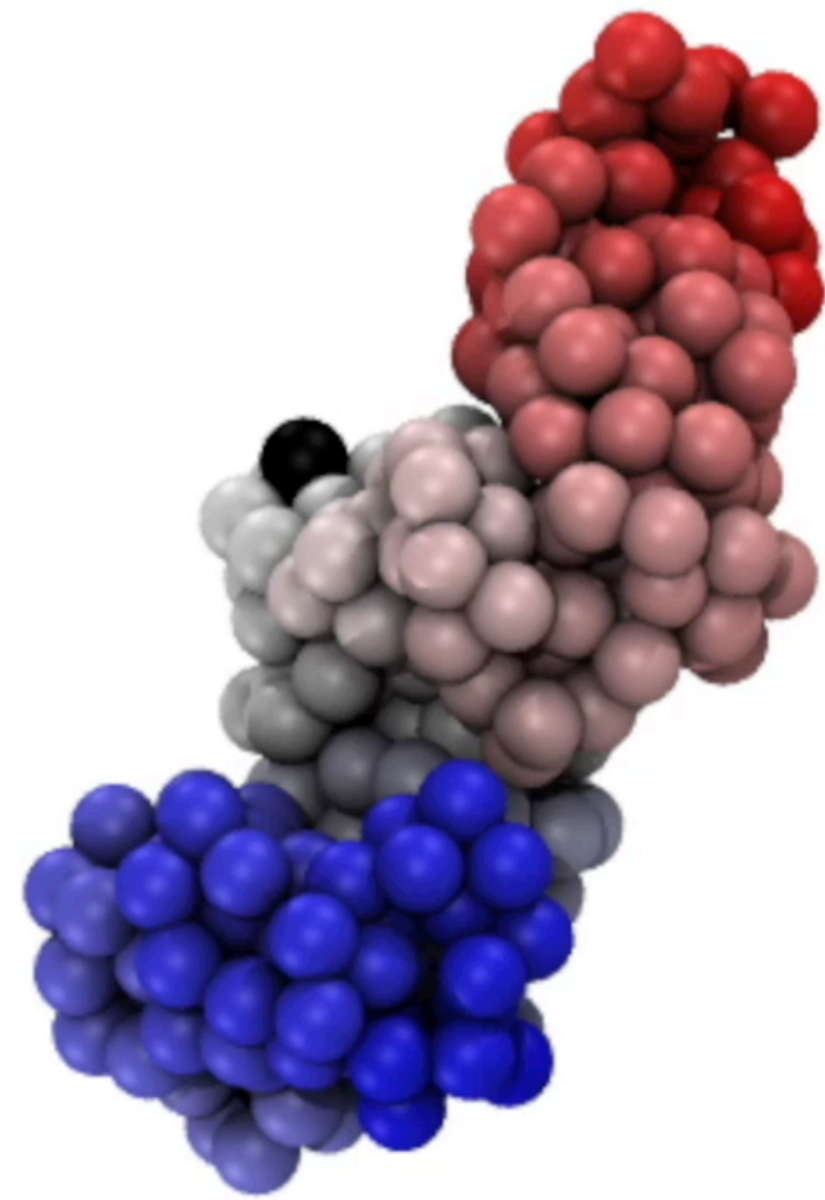
HarmonicLowerBound



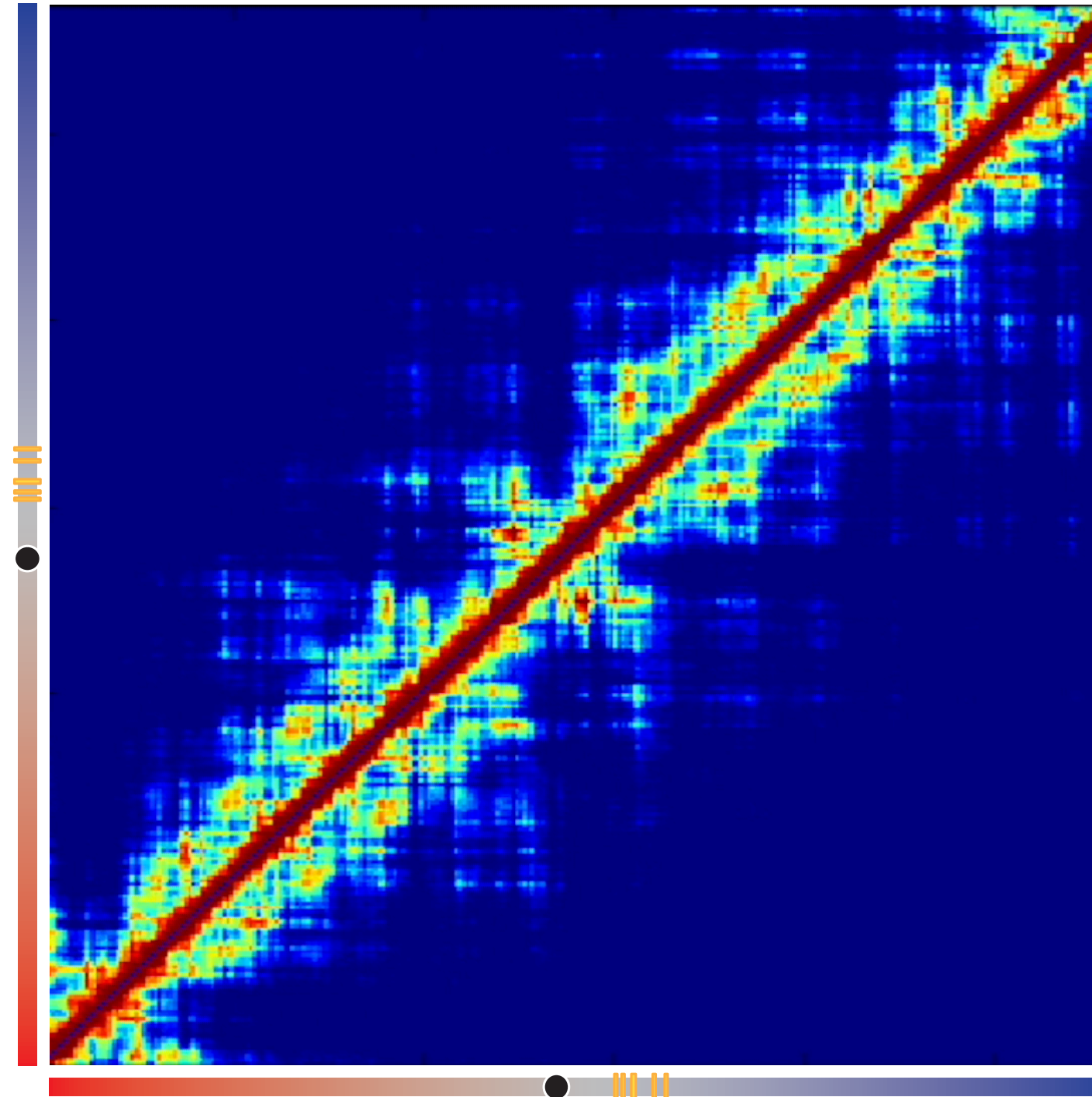
Transition	Stable	Vanishing	Raising
B -> B α	18,612	6,984	7,290
B α -> D2	18,512	7,390	6,687
D2 -> D4	18,369	6,830	6,893
D4 -> D6	18,971	6,291	7,289
D6 -> D8	20,167	6,093	6,250
D8 -> ES	20,679	5,738	6,173

SOX2 locus structural changes from B to PSC

Contacts

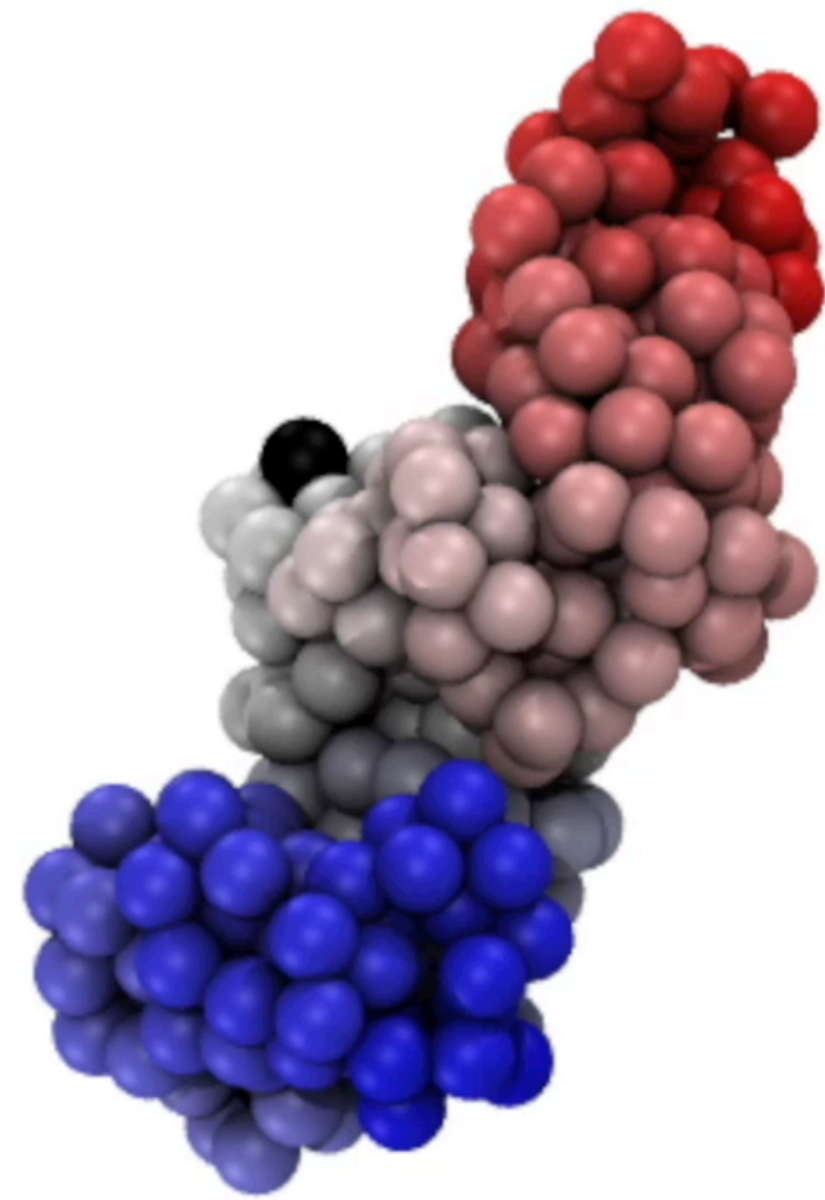


SE
SOX2

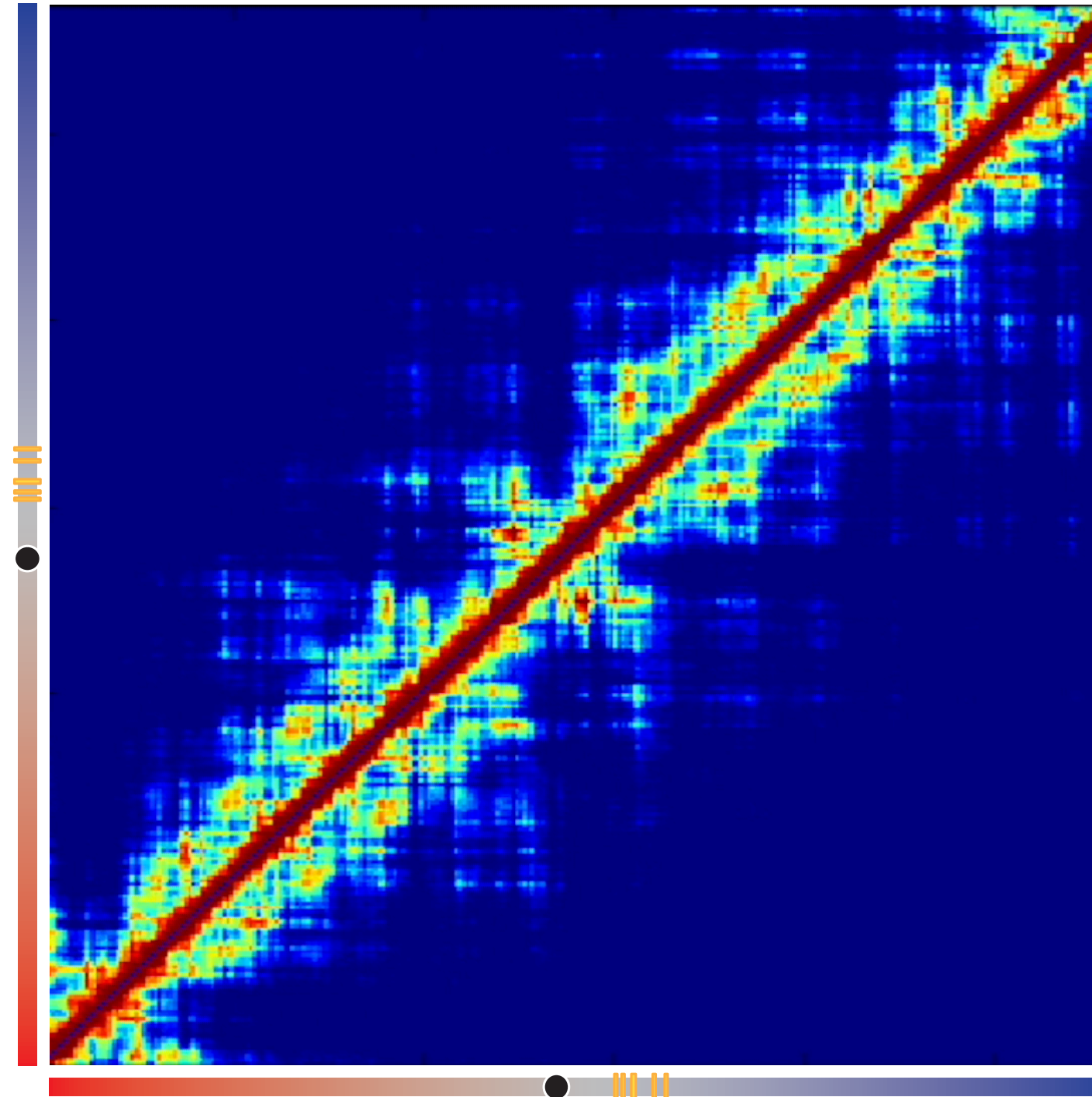


SOX2 locus structural changes from B to PSC

Contacts

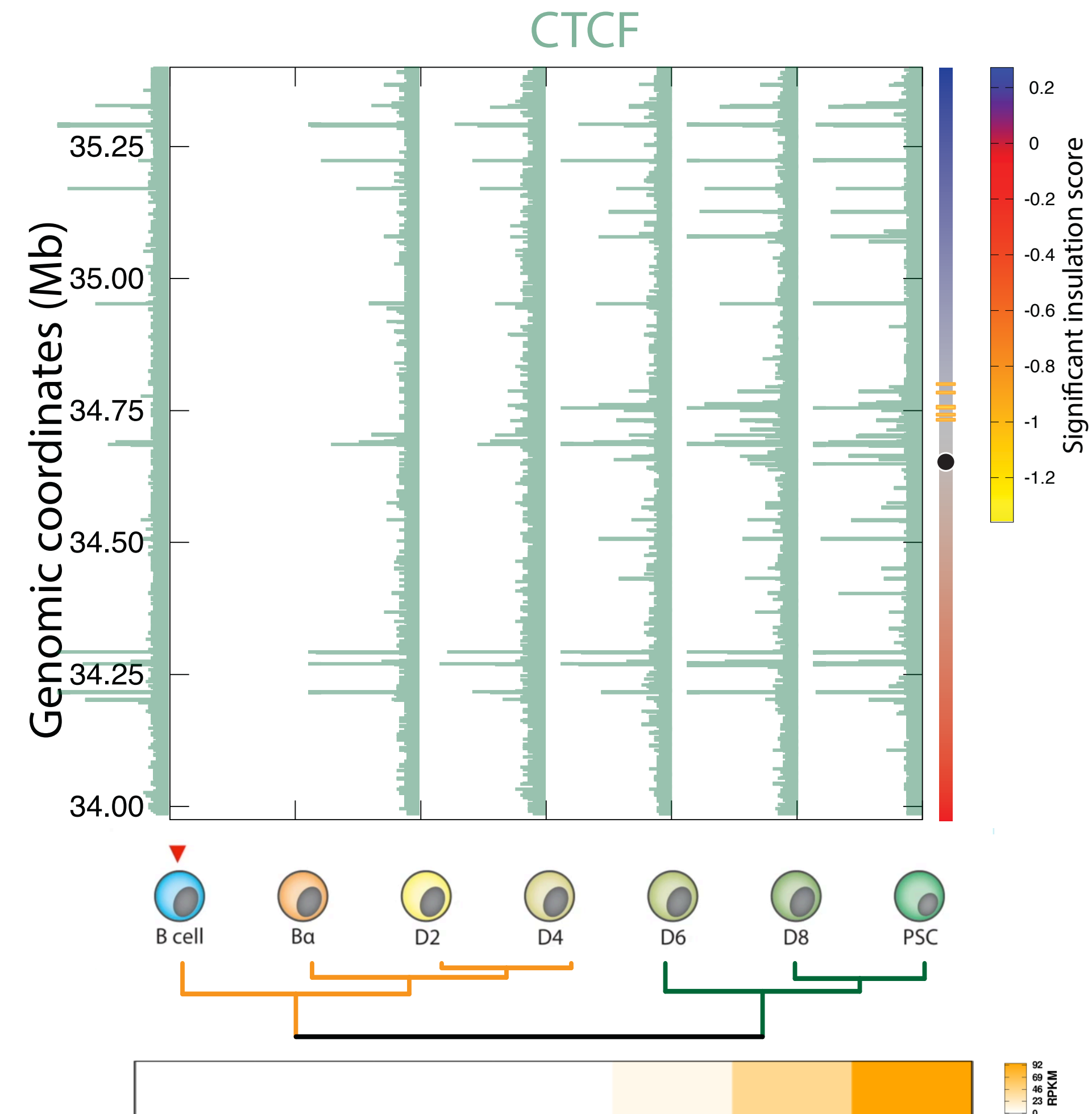
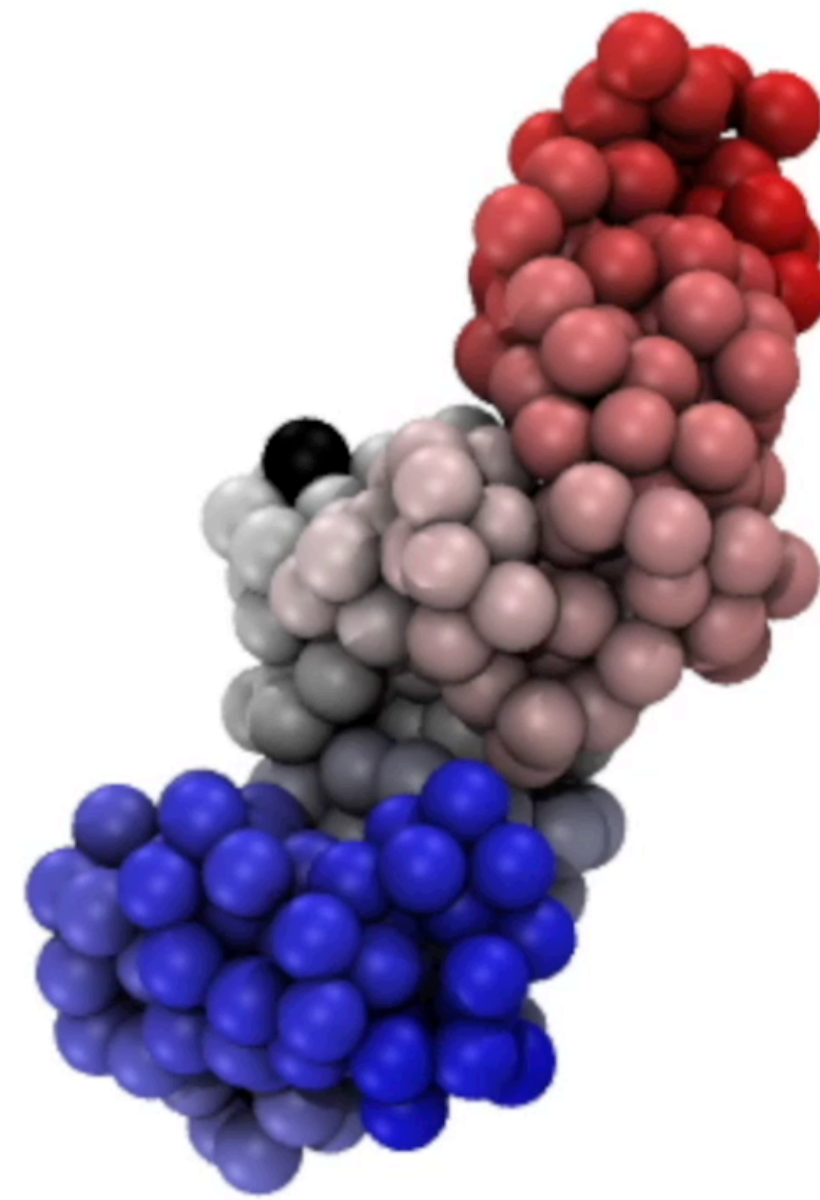


SE
SOX2



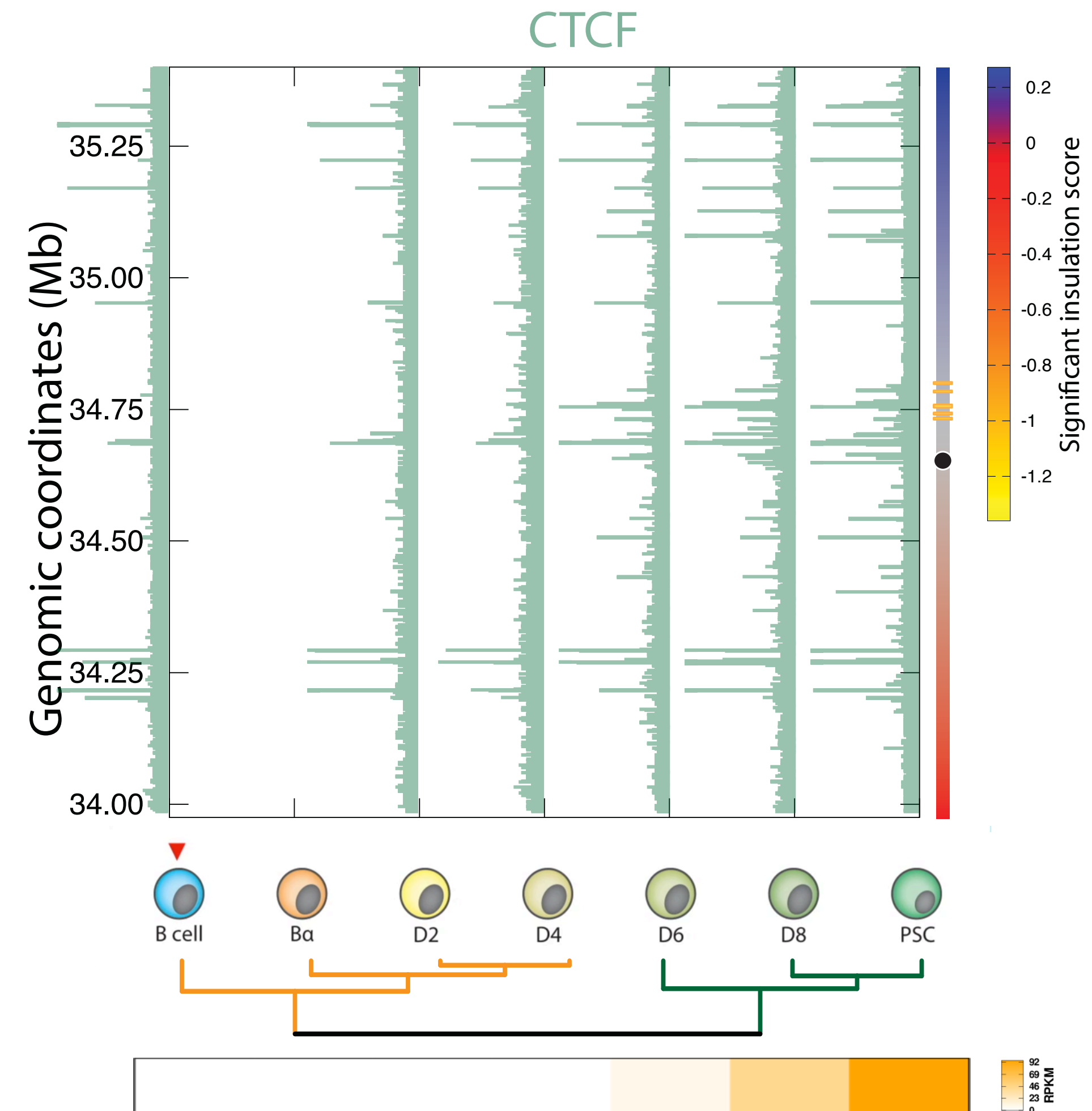
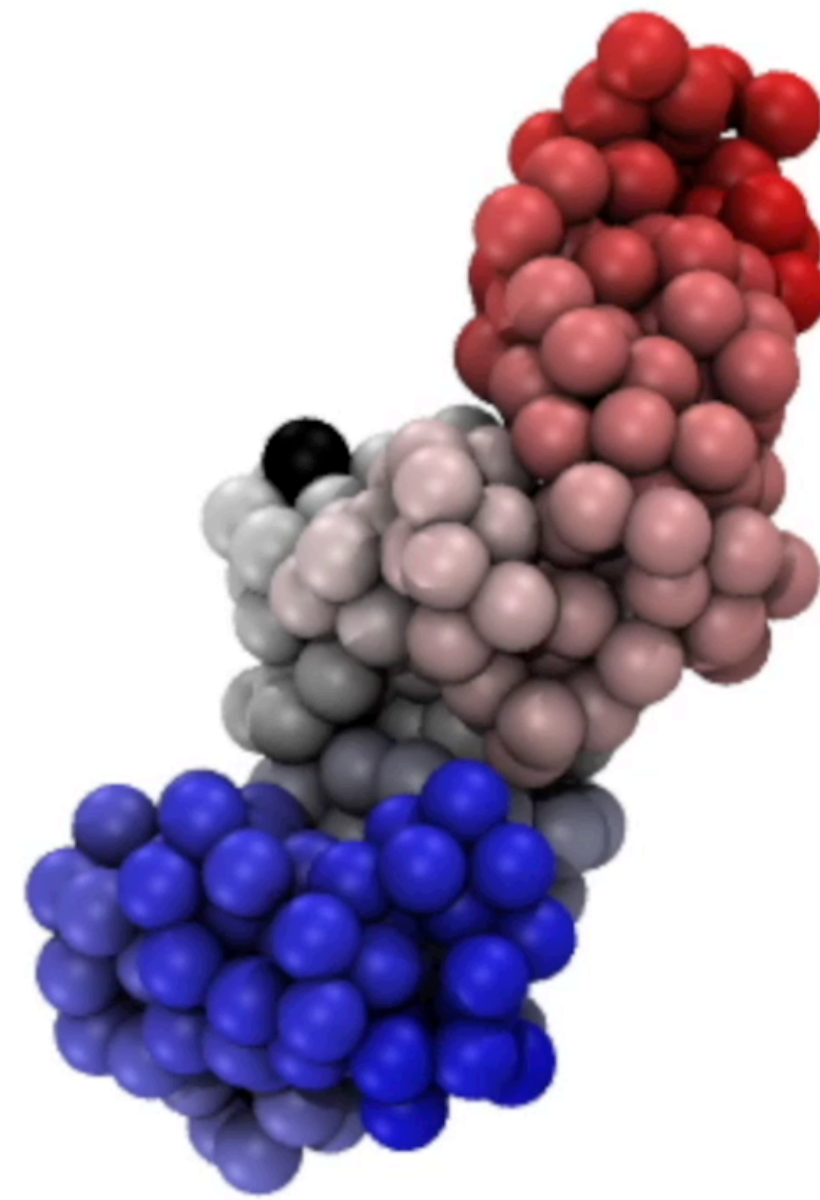
SOX2 locus structural changes from B to PSC

TAD borders



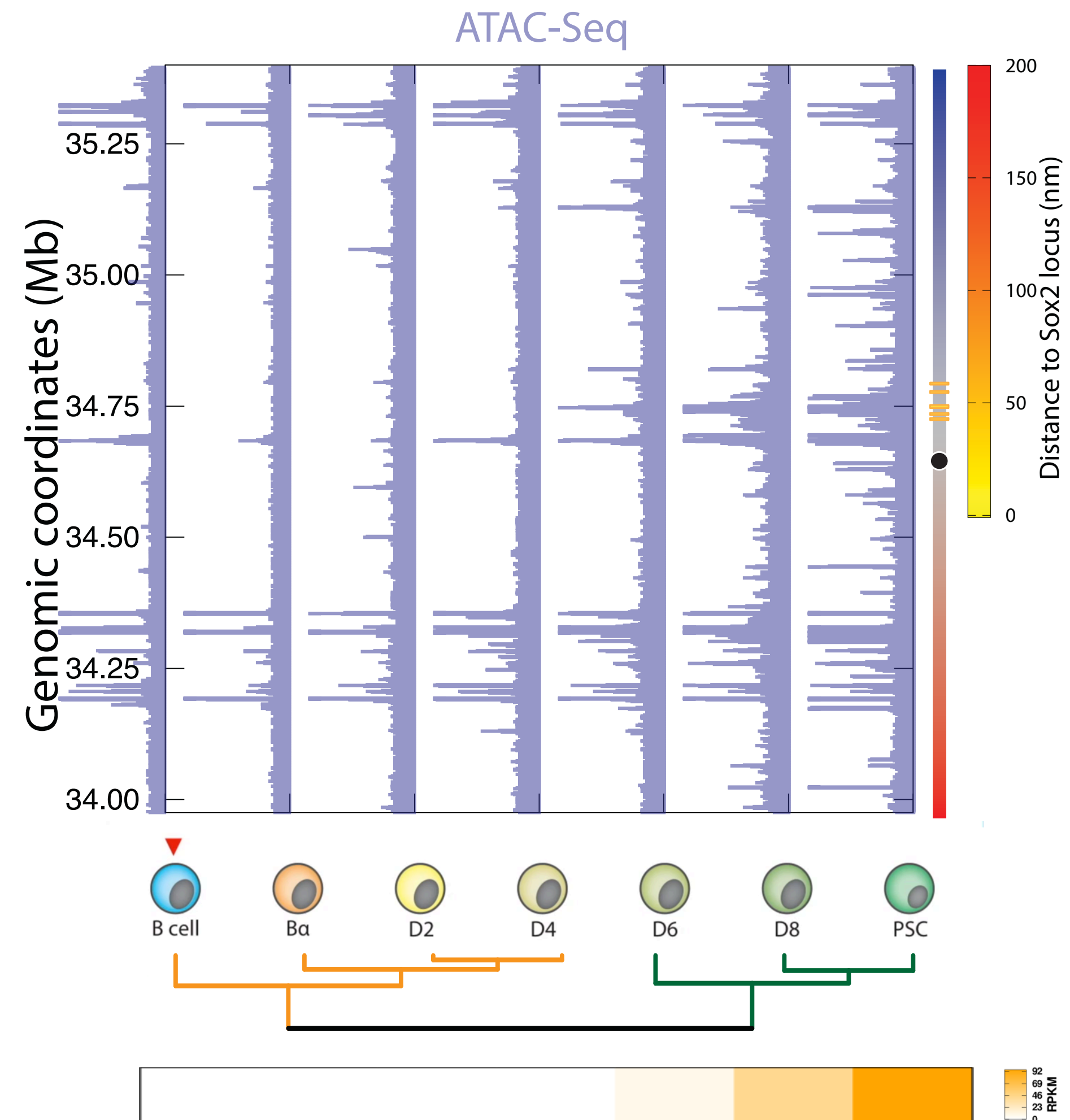
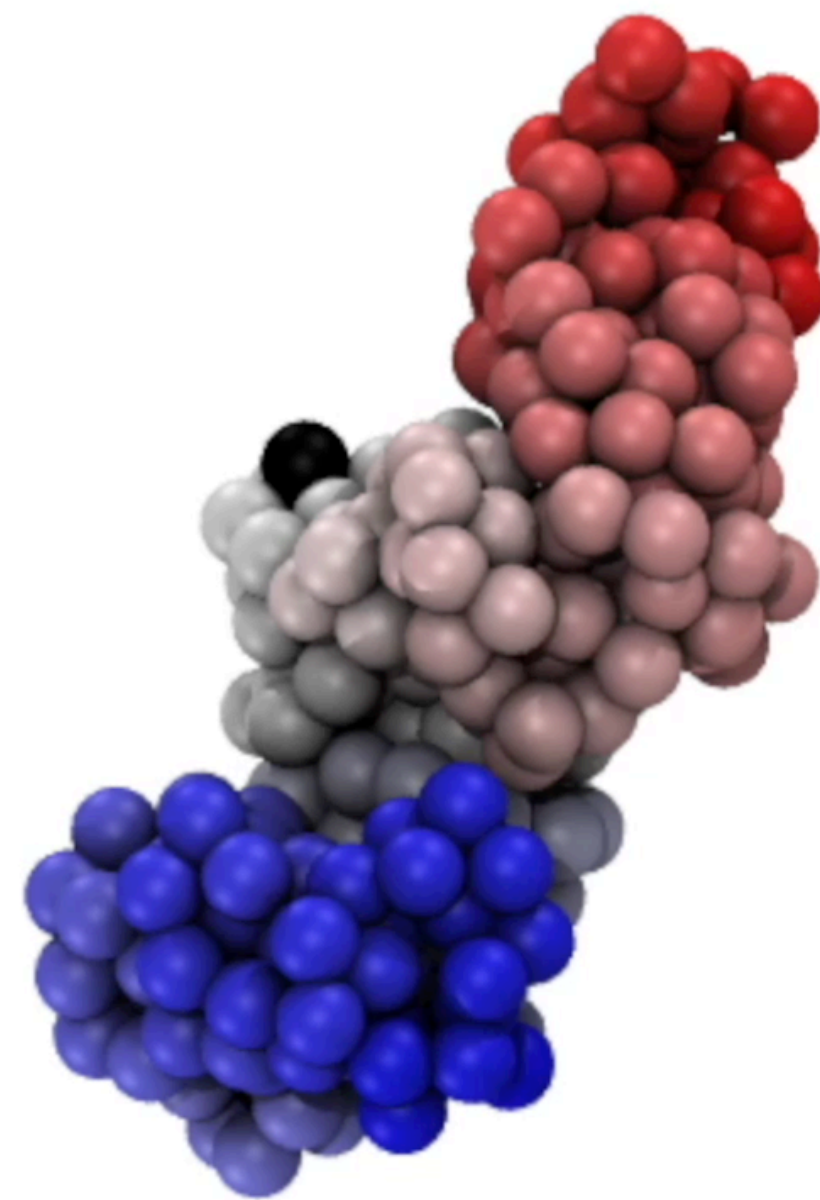
SOX2 locus structural changes from B to PSC

TAD borders



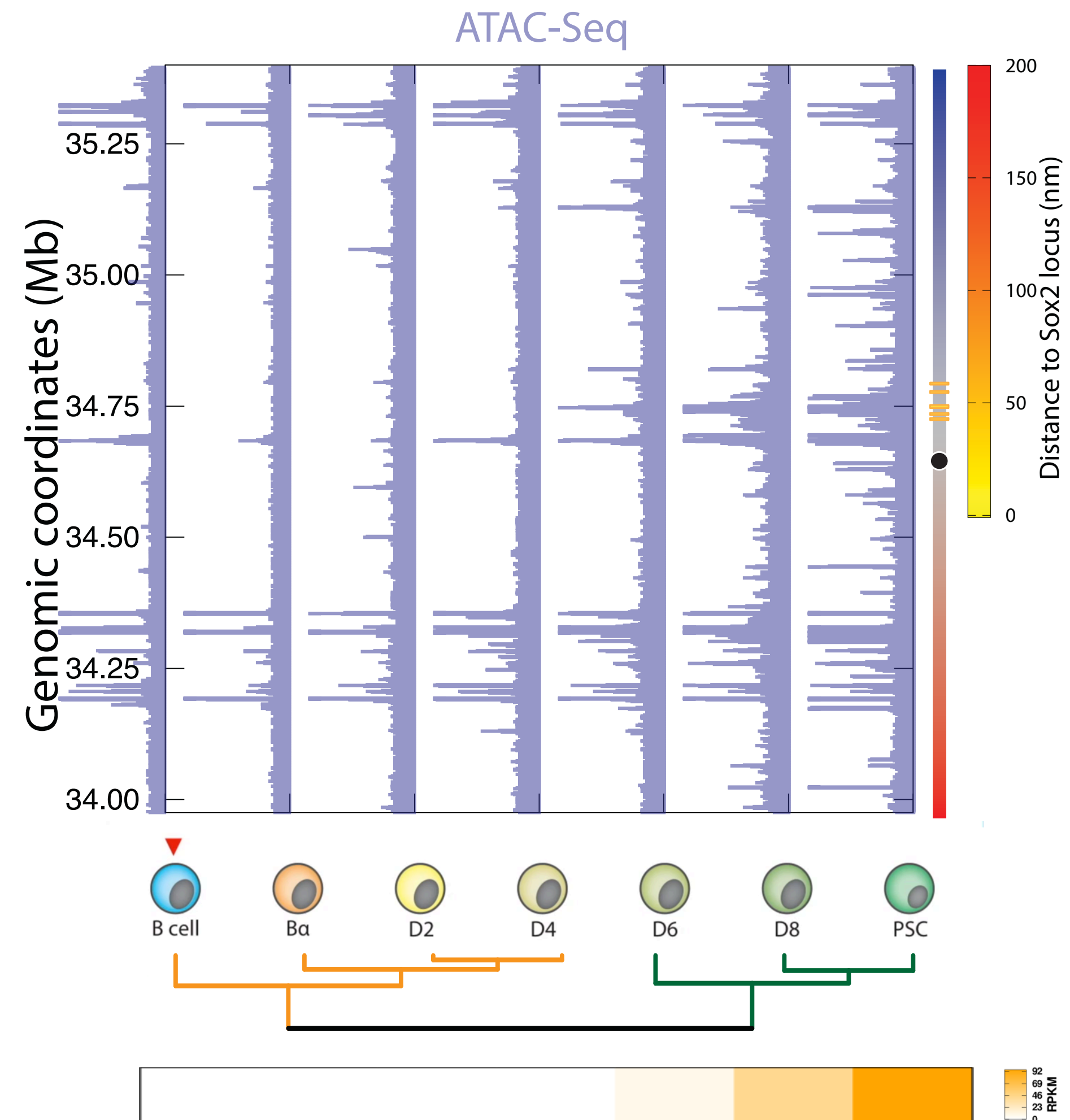
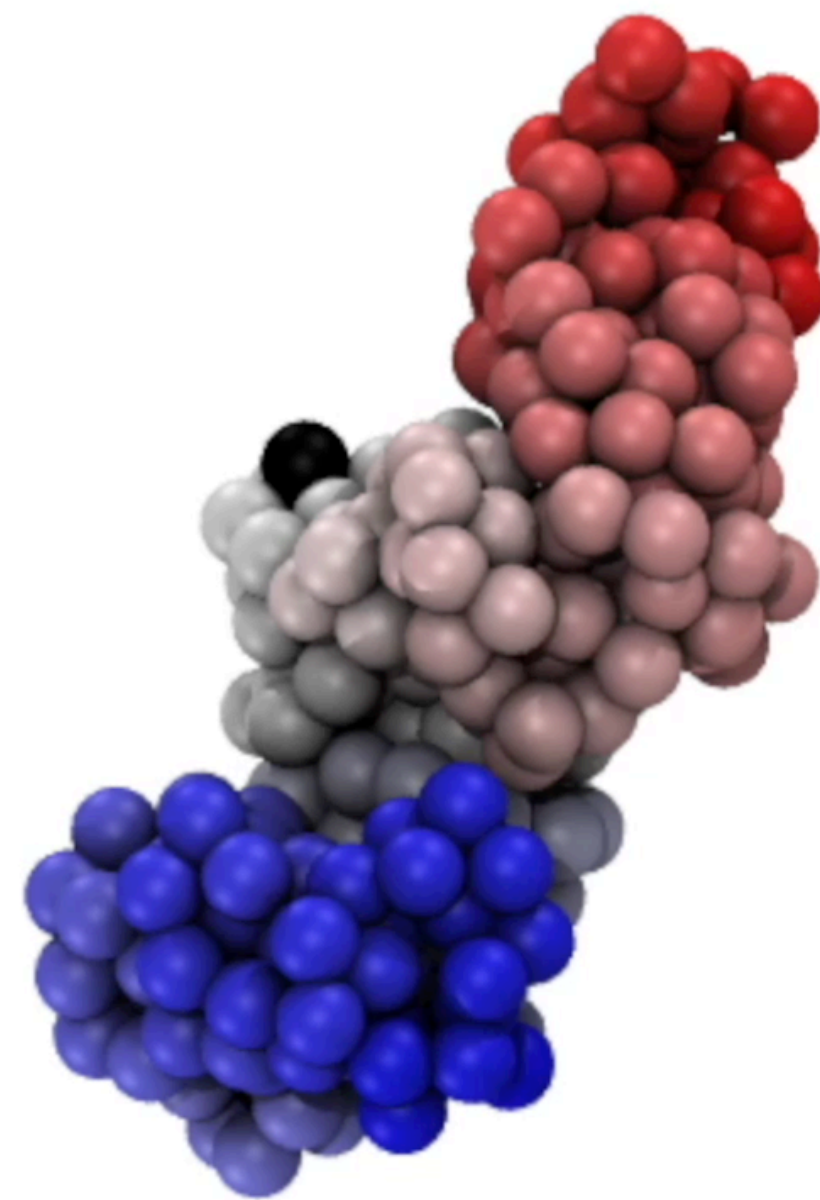
SOX2 locus structural changes from B to PSC

Distance to regulatory elements



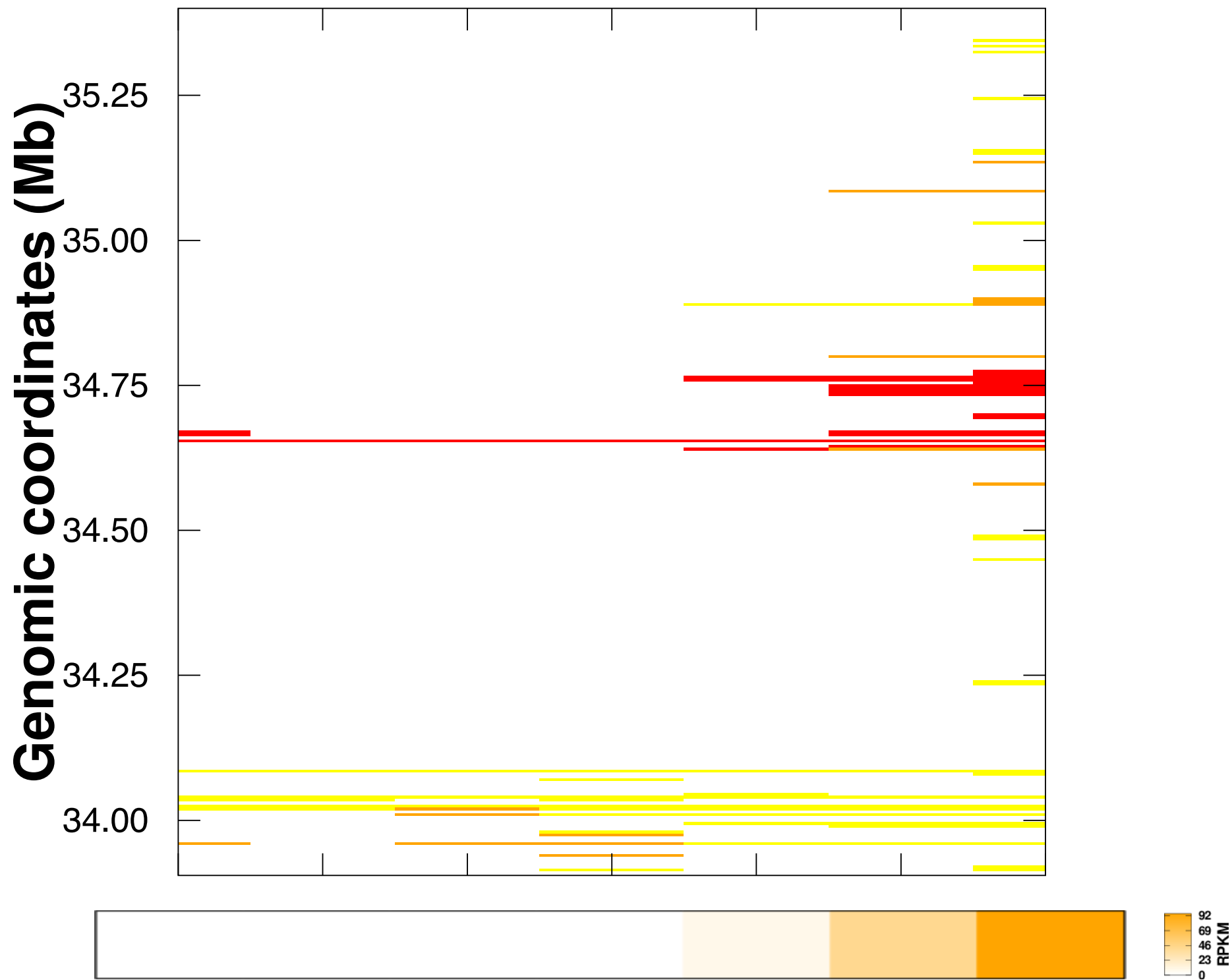
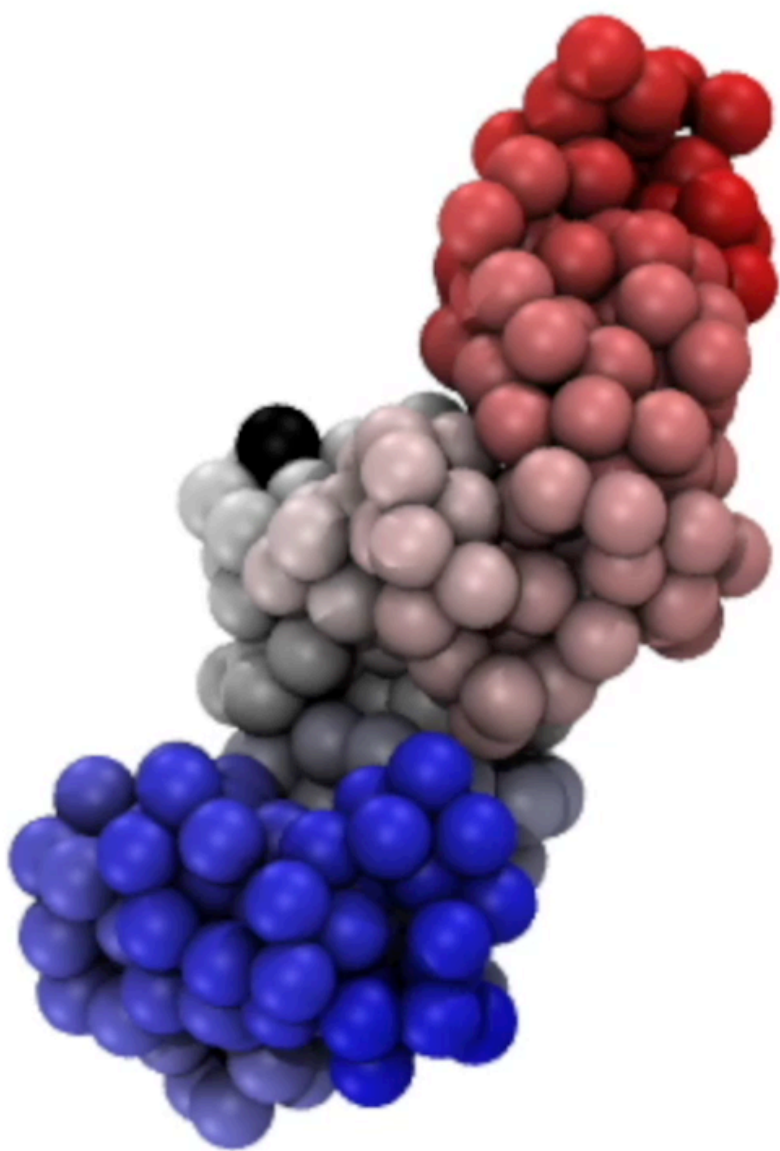
SOX2 locus structural changes from B to PSC

Distance to regulatory elements



SOX2 locus structural changes from B to PSC

Chromatin Activity



	B	Ba	D2	D4	D6	D8	PSC
A	9	6	7	13	13	22	48
AP	4	1	4	4	4	13	23
APD	3	1	1	1	4	10	15



B cell



Ba



D2



D4



D6



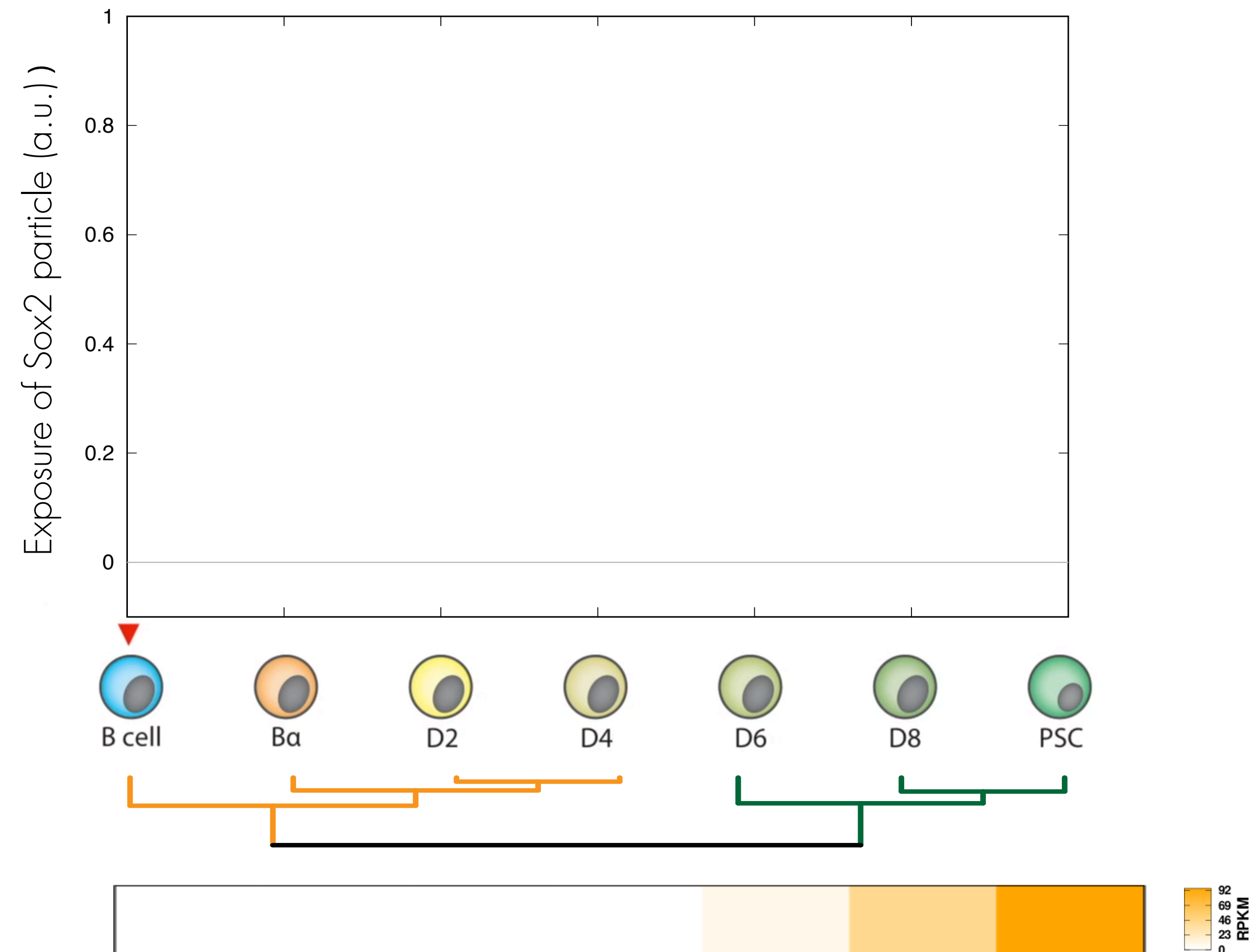
D8



PSC

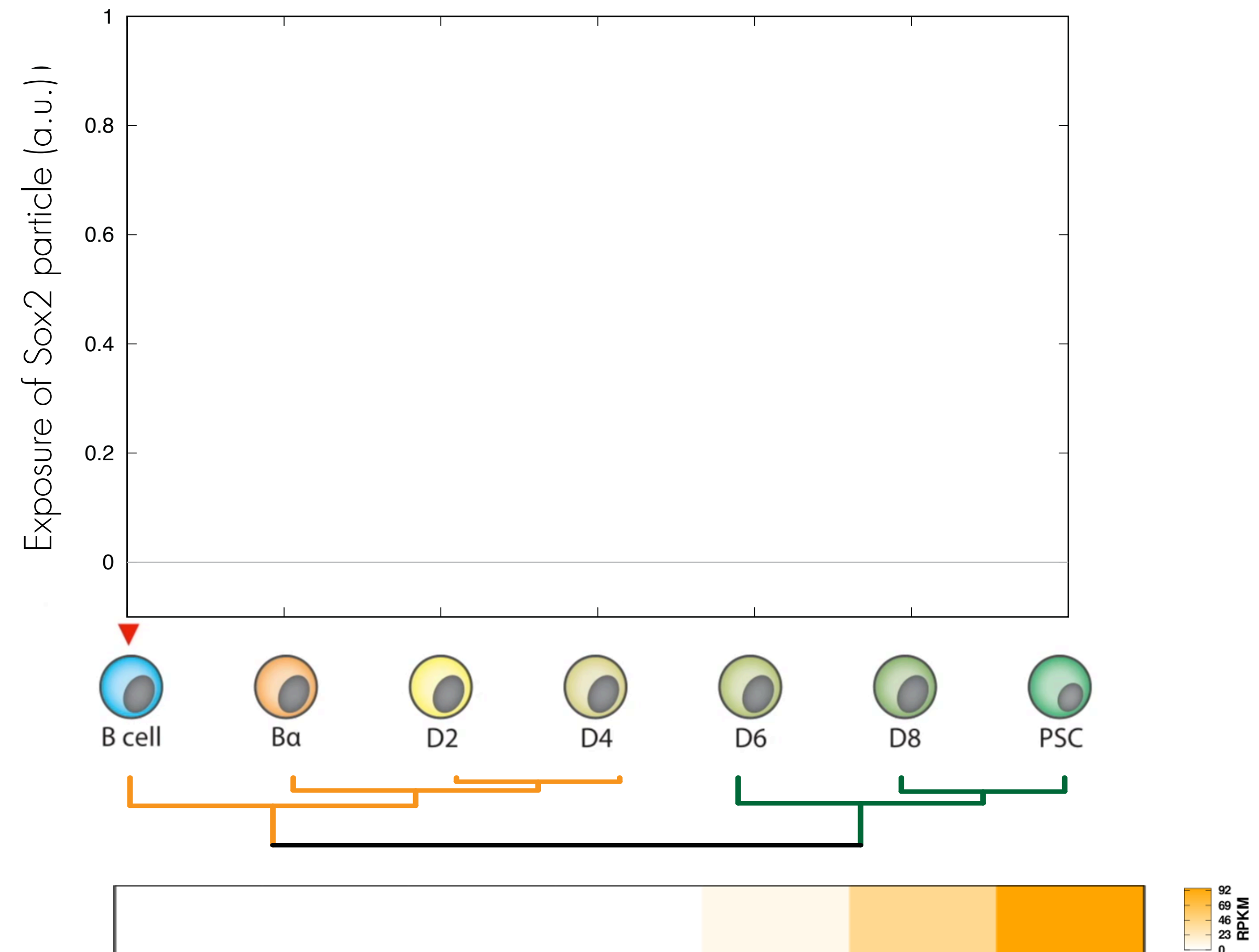
SOX2 locus structural changes from B to PSC

Structural exposure



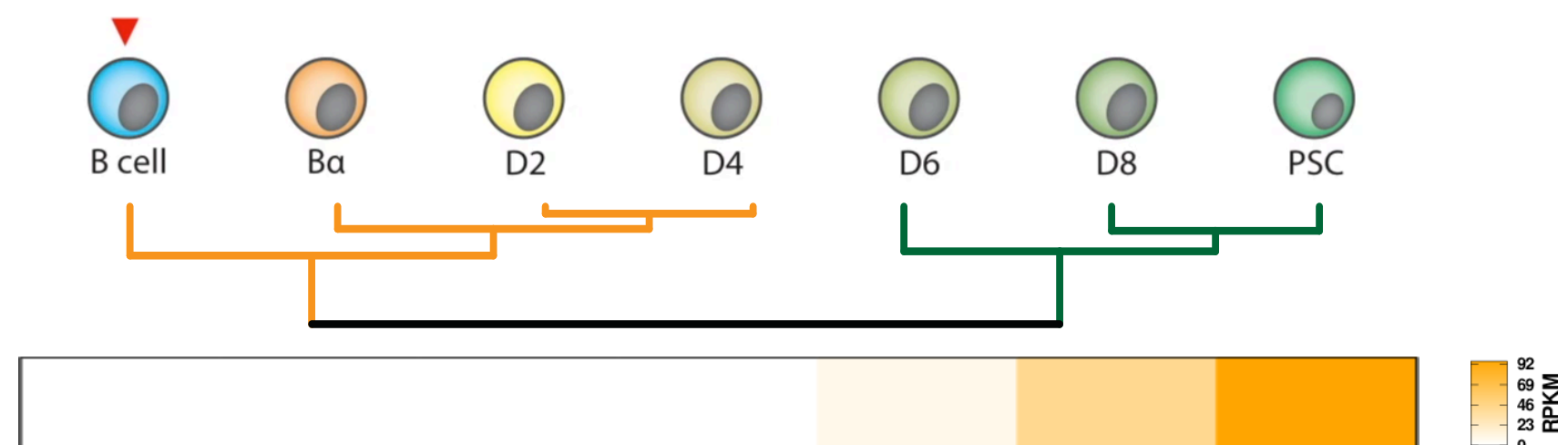
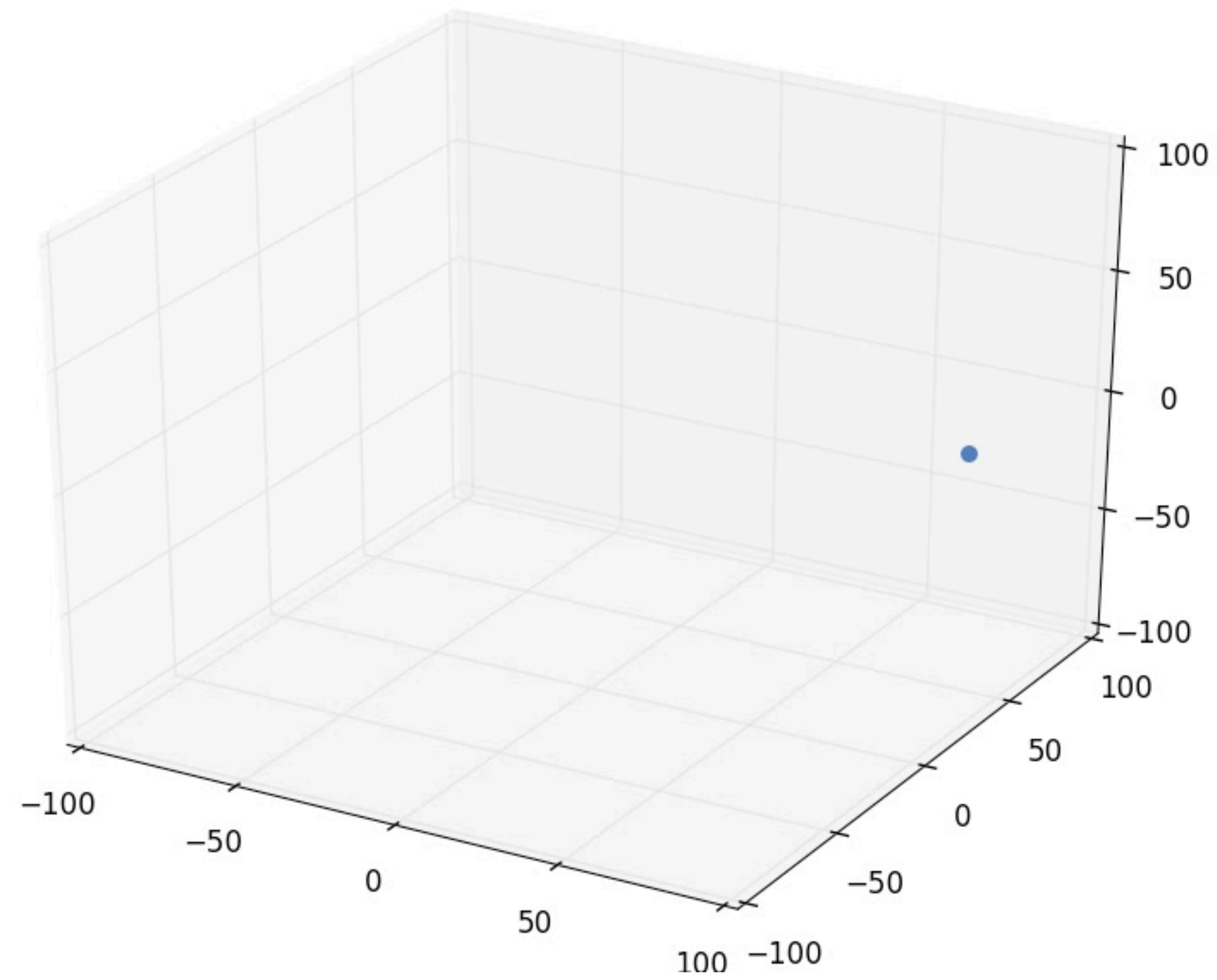
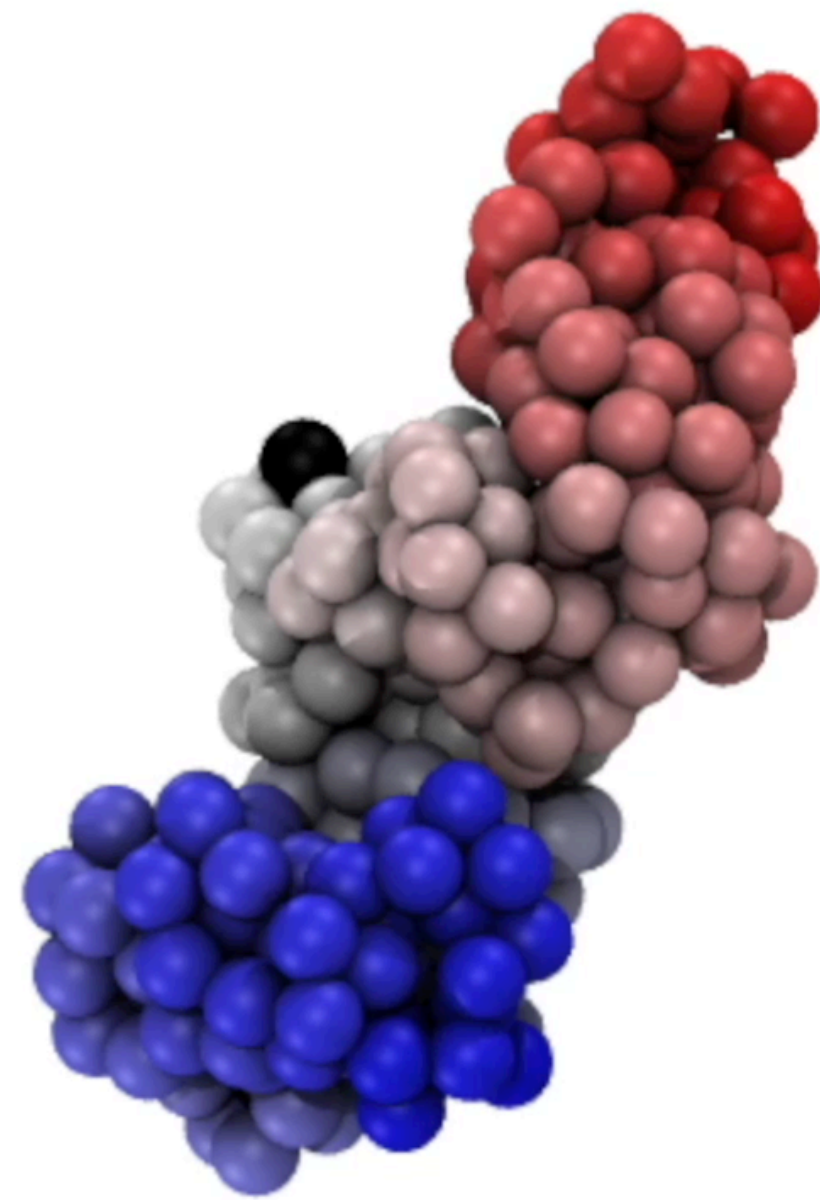
SOX2 locus structural changes from B to PSC

Structural exposure



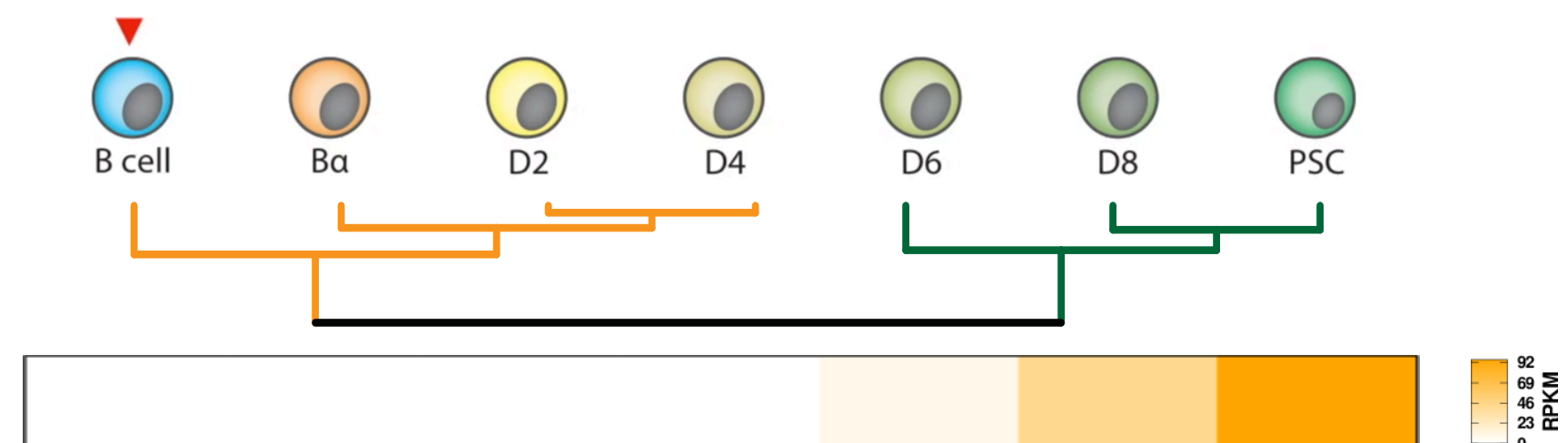
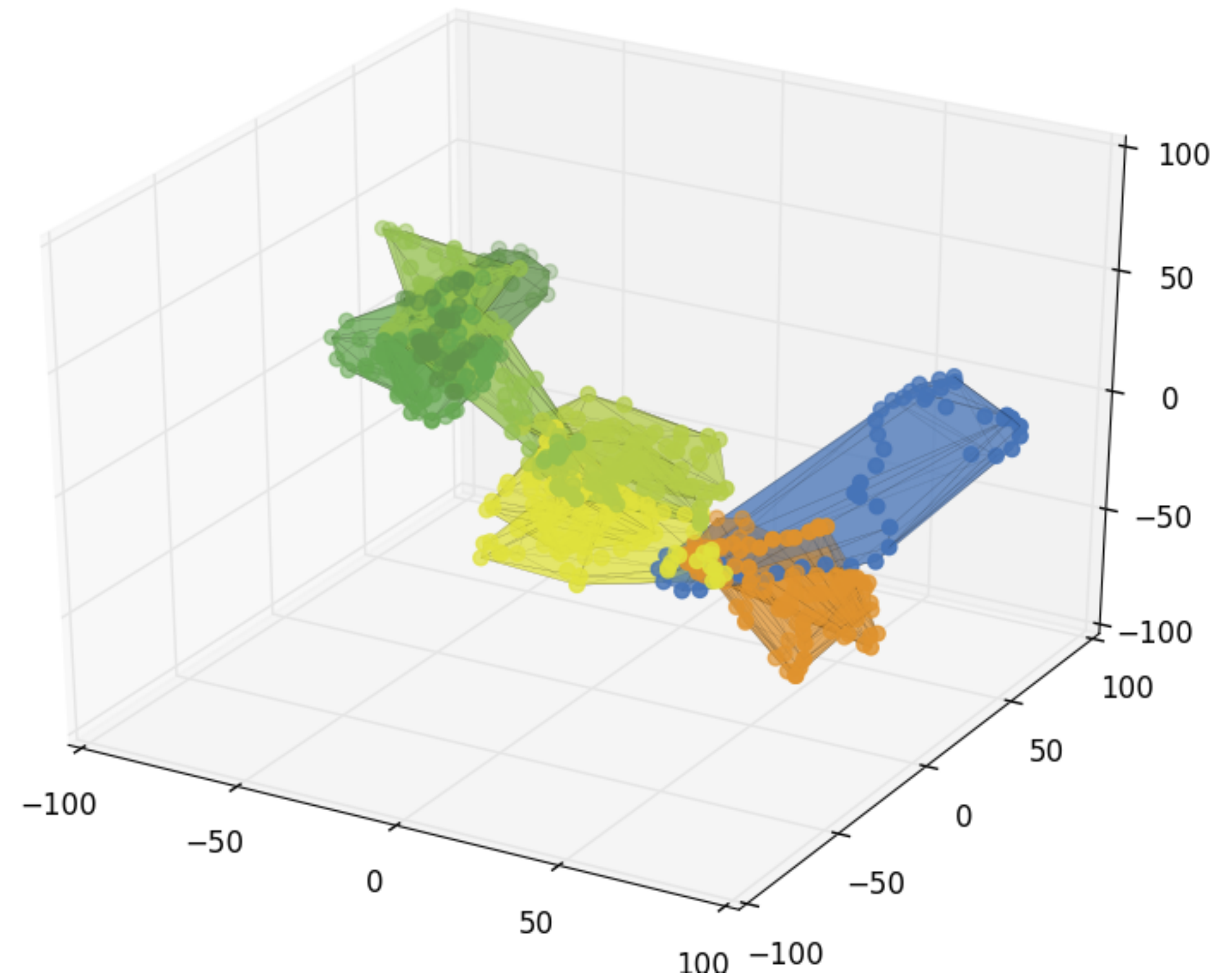
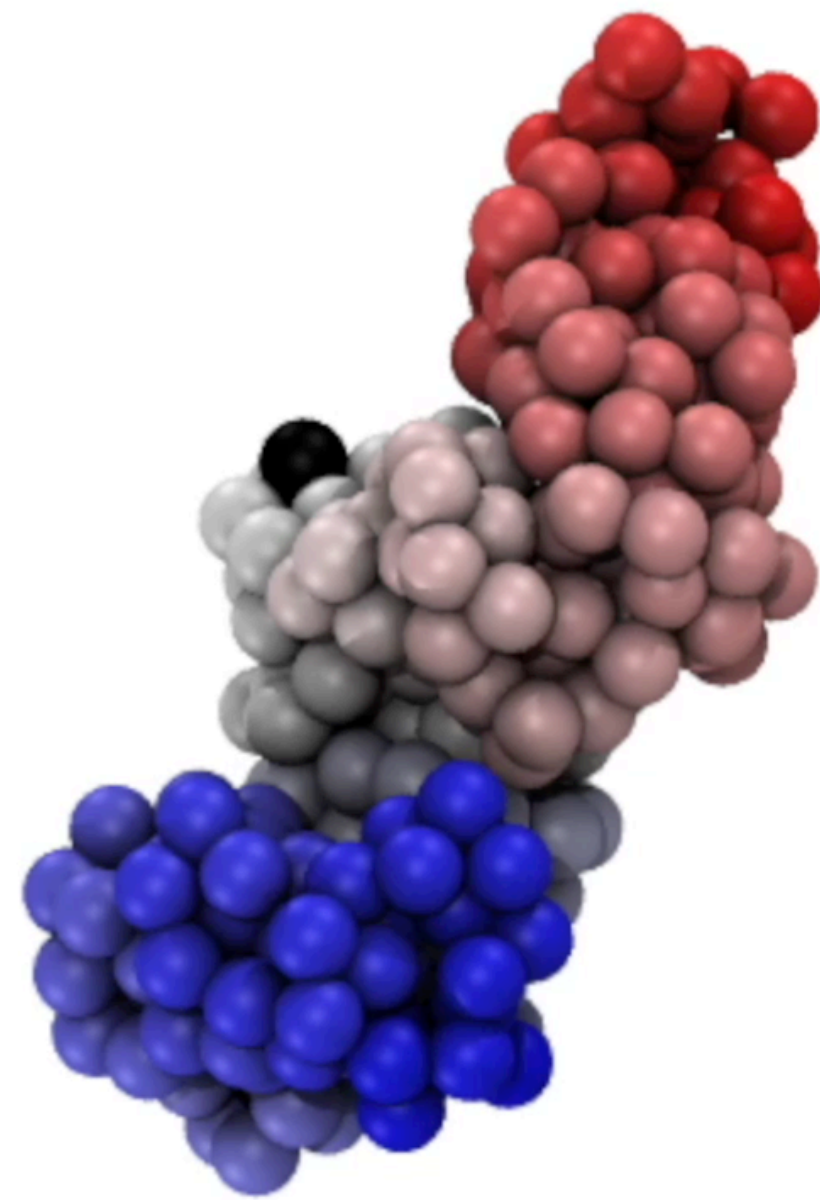
SOX2 locus dynamics changes from B to PSC

SOX2 displacement



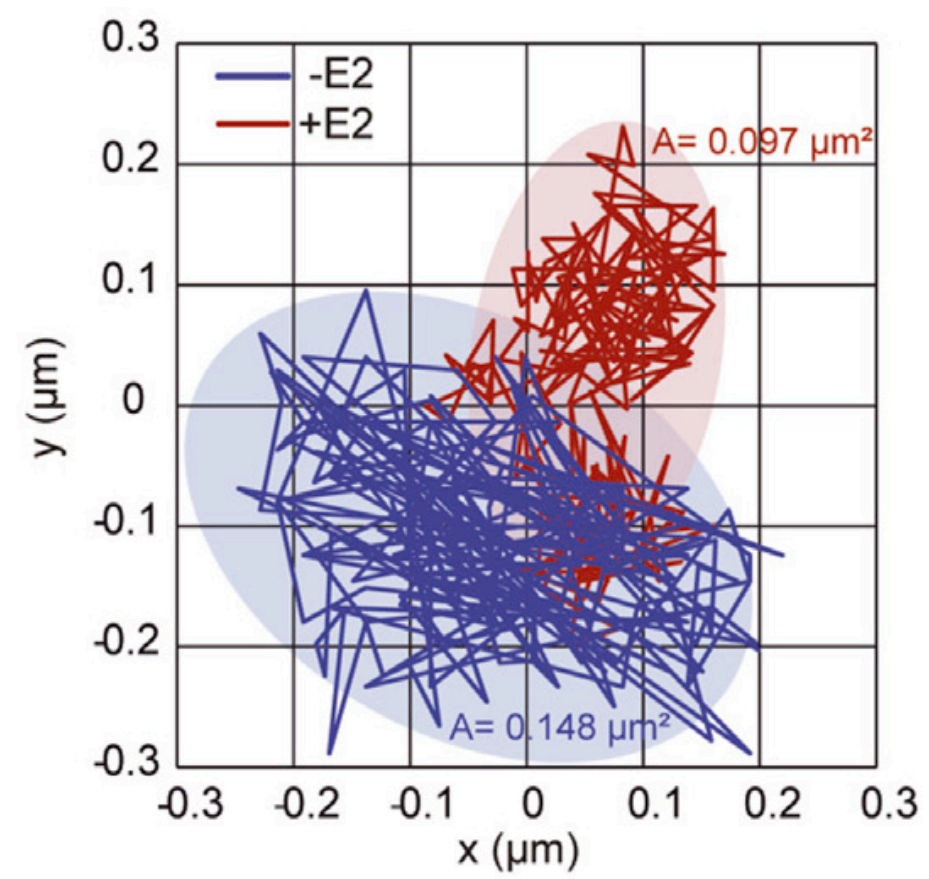
SOX2 locus dynamics changes from B to PSC

SOX2 displacement



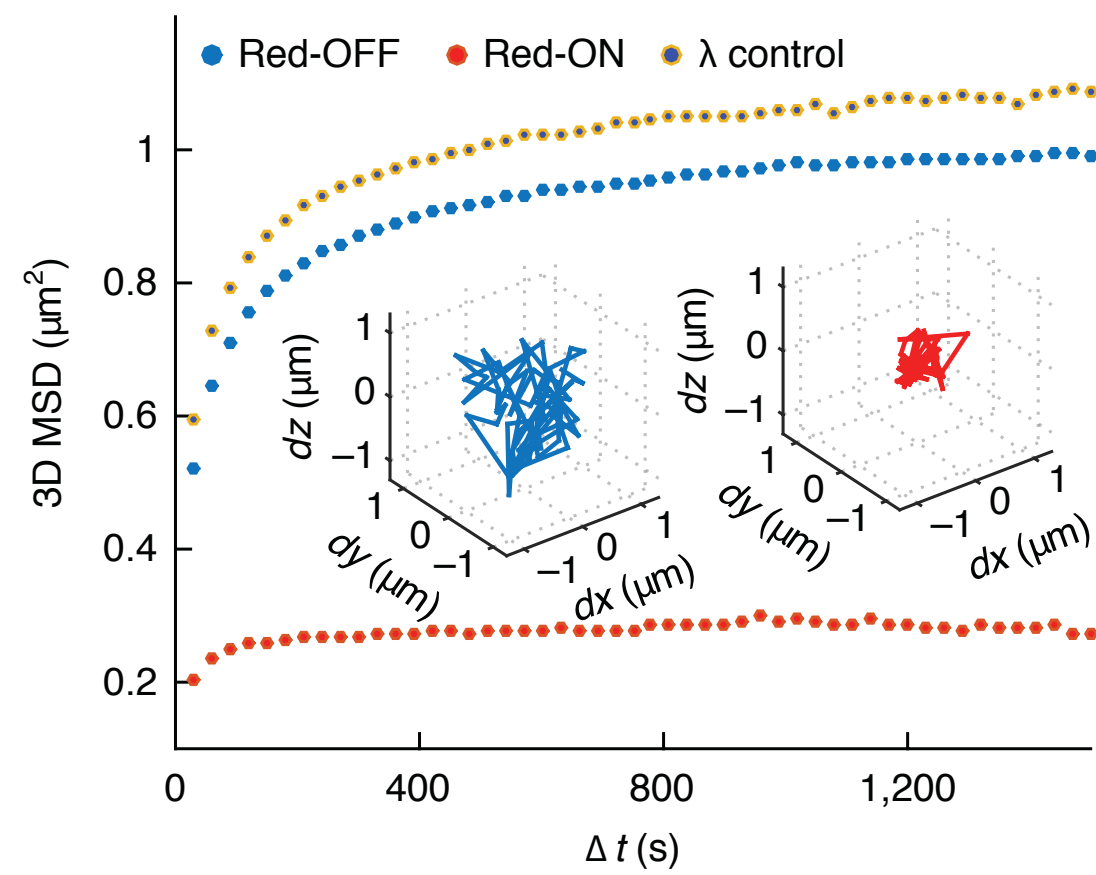
SOX2 locus dynamics changes from B to PSC

SOX2 displacement



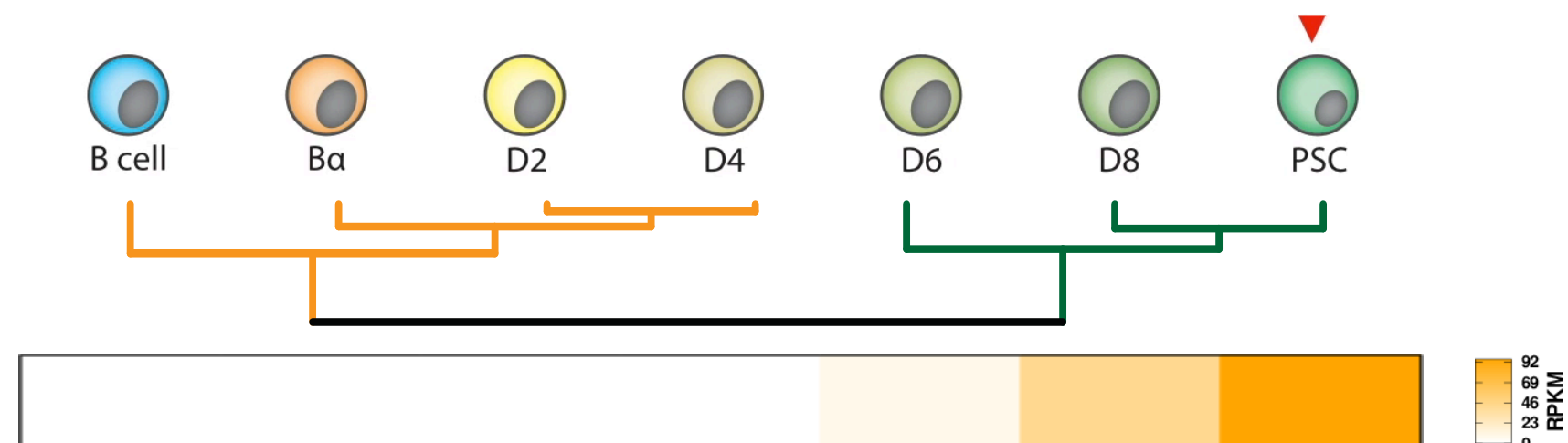
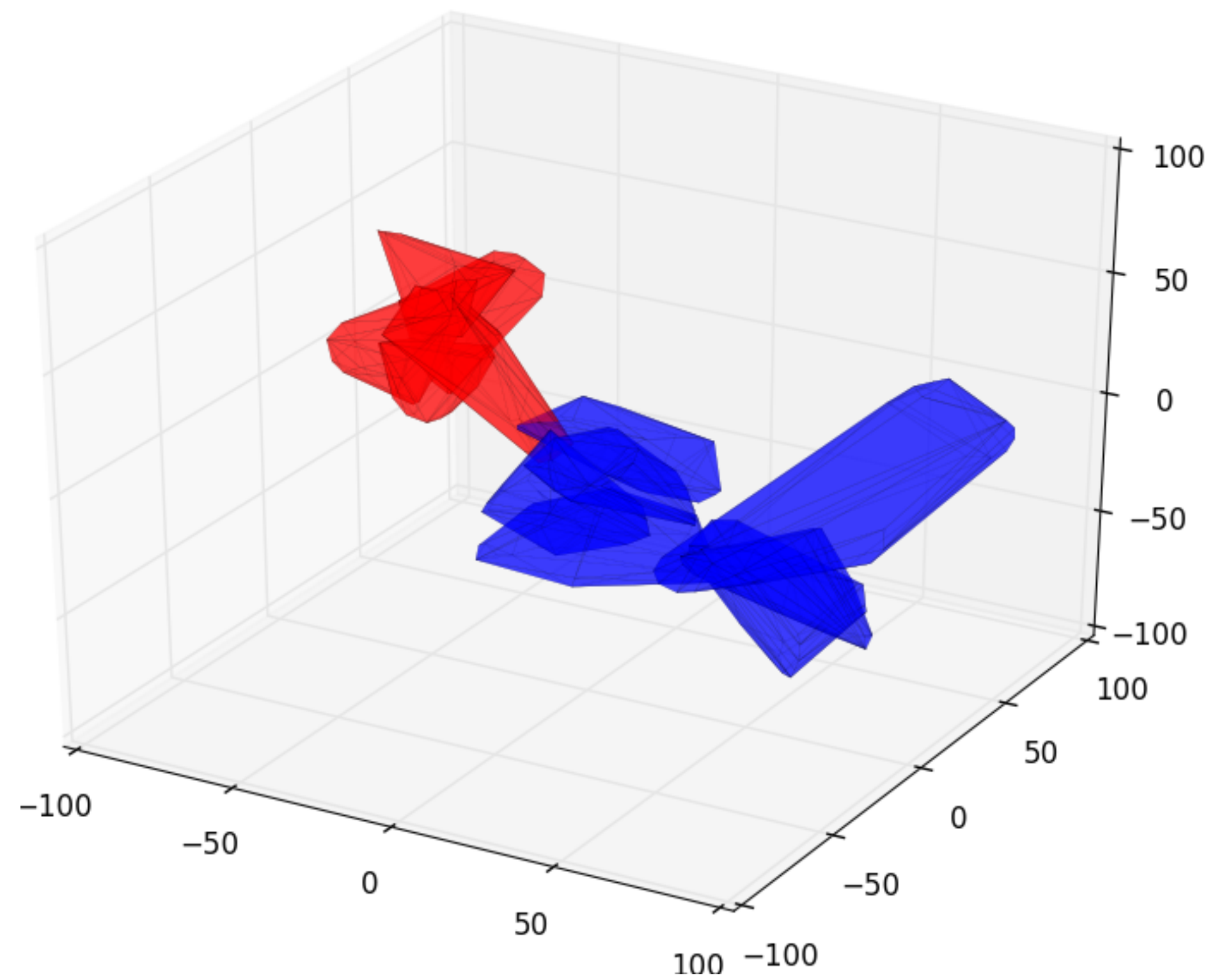
Two dimensional trajectories and area explored over 50s of the CCND1 locus recored before -E2 and after +E2 activation.

Germier ,T., et al, (2017) Blophys J.



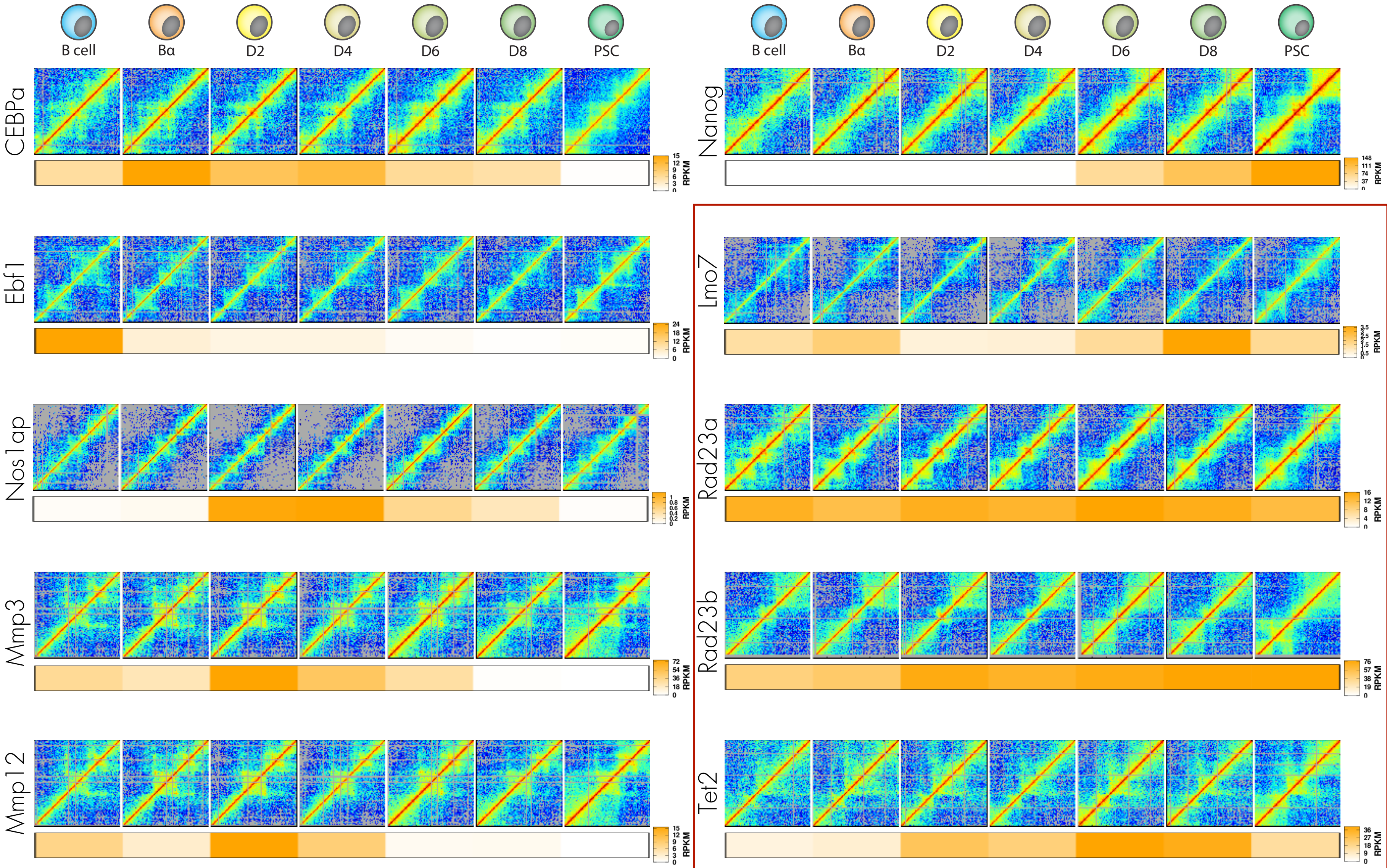
Transcription affects the 3D topology of the enhancer-promoted enhancing its temporal stability and is associated with further spatial compaction.

Chen ,T., et al, (2018) Nat. Genetics

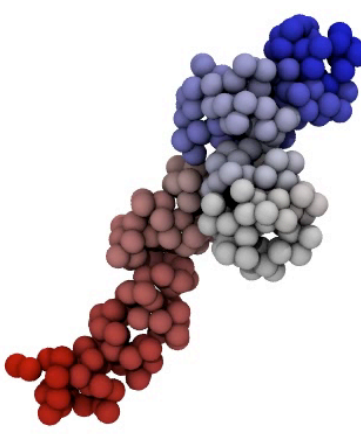


Structural changes from B to PSC

Other 10 loci



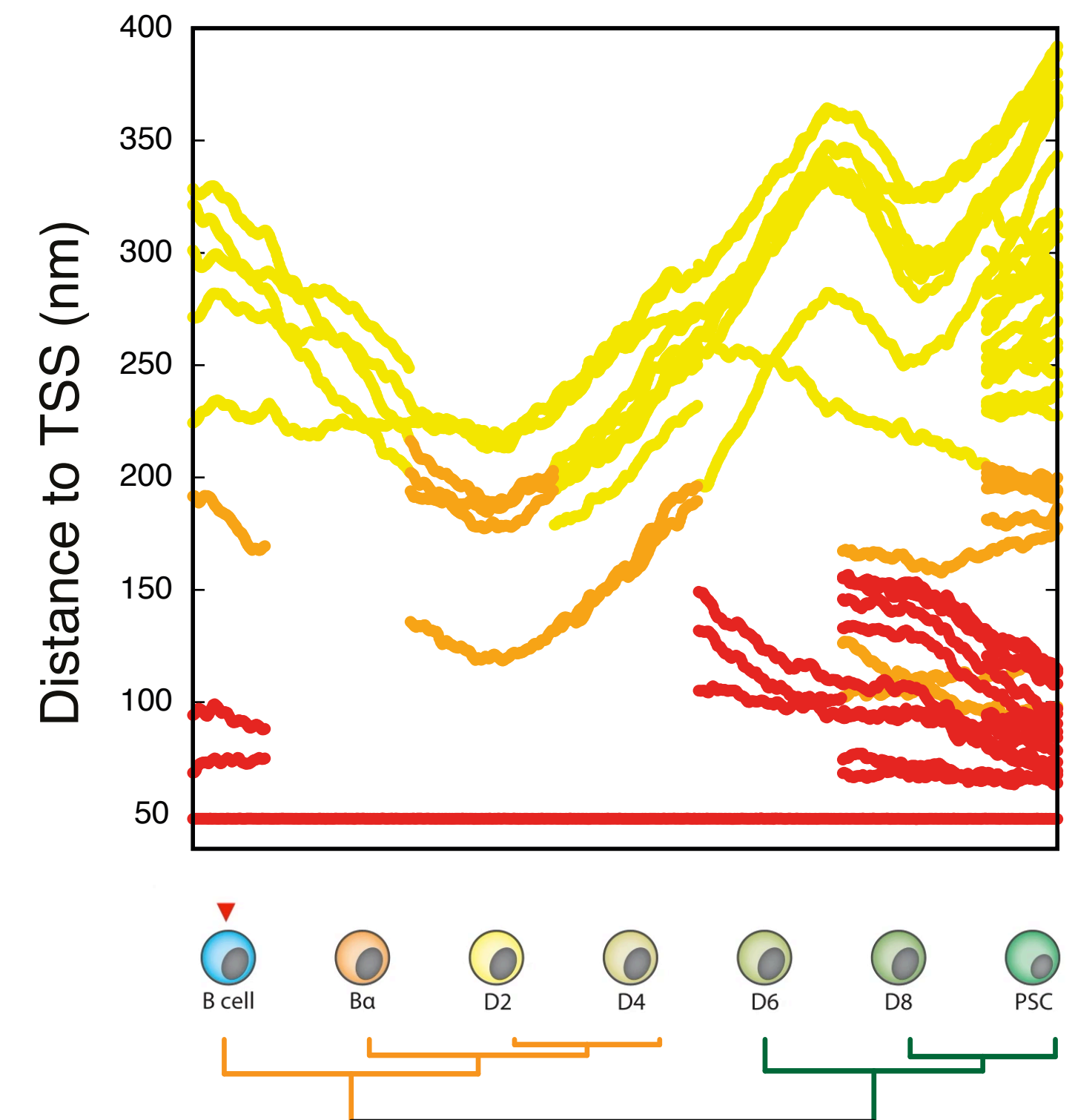
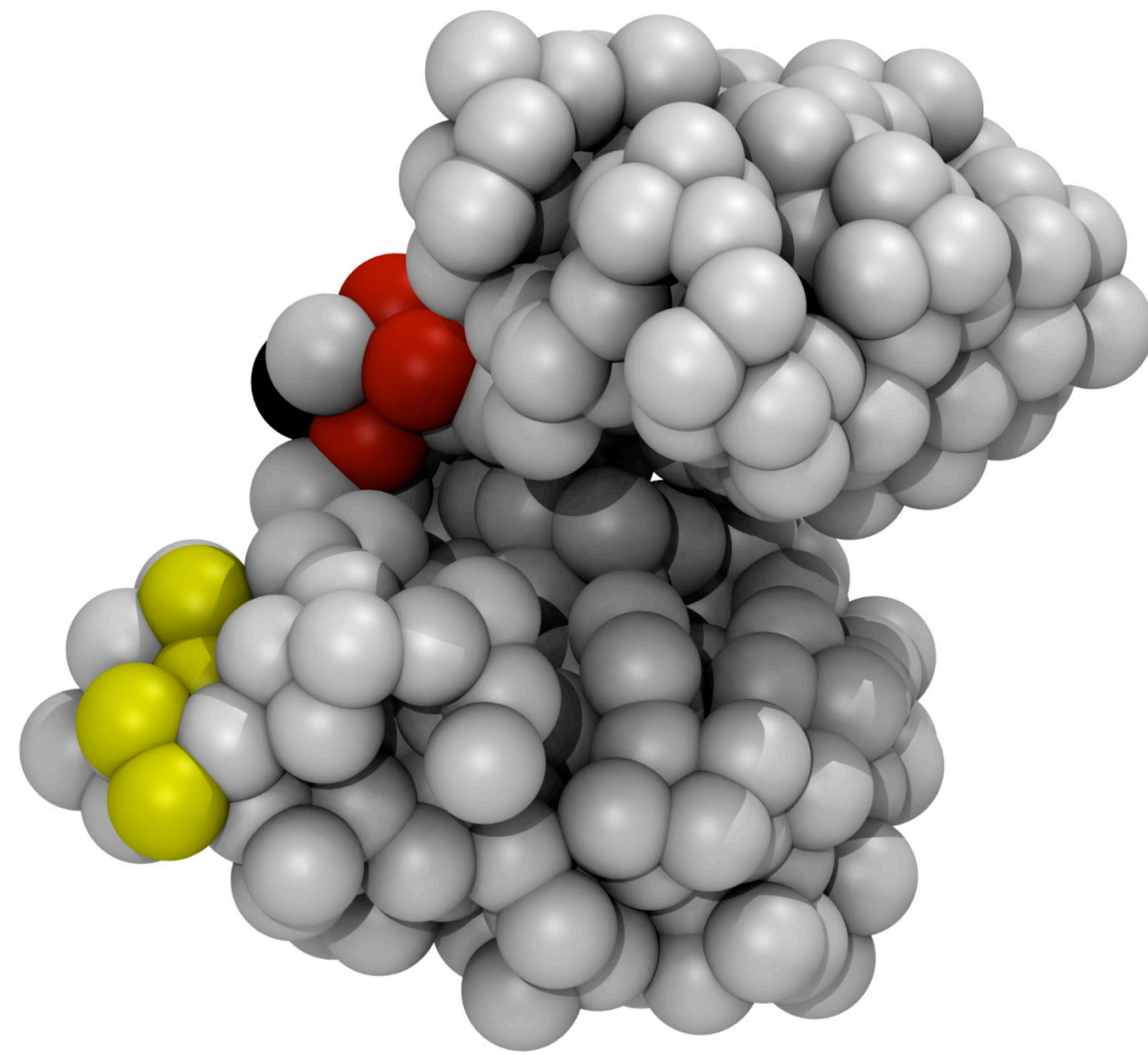
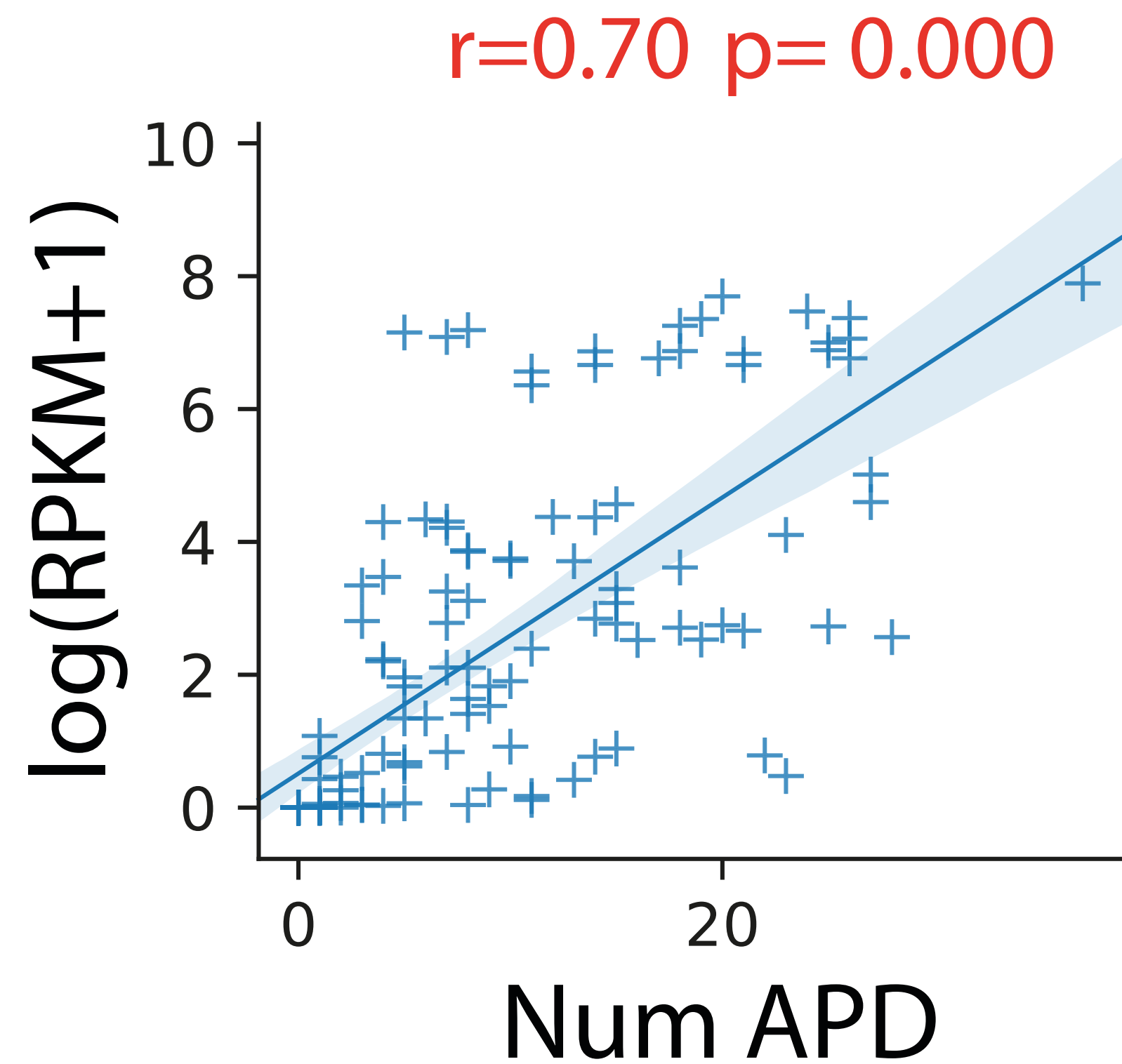
Always active



Switch

Dynamics of gene activation

3D enhancer hubs



<http://marciuslab.org>
<http://3DGenomes.org>

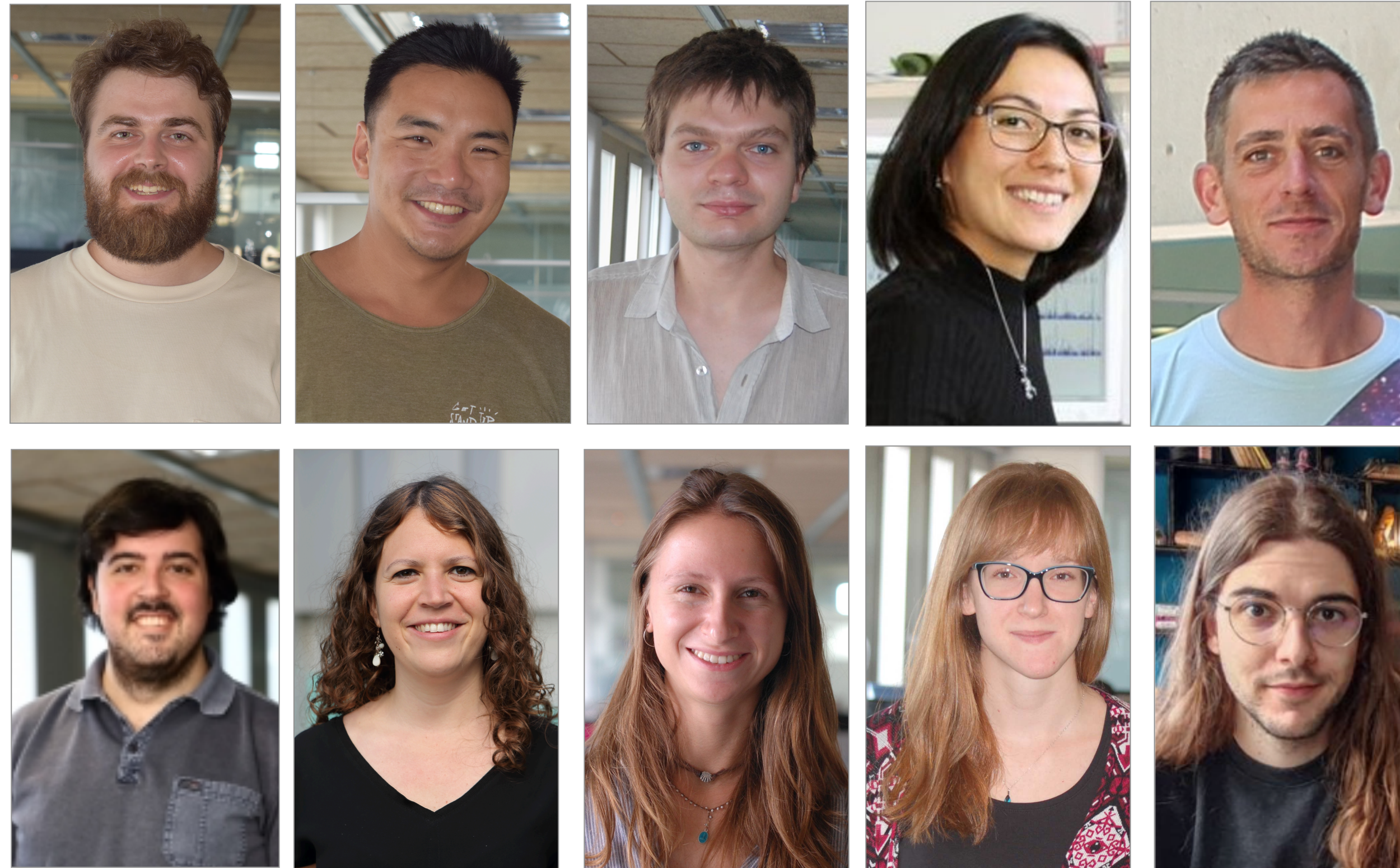
 @marciuslab
@mamartirenom

cnag

CRG
Centre
for Genomic
Regulation

 **ICREA**

Nikolai Bykov
Constantin Diekmann
Ronan Duchesne
Iana Kim
François Le Dily
Iago Maceda
Maria Marti-Marimon
Meritxell Novillo
Aleksandra Sparavier
Leo Zuber



David Castillo
Marco Di Stefano
Irene Farabella
Alicia Hernández
Francesca Mugianesi
Juan A. Rodriguez

.: Our current sponsors :.



.: Conflict of Interest Statement :.

Marc A. Marti-Renom serves as a consultant to Acuity Spatial Genomics, Inc., and receives compensation for these services.